

The
University
Of
Sheffield.

**Phosphorylation as a mode of post-translational
modification in *Campylobacter jejuni***

**A thesis submitted in part fulfilment for the degree of
Doctor of Philosophy.**

**Department of Molecular Biology and Biotechnology,
University of Sheffield**

Ashley Griffin

BSc University of Reading

December 2021

Abstract

Bacterial protein phosphorylation is known to be important in controlling metabolism, motility and virulence. Its global significance in *Campylobacter jejuni* is unknown, as only a limited number of phosphorylated proteins have previously been identified using low-resolution 2D-gel electrophoresis. Our aims were to: (i) comprehensively characterise the *C. jejuni* phosphoproteome using nano LC-MS/MS Orbitrap mass spectrometry, (ii) to identify the kinases and phosphatases responsible for phosphorylation and (iii) determine the physiological role of this modification in the infection biology of *C. jejuni*. A mass spectrometry workflow was devised which has identified up to ten times the number of S/T/Y phosphorylated proteins previously known in *C. jejuni*. Bioinformatic analyses identified several putative protein phosphatases and kinases and isogenic deletion mutants were constructed in these genes. Phosphopeptide analysis comparing wild type to a mutant strain with a deletion in a putative phosphatase revealed a number of putative substrates associated with glutamine metabolism. Whilst exploring the role of phosphorylation in glutamine metabolism in *C. jejuni*, growth experiments in a minimal media formula revealed that glutamine significantly stimulates growth on a variety of substrates suggesting its importance as an N-source for *C. jejuni* growth and survival. RNA-sequencing then revealed a variety of possible glutamine transporter candidates including an annotated putative amino-acid transport protein with homology to a sodium:alanine symporter that was highly down-regulated by excess glutamine. Further analysis using radio labelled glutamine in an uptake experiment confirmed this gene to encode the dominant glutamine transport protein. Protein phosphorylation on multiple proteins and residues is far more prevalent in *C. jejuni* than previously suspected. Mass spectrometry and physiological analyses using isogenic mutants can be used as a method to identify which enzymes are responsible for phosphorylation of target proteins. However, in this study it led to the identification of a novel glutamine transport protein using RNA-sequencing on chemostat culture samples with and without the addition of glutamine.

Acknowledgements

Firstly, I would like to thank Professor Dave Kelly for his patience and resilience through multiple mass spectrometry attempts. Not many supervisors would have been quite so supportive whilst watching the lab budget shrink so quickly. I have thoroughly enjoyed my PhD and will always look back on this experience with a great fondness. This was all made possible by Professor Kelly and the laboratory environment and traditions he has created over the years. I could not have asked for a better supervisor, and I wish him all the best in his retirement.

I would also like to thank the entire Kelly lab group in particular Dr. Aidan Taylor, Dr. Calum Pattrick, Dr. Joseph Webb, Dr. Thomas Puttick, Dr. Pete Walker and Dr. Abdulmajeed Alqurashi. The endless rounds of golf and Friday night beers have been a staple in my life for the past 4 years and I will miss these rituals dearly.

Finally, I would like to thank my family and friends for their unconditional support. I also extend my thanks to collaborators of this project including Dan Bennison, Dr. Rebecca Corrigan and Dr. Mark Collins.

Presentations

2019 Campylobacter, Helicobacter and Related Organisms Conference, Belfast. Talk presented

2021 CampyUK goes global conference, online. Talk presented

Contents

Chapter 1: Introduction.....	8
1.1 <i>Campylobacter jejuni</i> : importance, prevalence and general characteristics.....	8
1.2 Pathogenicity and virulence.....	9
1.2.1 Campylobacteriosis.....	9
1.2.2 Genetic Variation and natural transformation.....	10
1.2.3 Lipooligosaccharide and capsule.....	10
1.2.4 Motility and Chemotaxis.....	11
1.2.5 Adhesion and Invasion.....	13
1.2.6 Cytolethal Distending Toxin.....	14
1.2.7 Outer Membrane Vesicles.....	14
1.3 <i>C. jejuni</i> metabolism and growth.....	15
1.3.1 Microaerobic growth and oxidative stress.....	15
1.3.2 Gluconeogenesis and anaplerotic reactions.....	17
1.3.3 The Citric Acid Cycle and the electron transport chain.....	18
1.3.4 <i>C. jejuni</i> Carbon Sources – transport and metabolism.....	20
1.3.5 Nitrogen Metabolism.....	22
1.3.6 Capnophilic growth.....	23
1.4 Post-translational modification in <i>C. jejuni</i>	24
1.4.1 Post Translation Modifications Overview.....	24
1.4.2 Glycosylation.....	24
1.4.3 Acetylation.....	24
1.4.4 Bacterial Protein Phosphorylation.....	25
1.4.5 Two Component Systems.....	25
1.4.6 Serine/Threonine Phosphorylation.....	26
1.4.7 Tyrosine Phosphorylation.....	27
1.4.8 Other modes of Phosphorylation.....	29
1.4.9 Phosphorylation in <i>Campylobacter jejuni</i>	30
1.4.10 The use of mass Spectrometry in the Characterisation of Bacterial Phosphoproteomes.....	30
1.5 Project aims and objectives.....	31
Chapter 2: Materials and Methods.....	32
2.1 Stocks and Strains.....	32
2.2 Growth of <i>C. jejuni</i>	32
2.2.1 Routine growth of <i>C. jejuni</i>	32

2.2.2 Growth of <i>C. jejuni</i> in minimal media	32
2.3 Growth of <i>E. coli</i>	34
2.4 <i>E. coli</i> Strains used in this study	35
2.5 <i>C. jejuni</i> Strains used in this study	36
2.6 Antibiotics	38
2.7 DNA Manipulation	38
2.7.1 Isolation and purification of DNA	38
2.7.2 Polymerase Chain Reaction	38
2.7.3 Primers used in study	39
2.7.4 Agarose gel electrophoresis	44
2.7.5 Restriction Digestion of DNA	44
2.7.6 Ligation of DNA	44
2.7.7 DNA Sequencing	44
2.7.8 Plasmids used in this study	44
2.8 <i>E. coli</i> mutagenesis	45
2.8.1 Preparation of chemically competent <i>E. coli</i>	45
2.8.2 Transformation competent <i>E. coli</i>	46
2.9 <i>C. jejuni</i> mutagenesis	46
2.9.1 HiFi DNA assembly mutagenesis	46
2.9.2 Complementation Vector Construction	47
2.9.3 Preparation of chemically competent <i>C. jejuni</i>	47
2.9.4 Transformation of competent <i>C. jejuni</i>	47
2.10 Protein Work	47
2.10.1 Cell free extracts	47
2.10.2 Protein concentration determination	48
2.10.3 SDS-Polyacrylamide gel electrophoresis	48
2.10.4 Rapid Pro-Q Diamond Staining	48
2.10.5 Western Blotting	49
2.10.6 His-tagged protein purification	50
2.11 Assays	50
2.11.1 P-Nitrophenyl Phosphate Phosphatase Activity	50
2.11.2 Serine/Threonine Phosphatase Assay	50
2.11.3 Thermoflour Binding Assay	51
2.11.4 Disc Diffusion Assay	51
2.12 Phosphoproteomics by LC-MS	51
2.12.1 Sample preparation	51

2.12.2 Methanol/Chloroform precipitation.....	52
2.12.3 Reduction, Alkylation and Trypsin Digestion.....	52
2.12.4 Peptide desalting with sepPAK cartridges.....	52
2.12.5 IMAC enrichment of phosphopeptides.....	52
2.12.6 LC-MS Analysis.....	53
2.13 Chemostat Culture and RNA-seq.....	53
2.14 Glutamine transport assay.....	54
2.15 High resolution magic angle spinning (HRMAS) nuclear magnetic resonance (NMR) spectrometry	54
Chapter 3: Protein phosphorylation in <i>C. jejuni</i>	55
3.1 Introduction	55
3.2 Results.....	56
3.2.1 Putative protein kinases and phosphatases for investigation	56
3.2.2 Kinase/phosphatase mutant construction.....	59
3.2.3 Cytoplasmic proteins are extensively phosphorylated in <i>C. jejuni</i>	60
3.2.4 Blotting with antibodies to phospho-amino acids to identify changes in phosphorylation	62
3.2.5 Phosphatase activity of purified Cj1258	63
3.2.6 Selection of Cj0184c for phosphoproteome analysis using LC-MS/MS.....	65
3.2.7 Trial LC-MS/MS workflow.....	65
3.2.8 Deletion of Cj0184c has a significant impact on protein expression.....	68
3.2.9 Deletion of Cj0184c has a specific impact on the <i>C. jejuni</i> 11168 phosphoproteome	75
3.3 Discussion	78
Chapter 4: The relationship between Cj0184c and GlnQ.....	83
4.1 Introduction	83
4.2 A model for the relationship between Cj0184c and GlnQ.....	85
4.3 Results.....	86
4.3.1 Overexpression and purification of Cj0184c and S/T Phosphatase Assay	86
4.3.2 11168 Δ 0184c Sensitivity to Reactive Oxygen Species (ROS)	90
4.3.3 Growth on glutamine.....	91
4.3.4 paqPQ and glnPQ Mutant Construction	93
4.3.5 Glutamine ABC Transporters and growth on glutamine.....	95
4.3.6 NMR analysis using HRMAS.....	97
4.4 Discussion	99
Chapter 5 Identification of a novel glutamine transporter	103

5.1 Introduction	103
5.2 Results.....	105
5.2.1 Gene expression changes in chemostat culture during a transition from glutamine limitation to glutamine excess.....	105
5.2.2 Investigating the contribution of putative transport genes identified by RNA-seq to glutamine uptake	111
5.2.3 Glutamine but not ammonia stimulates the growth of <i>C. jejuni</i> 11168 in minimal media containing serine as a carbon source.....	114
5.2.4 Putative Amino Acid Binding Protein – GlnH	115
5.2.5 Inactivation of Cj0903c but not PaqPQ or GlnP reduces the susceptibility of <i>C.</i> <i>jejuni</i> to toxic glutamine analogue Gamma-L-Glutamyl hydrazide (GGH)	116
5.2.6 Cj0903c is likely the sole glutamine transporter in NCTC11168 <i>Campylobacter</i> <i>jejuni</i>	118
5.3 Discussion	119
Chapter 6 Final conclusions and further work.....	126
Chapter 7 References	128

Chapter 1: Introduction

1.1 *Campylobacter jejuni*: importance, prevalence and general characteristics

Campylobacter jejuni is a common cause of gastroenteritis worldwide. Campylobacteriosis is responsible for up to 46% of laboratory-confirmed cases of bacterial gastroenteritis followed by salmonellosis (28%), shigellosis (17%) and *Escherichia coli* O157 infection (5%) (Altekruse et al., 1999). Therefore, annual losses associated with *Campylobacter* in the USA are estimated to be between \$1.3 – 6.2 billion as a result of clinical expenditures and loss of working hours (Forsythe, 2000). *C. jejuni* is widely considered a commensal of chickens and is predominantly found in the gut growing at 42°C; once excreted unlike other causative agents of gastroenteritis *C. jejuni* does not multiply in the environment however viability is maintained in a conventionally unculturable dormant phase (Rollins & Colwell, 1986). The acquisition of *Campylobacter jejuni* by the consumption and handling of poultry is usually followed by a self-limiting gastrointestinal illness characterized by diarrhoea, abdominal cramping and fever. In rare instances a postinfectious complication known as Guillain-Barré syndrome (GBS) may occur. GBS is an acute demyelinating disease of the peripheral nervous system and the most common cause of acute neuromuscular paralysis. The risk of developing *Campylobacter* associated GBS is relatively low (<1 in 1000 cases) however, it is suggested that up to 30% of patients with Guillain-Barré have reported having campylobacteriosis within 12 weeks before the onset of neurological symptoms (Allos, 1997; Rees et al., 1995). Antimicrobial resistance in enteric infections is concerning and particularly prevalent in the developing world. An increase in resistance to macrolides, such as erythromycin, and fluoroquinolones, such as ciprofloxacin has been observed in *C. jejuni* (Post et al., 2017). Subsequently ongoing research in the understanding of *Campylobacter jejuni* metabolism, virulence and survival is crucial to aid in the control and prevention of infection worldwide.

Chickens are the main reservoir for human campylobacteriosis cases however *C. jejuni* is also known to asymptotically colonise the intestines of cattle, pigs, sheep, wild and domesticated birds (Altekruse et al., 1999; Cha et al., 2017; Harris et al., 1986; Stanley & Jones, 2003). Interestingly in the UK both chicken and cattle are considered to contribute equally to reported number of human campylobacteriosis (Wilson et al., 2008). Due to the widespread presence of *C. jejuni* in livestock; contamination of the environment via run-off water from farming and meat processing also provides an additional source for human infection. However, the importance of chickens as a natural reservoir should not be

underestimated. The European Food Safety Authority (EFSA) survey indicates that 71.2% of broiler flocks in the EU were *Campylobacter* positive in 2008 (EFSA, 2010). In addition the UK Food Standards Agency (FSA) have reported that 72.8% of chicken skin and 6.9% of packaging was contaminated with *C. jejuni* across all major supermarkets (FSA, 2015).

Campylobacter jejuni is a gram-negative, non-saccharolytic, non-spore forming, motile, catalase and oxidase positive bacterium belonging to the epsilon class of proteobacteria in the order of Campylobacteriales. This order includes both *Helicobacter* and *Wolinella*. *C. jejuni* has a small genome of only 1.6 – 1.7 Mbps with a guanine and cytosine ratio of approximately 30% (Ketley, 1997; Parkhill et al., 2000). The small genome may explain the inability of *C. jejuni* to ferment carbohydrates and the requirement for complex media. *C. jejuni* is a microaerophile with optimum growth at 42°C, utilising amino acids as the primary carbon source (Debruyne et al., 2008). *C. jejuni* are spiral shaped rods approximately 0.2 to 0.8µm wide and 0.5 to 5 µm long. Motility is achieved in a corkscrew like motion via polar unsheathed flagellum (Ketley, 1997; Wassenaar et al., 1991). The first *C. jejuni* genome sequence was published in 2000 and this has provided the gateway to a new era of *C. jejuni* research (Parkhill et al., 2000).

1.2 Pathogenicity and virulence

1.2.1 *Campylobacteriosis*

Transmission to humans occurs primarily by ingestion of undercooked poultry and/or the cross contamination of food prepared in the same vicinity. Alternative less common routes of infection include contaminated water and direct contact with infected animals including pets. Human-to-human transmission is also possible however rarer (Blaser, 1997). After ingestion, the usual incubation period of *C. jejuni* is 24-72 hours. Prodromal symptoms such as headaches, chills and fever can last greater than 24 hours however the major symptom is acute diarrheal illness with abdominal cramping. The diarrhoea can be watery and often becomes bloody. The duration of illness ranges from 2 days to 1 week, but some cases can last longer. The illness is self-limiting however in severe cases and in compromised patients' erythromycin is the treatment of choice with fluoroquinolones and tetracyclines used as alternatives. If untreated a relapse can occur in up to 20% of cases (Blaser, 1997).

1.2.2 Genetic Variation and natural transformation

C. jejuni has a high degree of genetic variation from intragenomic mechanisms. Equally *Campylobacters* are also highly competent and therefore further diversity can arise from genetic exchange between strains. The genome sequenced published by Parkhill et al. (2000) reveals the presence of hypervariable regions that consist of homopolymeric tracts. A high frequency of variation is observed within these sequences and can be partially explained by the lack of DNA-repair gene homologues. Interestingly the majority of these hypervariable regions are located in regions that encode proteins involved in the biosynthesis or modification of surface structures such as the capsule, lipooligosaccharide and flagellum (Parkhill et al., 2000). Variation in these structures can occur conventionally by mechanisms such as gene duplication, deletions, frameshifts and point mutations (Gilbert et al., 2002). However, variation can also arise bidirectionally via a mechanism known as phase variation. An example of phase variation in *C. jejuni* is the transition between flagellated (Fla⁺) and aflagellated (Fla⁻) phenotypes in culture which can occur at rates as high as 3.1×10^{-3} per cell per generation (Caldwell et al., 1985).

C. jejuni can readily take up DNA from the environment due to its naturally competent state. Both plasmid and chromosomal DNA can be shared between strains via horizontal transfer. This phenomenon has been observed *in vitro* and showed that specifically the transfer of the *tetO* gene can occur rapidly without antimicrobial selection in chickens (Avrain et al., 2004). Another study has also shown that *C. jejuni* displays a significant preference for its own DNA at the species level and is affected by environmental factors such as carbon dioxide levels and bacterial cell density (Wilson et al., 2003) This mechanism of recombination between strains could play an important role on genome plasticity and the spread of antibiotic resistance in *C. jejuni*.

1.2.3 Lipooligosaccharide and capsule

The *C. jejuni* lipooligosaccharide (LOS) capsule is highly variable and plays a major role in immune cell avoidance. The LOS structures are thought to exhibit molecular mimicry resembling human neuronal gangliosides. This characteristic of the LOS is thought to lead to autoimmune disorders such as Guillain-Barré syndrome (GBS) and Miller-Fisher syndrome (GBS variant). Acute motor axonal neuropathy (AMAN) is a variant of GBS and is characterised by acute paralysis and loss of reflexes without sensory loss. Komagamine & Yuki (2008) showed that sensitization with *C. jejuni* LOS or GM1 ganglioside induced acute

motor axonal neuropathy in rabbits. It is therefore hypothesized that *C. jejuni* infection may induce anti-ganglioside antibodies resulting in AMAN.

Capsular polysaccharide (CPS) is structurally independent of LOS, anchored to the membrane by a dipalmitoyl-glycerophosphate lipid anchor (Corcoran et al., 2006). The CPS is possibly the most promising vaccine against campylobacteriosis. A CPS vaccine has been shown to elicit a robust immune response and significantly reduced disease in mice as well as 100% protection against disease in New World monkeys (Monteiro et al., 2009). As well as a vaccine target the *C. jejuni* CPS is also strongly linked with the development of post sequalae infections such as GBS. Specifically capsular types HS1/44c, HS2, HS4c, HS19, HS23/36c and HS41 in combination with sialylated LOS are crucial markers for GBS (Heikema et al., 2015). The *C. jejuni* CPS is composed of complex heptoses and O-methyl phosphoramidate (MeOPN), the substantial variation in the capsule has been attributed to genetic variation mechanisms including phase variation of structural genes (Karlyshev et al., 2005). Additionally the unique phase-variable MeOPN modification found in up to 70% of *C. jejuni* isolates also participates in the variation of the capsule (McNally et al., 2007). Four potential MeOPN biosynthesis genes have been identified, *cj1415-cj1418*, and two enzymes Cj1421 and Cj1422 that encode transferases responsible for the addition of MeOPN to C-3 of β -D-Gal β Nac or to C-4 of D-glycero- α -L-gluco-Hep, respectively (McNally et al., 2007)(Van Alphen et al., 2014). The commonality of MeOPN modification in *C. jejuni* suggest an important biological role. Recently MeOPN has been shown to act as a lytic bacteriophage receptor (Sørensen et al., 2011). Additionally, an MeOPN biosynthesis mutant showed a significant decrease in insecticidal activity in the *Galleria mellonella* model of infection (Champion et al., 2010). MeOPN has also been associated with both serum resistance and colonization in various models, these findings suggest MeOPN is important for both cellular interactions and infection (Maue et al., 2013; Van Alphen et al., 2014).

1.2.4 Motility and Chemotaxis

Motility and chemotaxis are fundamental mechanisms in *C. jejuni* virulence and therefore have been studied extensively. The flagellum has been shown to be essential for the establishment of infection in range of models (Caldwell et al., 1985; Morooka et al., 1985). *C. jejuni* has two flagellin genes *flaA* and *flaB* transcribed from σ^{28} and σ^{54} promoters, respectively (Guerry et al., 1991). Further regulation of the flagella is coordinated by the phase variable two-component system FlgRS (Young et al., 2007). The flagella complex in *C. jejuni* includes an (IM) type-3 secretion system (T3SS) and accessory proteins FlhS and FlhW

responsible for chaperoning FlaAB through the T3SS to polymerise the filament (Boll & Hendrixson, 2013). Glycosylated species are abundant in the filament proteins and in some cases can account for up to 10% of the cells observed mass (Thibault et al., 2001). The chaperone protein FliS has a higher specificity for glycosylated FlaAB to ensure the presence of glycosylated species. This O-linked glycosylation of the structural filament proteins FlaA and FlaB is thought to be important for host immune evasion and/or host-cell interactions (Radomska et al., 2017).

Bacterial chemotaxis is the preferential movement towards or away from high concentrations beneficial or toxic chemicals, respectively. These chemicals are known as chemoattractants and chemorepellents and flagellated bacteria such as *C. jejuni* direct their locomotion to favourable conditions in response to changes in the environmental concentration of both substances. Environmental attractants and repellents are detected by eleven methyl-accepting chemotaxis proteins (MCPs) known as transducer-like proteins (Tlps) in *C. jejuni* (Zautner et al., 2012). These chemoreceptors exist as integral membrane or cytoplasmic proteins sharing a common two component system consisting of membrane associated histidine autokinase (CheA) and a cytoplasmic response regulator (CheY) for signal transduction (Hazelbauer & Lai, 2010). A scaffold protein, CheW, is responsible for interacting with MCPs carrying a signal and attaching to CheA blocking the P1 phosphorylation domain and therefore reducing the phosphorylation of CheY the response regulator (Zautner et al., 2012). The phosphorylated or dephosphorylated state of CheY determines the direction of flagella rotation via interactions with FliM, a switch protein of the flagella motor (Zautner et al., 2012). Finally, phosphatases CheZ and FliY are responsible for quenching environmental signals by dephosphorylating phosphate-activated CheY and CheR. CheB can methylate and demethylate, CheY and CheR, respectively to control adaptation to sustained conditions (Lertsethtakarn et al., 2011). Recent studies have revealed the role of specific transducer-like proteins. Capillary chemotaxis assays have shown that Tlp12 plays a role in chemotaxis towards glutamate and pyruvate and the deletion of the Tlp12 gene influences physiological features such as growth rate and invasiveness (Lübke et al., 2018). It is clear that the chemosensory pathway plays an essential role in colonisation and pathogenesis. This statement is vindicated by studies which show the disruption of just a single potentially redundant chemosensory receptor can have significant deleterious effects on colonisation (Korolik, 2019).

1.2.5 Adhesion and Invasion

Bacteria often utilise surface appendages such as pili to adhere to host cells. However, there are no obvious pili or pilus like encoding open reading frames in the *C. jejuni* genome (Parkhill et al., 2000). Despite the lack of pilus encoding regions several *C. jejuni* strains have been shown to bind components of the extracellular matrix. Western blots have shown *C. jejuni* outer membrane protein (OMP) extracts bind radioactive fibronectin, specifically a 37 kDa protein known as CadF (Konkel et al., 1997, 2005). CadF contains a novel fibronectin binding motif at amino acids 134-137 (FRLS) and is required for maximal binding and invasion in vitro (Monteville et al., 2003). In 2009 another fibronectin binding protein was identified in *C. jejuni* known as FlpA for Fibronectin-like protein A (Flanagan et al., 2009). The deletion either *cadF* or *flpA* results in a reduction in chicken colonization compared to wildtype (Flanagan et al., 2009; Konkel et al., 2020). Two surface exposed *C. jejuni* lipoproteins, JlpA and CapA, have been suggested to play a role in adhesion. JlpA is important for Hep-2 cell binding which is suggested to contribute to the proinflammatory response triggered during *C. jejuni* infection (Jin et al., 2001, 2003). CapA is an autotransporter and in CapA-deficient mutants a reduction in adherence to Caco-2 cells is observed as well as decreased colonization and persistence in a chick model (Ashgar et al., 2007). Another putative adhesin is Peb1, a periplasmic protein with homology to amino acid ATP-binding cassette (ABC) transporters (Pei & Blaser, 1993). Peb1 has been shown to bind both aspartate and glutamate with high affinity and is essential for growth on both these major carbon sources (Leon-Kempis et al., 2006). However, Peb1 has also been shown to be crucial for adherence to HeLA cells and *peb1*-deficient mutants colonize mice poorly (Young et al., 2007).

C. jejuni adheres to and invades intestinal epithelial cells after passage through the GI tract. In order for the cells to efficiently invade production and secretion of *Campylobacter* invasion antigens (Cia) must be regulated. Cia protein synthesis is stimulated by bile, specifically deoxycholate in the small intestine although secretion through the flagella is not stimulated until after adherence at the site of invasion has been established (Rivera-Amill et al., 2001). Internalisation of *C. jejuni* is thought to occur in an actin-independent microtubule-dependent fashion as opposed to the more common microfilament-dependent mechanism utilised by other invasive bacteria (Oelschlaeger et al., 1993). Once internalised, *C. jejuni* survives and replicates within a vacuole known as a *Campylobacter* containing vacuole (CCV). This CCV travels along microtubules towards the perinuclear

avoiding delivery into lysosomes in a mechanism not yet entirely determined (Watson & Galán, 2008; Young et al., 2007).

1.2.6 Cytolethal Distending Toxin

The most well characterised toxin in *C. jejuni* is the cytolethal distending toxin (CDT). CDT is also produced by a number of other bacterial species such as *E. coli*, *Acinetobacillus actinomycetemcomitans*, *Haemophilus ducreyi* and *Helicobacter hepaticus*. The genetic locus for CDT contains genes *cdtABC* which are essential for the formation of the tripartite active holotoxin complex (Lara-Tejero & Galán, 2001). CDT causes arrest at the G₁/S or G₂/M transition of the cell cycle by attacking host DNA to introduce double strand breaks induce senescence and apoptosis (Young et al., 2007). CdtB shares homology with DNase I-like proteins and possesses both DNase and phosphatidylinositol 3-4-5 triphosphate phosphatase activities, this is the subunit responsible for introducing double stranded DNA breaks (Lara-Tejero & Galán, 2001). The role of CdtA and CdtC is less well understood however their primary role must be to support CdtB to exert cytomodulatory and cytotoxic effects by facilitating the localisation of CdtB into the nucleus. It has been shown in some organisms that CdtA and CdtC can both independently support intoxication by CdtB (Dixon et al., 2015). CdtA and CdtC have been shown to bind cholesterol rich lipid rafts on the cell surface which result in changes to intracellular uptake and trafficking pathways enabling delivery of CdtB to the nucleus (Dixon et al., 2015). It is unknown why a pathogen which establishes long-term asymptomatic associations in hosts such as the chicken has maintained genetic instructions for a toxin such as CDT. However there is evidence in mice that suggest CDT may function in immune modulation and persistent colonisation (Ge et al., 2005; Pratt et al., 2006).

1.2.7 Outer Membrane Vesicles

A key mechanism of survival and pathogenesis in enteric bacteria is the secretion of virulence factors. However, there are no obvious virulence-associated secretion systems encoded in the *C. jejuni* genome. Instead, *C. jejuni* utilises outer membrane vesicles (OMVs) for the delivery of multiple virulence factors in a concerted package to host cells. OMVs are 10 to 500 nm spherical proteoliposomes produced by growing cells containing both outer membrane and periplasmic proteins as well as phospholipids and lipooligosaccharides (LOS) (Kuehn & Kesty, 2005; Mashburn-Warren et al., 2008). It was only recently when CDT was

identified as a constituent of *C. jejuni* OMVs that the significance of this mechanism was realised (Lindmark et al., 2009). Therefore, it has can be hypothesised that OMVs are bestowed by *C. jejuni* in order to promote cellular adhesion and invasion. Proteome analysis of OMVs in *C. jejuni* has revealed at least 151 proteins are present with the OMVs including N-linked glycoproteins, potentially explaining the purpose of N-linked glycosylation of periplasmic proteins which have been shown to enhance immune cell evasion (Elmi et al., 2012). Furthermore, OMVs in *C. jejuni* have been shown to induce the host immune response including IL-8, IL-6, and TNF- α potentially causing a loss of host cell membrane integrity (Elmi et al., 2012).

A transport system responsible for the synthesis and release of OMVs in *Campylobacter* has been identified as the maintaining outer membrane lipid asymmetry (Mla) system (Malinverni & Silhavy, 2009). This transport system includes an OM (MlaA) associated protein, periplasmic lipid binding protein (MlaC) and an inner membrane ABC-type transporter complex (MlaBDEF). The Mla system is responsible for the recycling of aberrant phospholipids from the outer leaflet of the OM however, the suppression of this system induces the spontaneous budding of vesicles and thus the release of OMVs (Roier et al., 2016). Recently bile components such as sodium taurocholate have been shown to reduce expression of both *mlaA* and *mlaC* resulting in an increase in OMV production (Davies et al., 2019). Similarly the concentration of bile has been suggested to influence OMV protein content and facilitate both adhesion and invasion (Taheri et al., 2018). Bile composition is affected by both diet and microbiota and therefore these finding highlight the importance of lifestyle factors in disease presentation.

1.3 *C. jejuni* metabolism and growth

1.3.1 Microaerobic growth and oxidative stress

C. jejuni must survive in a range of environmental niches and endure variable stresses such as oxygen concentration. *C. jejuni* grows best at 5% O₂, 10% CO₂ and 85% N₂ and is therefore designated a microaerophile (Altekruse et al., 1999). The intestines where *C. jejuni* colonises its host is often lower than the desirable 5% oxygen concentration. In order to combat this *C. jejuni* preferentially colonises the mucus layer and the intestinal crypt where oxygen tension is higher. *C. jejuni* also has a complex set of electron transport chains which allows the use of a variety of electron donors and electron acceptors besides oxygen

(Hofreuter, 2014). Two terminal, membrane-bound oxidases, cytochrome c oxidase CcoNOQP and bd-like quinol oxidase CioAB, in the electron transport chain are suggested to mediate the oxygen dependent respiration of *C. jejuni*. CcoNOQP has a far higher affinity for oxygen than CioAB and deletion of cconN results in complete attenuation in a chicken colonisation model whilst a *cioM* mutant demonstrates no attenuation. These findings suggest CcoNOQP to be the major terminal complex for oxygen dependent respiration in *C. jejuni* (Jackson et al., 2007; Weingarten et al., 2008). Despite the presence of these two oxidases atmospheric oxygen levels will result in growth inhibition. This is in part due to the presence of oxygen sensitive enzymes encoded in the *C. jejuni* genome. A key example is centred around the metabolism of serine, a key carbon source for *C. jejuni*. L-serine dehydratase enzyme (SdaA) converts serine into ammonia and pyruvate. Pyruvate and 2-oxoglutarate:acceptor oxidoreductases (Por and Oor) are then responsible for oxidative decarboxylation of intermediates in the TCA cycle to acetyl-coenzyme A (acetyl-CoA) and succinyl-CoA, respectively (Kendall et al., 2014). SdaA, Por and Oor all possess iron-sulphur clusters which are oxygen labile (Velayudhan et al., 2004). Iron sulfur cluster enzymes are found in many anaerobic bacteria as they are extremely susceptible to inactivation by molecular oxygen. Despite the possession of oxygen labile enzymes *C. jejuni* cannot grow under anaerobic conditions (Véron et al., 1981). This is in part due to the class I ribonucleotide reductase (Nrd-AB-type RNR) requiring low amounts of oxygen for deoxyribonucleotide synthesis (Sellars et al., 2002).

The requirement for oxygen in an organism which possesses oxygen labile enzymes results in the need for mechanisms to counteract non-specific electron transfer and the action of reactive oxygen species (ROS). For this reason *C. jejuni* harbours a variety of ROS-detoxifying enzymes such as superoxide dismutase (SodB), catalase (KatA), cytochrome c peroxidases, thiol peroxidases and alkyl hydroperoxide (AhpC), (Hofreuter, 2014). Hemerythin proteins HerA and HerB also partially protect POR and OOR however *C. jejuni* lacks the ability to repair either enzyme once damaged by atmospheric oxygen concentrations (Kendall et al., 2014).

1.3.2 Gluconeogenesis and anaplerotic reactions

The inability of *C. jejuni* to utilize glucose and other hexose sugars is attributed to the lack of sugar transporters and key glycolytic enzymes in the genome (Parkhill et al., 2000)(Figure 1.1). *C. jejuni* lacks a glucokinase for the phosphorylation of extracellular glucose and a 6-phosphofructokinase, a key glycolytic enzyme responsible for the irreversible phosphorylation of fructose-6-phosphate to fructose 1,6-diphosphate. However, homologues of all the enzymes for gluconeogenesis from phosphoenolpyruvate (PEP) are present suggesting that the Embden-Meyerhof pathway functions in gluconeogenesis (Velayudhan & Kelly, 2002). Other anaplerotic enzymes including pyruvate carboxylase (PYC), phosphoenolpyruvate carboxykinase (PCK) and malic enzyme (MEZ) are also present in the *C. jejuni* genome potentially for the synthesis of oxaloacetate (OAA) from pyruvate or PEP in order to feed the citric acid cycle for both its energy generating and biosynthetic roles (Parkhill et al., 2000; Velayudhan & Kelly, 2002). Interestingly pyruvate kinase (PYK), which catalyses the irreversible final step of glycolysis (phosphoenolpyruvate to pyruvate) is present in the *C. jejuni* genome (Parkhill et al., 2000). Velayundhan and Kelly (2002) suggest the role of PYK could be to metabolize an alternative substrate such as one of the pentose phosphate pathways to bypass 6-phosphofructokinase.

A novel L-fucose pathway has been identified in some *C. jejuni* strains. The L-fucose permease FucP has been identified within a genomic island with 37.2% amino acid identity to the L-fucose permease in *E. coli* (Muraoka & Zhang, 2011; Stahl et al., 2011). The precise mechanisms of the pathway are unknown however it was shown to be essential for fucose uptake and metabolism and was advantageous for colonisation in certain hosts (Stahl et al., 2011).

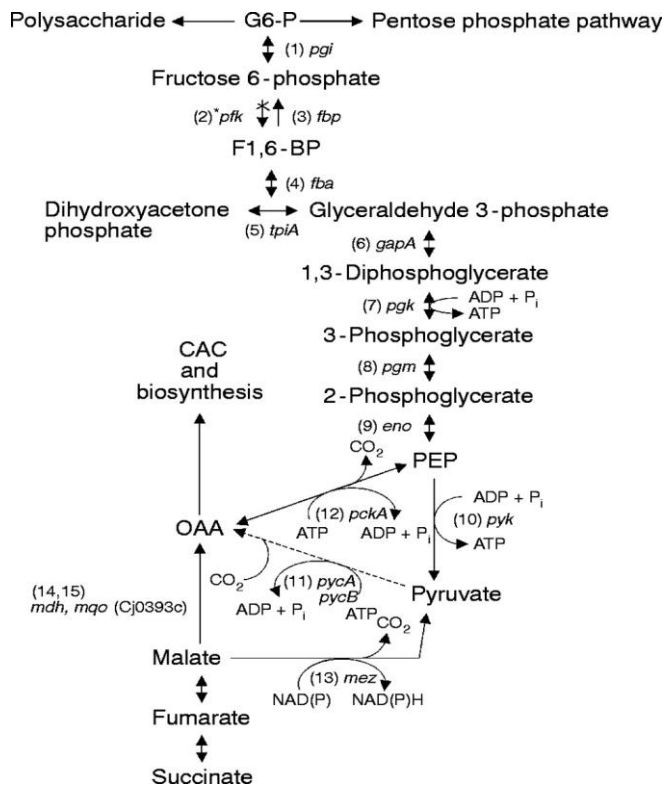


Figure 1.1 Gluconeogenic and anaplerotic reactions of *C. jejuni*. The gluconeogenic and anaplerotic pathways are shown with the corresponding enzymes. An asterisk indicates that enzyme is missing from the *C. jejuni* genome. The dotted line shows reactions which replenish the citric acid cycle (Diagram taken from Velayudhan & Kelly, 2002).

1.3.3 The Citric Acid Cycle and the electron transport chain

C. jejuni is heavily dependent on the citric acid cycle (CAC) to meet its energy requirements. The CAC is similar to the one seen in model organism *E. coli* except pyruvate dehydrogenase and 2-oxoglutarate dehydrogenase are replaced with pyruvate oxidoreductase (POR) and oxoglutarate oxidoreductase (OOR), respectively. The majority of the amino acid pathways produce CAC intermediates which are fed into the CAC. However, *C. jejuni* can also transport several intermediates directly. For example, the KgtP permease can transport 2-oxoglutarate. Additionally fumarate and malate can be transported by C4-dicarboxylate transporters DcuA and DcuB (Guccione et al., 2008). Some strains such as NCTC11168 also possess a citrate transporter (Cj0203) (Parkhill et al., 2000). Interestingly growth on pyruvate has also been observed in *C. jejuni* however no pyruvate transporters have been identified (Velayudhan & Kelly, 2002). Pyruvate is the key carbon source for all CAC intermediates and is degraded to CO₂ or fermented to acetate after being decarboxylated to acetyl-CoA by POR (Gao et al., 2017).

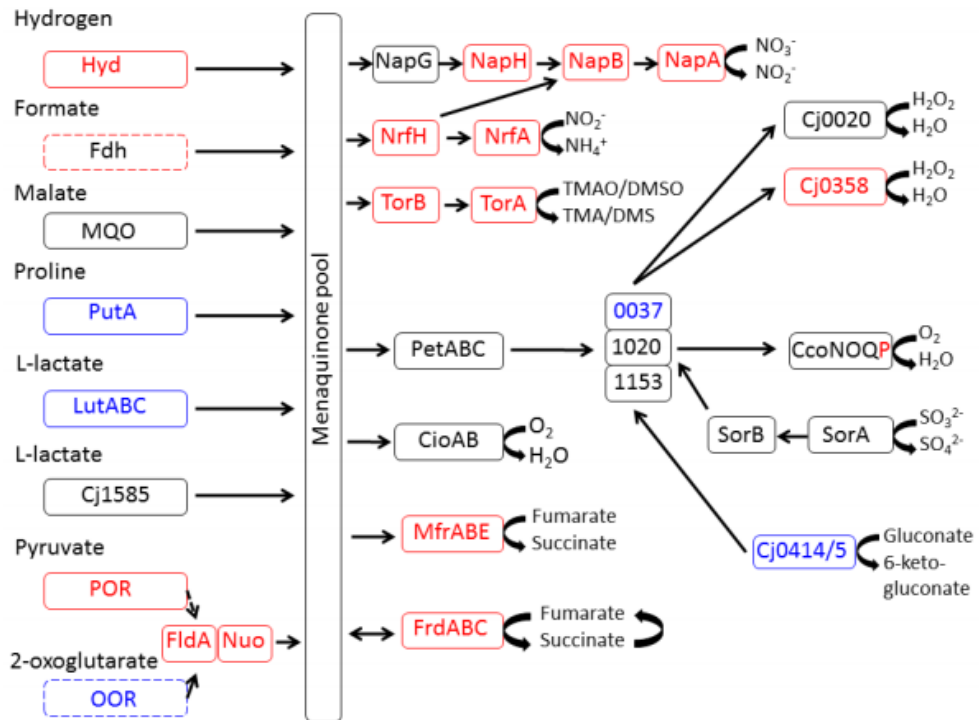


Figure 1.2 C. jejuni electron donors and acceptors. Pathways show the range of alternative electron donors utilized. Pathways in red are upregulated during oxygen limitation. Blue pathways are upregulated in the presence of oxygen (Diagram taken from Guccione et al. 2017)

Campylobacter jejuni utilises a range of alternative electron donors to oxygen and therefore has a highly branched electron transport chain as seen in Figure 1.2. Under anaerobic or aerobic metabolism *E. coli* utilises menaquinone or ubiquinone, respectively as the electron carrier in the ETC. However, *C. jejuni* relies entirely on menaquinone which is synthesised via a futasoline pathway yielding MQ with a C30 prenyl side chain (Li et al., 2011). As mentioned previously pyruvate and 2-oxoglutarate:acceptor oxidoreductases (Por and Oor) are responsible for the oxidative decarboxylation of intermediates in the TCA cycle to acetyl-coenzyme A (acetyl-CoA) and succinyl-CoA, respectively. POR and OOR also reduce flavodoxin (FldA) and direct electron flow to the Nuo complex. Label-free proteomics has revealed insights into the gene regulation patterns of important ETC genes seen in figure 1.2 (Guccione et al., 2017). Molecular oxygen is the preferred terminal electron acceptor and is utilised by the CioAB and CcoNOQP complexes (Sellars et al., 2002).

1.3.4 *C. jejuni* Carbon Sources – transport and metabolism

Amino acids are the primary nutrient and carbon source for *C. jejuni*. Serine, aspartate, asparagine, glutamate and proline are the preferred amino acids, in that order and their respective transport pathways can be visualised in Figure 1.3. Interestingly serine, glutamate, aspartate and proline are readily found in chick excreta possibly explaining why these amino acids are central in *C. jejuni* metabolism (Parsons, 1984). Serine is particularly favoured and can be utilised by the action of SdaC, a serine transporter and SdaA an L-serine dehydratase (Velayudhan et al., 2004). SdaC is a high capacity, low affinity transporter with the ability to transport other amino acids such L-threonine. However SdaC is essential for serine uptake as shown in a SdaC deficient strain (Velayudhan et al., 2004). Deletion of either *sdaA* or *sdaC* also completely impairs the ability of *C. jejuni* to colonise chicks however does not prevent growth *in vitro* suggesting serine is not essential for growth (Velayudhan et al., 2004). Once in the cell serine can be deaminated to pyruvate which is then used as an energy source for the CAC after decarboxylation to acetyl-CoA (Gao et al., 2017). The Peb1 system in *C. jejuni* is responsible for both aspartate and glutamate uptake. The Peb1a protein is a periplasmic protein which mediates epithelial cell adhesion as well as acting as a periplasmic binding protein binding both L-aspartate and L-glutamate (Fauchère et al., 1989; Leon-Kempis et al., 2006). A Peb1a deficient strain was completely impaired for L-glutamate uptake however some residual L-aspartate uptake was detected. The C4-dicarboxylate transporters (DctA, DcuA and DcuB) have been suggested to be an alternative route for L-aspartate uptake however without an intact Peb1 system the C4-dicarboxylate transporters do not permit growth on L-aspartate (Leon-Kempis et al., 2006). Within the cell glutamate can be transaminated by AspB to produce aspartate and 2-oxoglutarate in a reversible reaction. The aspartate can then be deaminated by aspartase AspA to fumarate for use in the citric acid cycle (Guccione et al., 2008). Proline uptake has been associated with proteins PutP and PutA. PutP is predicted to be the major proline permease and then PutA is responsible for the oxidation of L-proline to L-glutamate (Parkhill et al., 2000). PutA and PutB are both upregulated during stationary phase when other nutrient sources become limited; this upregulation coincides with a decline in L-proline levels *in vitro* (Wright et al., 2009). Currently an asparaginase gene (*ansB*) but no asparagine transporter has been identified in *C. jejuni*. For this reason many strains are unable to grow on asparagine however some strains including 81-176 possess an *ansB* gene with a Sec-dependent secretion signal peptide allowing transport of the asparaginase to the periplasm where it can deaminate periplasmic asparagine to aspartate (Hofreuter et al.,

2008). It is generally accepted that glutamine cannot be utilised as a primary carbon source and does not support growth in the majority of *C. jejuni* strains due to the absence of a γ -glutamyltranspeptidase (GGT). However, two glutamine uptake systems have been annotated. One has not been studied experimentally but has homology to widely distributed glutamine ABC transport system GlnPQ from other bacterial species. The other system is proposed by Lin et al., (2009), as the PaqPQ system, encoded by the genes *cj0467* (*paqP*), *cj0468* and *cj0469* (*paqQ*). PaqPQ is suggested to be responsible for glutamine uptake in a GGT independent manner. Lin et al. (2009) report that a $\Delta paqQ$ mutant was defective in the uptake of glutamine, glutamate, cysteine and aspartate. The reduction in uptake was most significant in glutamine although some residual glutamine transport was still observed. They speculate that the residual uptake could be due to a redundant mechanism for glutamine transport existing in the genome such as *cj0940c* and *cj0902* which are annotated *glnP* and *glnQ*, respectively. These findings are supported by observations that a *ggt* mutant can reach higher OD_{600nm} when grown on DMEN plus glutamine compared to DMEM alone (Stel et al., 2015). Based on these observations one current hypothesis is that when other carbon sources are present PaqPQ most likely imports glutamine and the role of GGT may be of greater importance when other energy sources than glutamines are unavailable.

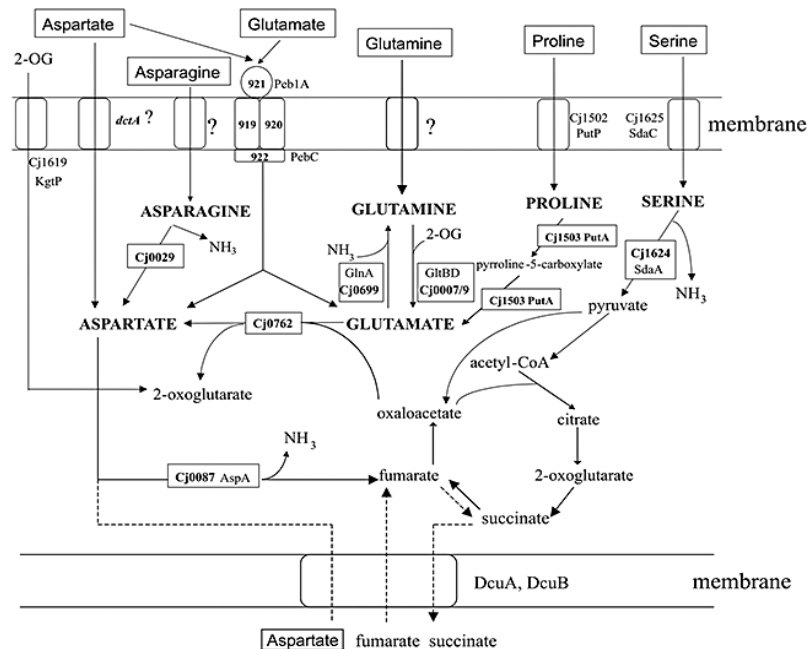


Figure 1.3 Amino acid transport pathways in *C. jejuni* NCTC11168. Pathways have been depicted based on annotated genes (Parkhill et al., 2000) and biological data. Dotted lines indicated pathways of importance under oxygen limited conditions. Glutamine transport is yet to be conclusively determined however the PaqPQ system is the current published transport which has been associated with glutamine transport. Pyruvate can also enter the cyclic acid cycle from anaplerotic reactions not shown here. Diagram taken from Guccione et al., 2008.

1.3.5 Nitrogen Metabolism

Nitrogen is essential for the synthesis of amino acids, pyrimidines and purines, NAD and amino sugars. Typically, gram-negative organisms use ammonia as an inorganic nitrogen compound when growing aerobically and nitrate or nitrite when growing anaerobically (Reuse & Skouloubris, 2001). Ammonia is crucial in nitrogen anabolism and assimilation. Ammonia can often be transported directly into the cell or can be generated by the deamination of amino acids (Reuse & Skouloubris, 2001). Glutamine and glutamate typically constitute the central reservoir of nitrogen in bacteria and their synthesis is regulated by the GS-GOGAT pathway (Figure 1.4). Glutamine synthetases (GS) catalyse the incorporation of ammonia into glutamate to produce glutamine, at the expense of one ATP molecule. Glutamate synthase (GOGAT) can then convert glutamine back to glutamate with the addition of 2-oxoglutarate. In energy limiting conditions a glutamate dehydrogenase (GDH) can synthesise glutamate directly by the amination of 2-oxoglutarate. The enzyme γ -glutamyl transpeptidase (GGT) is present in prokaryotes and is secreted into the periplasm of gram-negative bacteria where it hydrolyses either glutamine to glutamate and ammonia, or glutathione to glutamine and a γ -glutamylcysteine (Shibayama et al., 2007). This allows bacteria to utilize glutamine and glutathione as a source of amino acids. *C. jejuni* NCTC11168 has a functional GS:GOGAT system however GDH and GGT are absent. Therefore, NCTC11168 cannot utilise glutamine as a primary carbon source. Interestingly the GGT activity is present in other *C. jejuni* strains and Barnes et al. (2007) suggest the prevalence of *ggt* to be as low as 19.4% amongst a large strain collection. Examples of strains with an intact *ggt* gene are 81-176 and 81116. *In vitro* the deletion of *ggt* does not result in any growth abnormalities however in strain 81-176 it impairs colonisation of MyD88^{-/-} deficient mice and in 81116 GGT activity is required for persistent colonisation of the avian gut (Barnes et al., 2007; Hofreuter et al., 2008). Despite this strains like 11168 are perfectly capable of colonising its hosts and therefore must be compensated by the presence of alternative metabolic pathways such as the recently identified fucose acquisition and metabolic pathway (Stahl et al., 2011). Glutamine clearly plays a pivotal role in the assimilation of nitrogen as discussed. However, in *C. jejuni* this role could be even more critical as the ammonium transporter gene *amt* (*Cj0501*) appears to have at least one frameshift which likely renders the gene non-functional and thus a pseudogene (Parkhill et al., 2000). With no known ammonium transporter in the genome, glutamine which is readily available in the colon could potentially be the key source of nitrogen for *C. jejuni*.

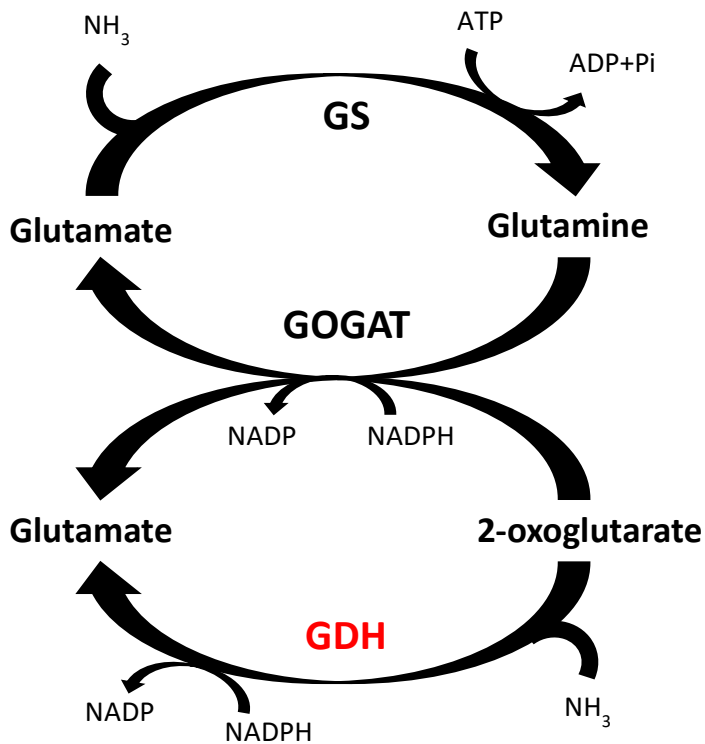


Figure 1.4 Nitrogen metabolic circuit in enteric bacteria. Glutamate can be converted to glutamine and nitrogen assimilated in the process in a reaction catalyzed by GS. Glutamate can then be synthesized by either GOGAT or GDH. GDH (red) is not present in *Campylobacter jejuni*.

1.3.6 Capnophilic growth

C. jejuni requires low environmental oxygen but also high carbon dioxide (5-10%) for optimum growth and is therefore designated a capnophile. As seen in Figure 1.2 pyruvate carboxylase requires CO₂ to catalyse the ATP-dependent carboxylation of pyruvate to yield OAA in the CAC (Velayudhan & Kelly, 2002). Bicarbonate is formed by the hydration of CO₂ and in this form is required by carboxylases such as PYC to function. Inefficient conversion of CO₂ to bicarbonate could be another factor explaining the capnophilic nature of *C. jejuni*. CanB is beta-class carbonic anhydrase present in the *C. jejuni* genome and deletion of this gene alone prevents growth at low CO₂ (1% v/v) and significantly reduces growth at high CO₂ (5% v/v). Purified CanB was also shown to only hydrate CO₂ at low affinity above pH 8 (K_m 34 mM) (Al-Haideri et al., 2016). These properties of CanB could explain the inefficient conversion of CO₂ to bicarbonate in *C. jejuni* explaining the organism's requirement for high atmospheric CO₂ concentrations.

1.4 Post-translational modification in *C. jejuni*

1.4.1 Post Translation Modifications Overview

The number of coding regions within a genome is often too low to explain the diversity of its proteome and cannot be explained by the central dogma of molecular biology. This complexity can be explained by post translational modifications. The role of post translational modifications in the regulation of many cellular processes in eukaryotes has been observed for decades. Until recently it has been assumed this level of modification is limited to higher more 'complex' organisms however, it is now generally accepted to be an important regulatory step in many bacterial processes (Cain et al., 2014). The recent improvement in mass spectrometry techniques has facilitated the high-throughput identification and quantifications of PTMs revealing an extensive array of PTMs in bacteria (Gupta et al., 2007).

1.4.2 Glycosylation

It is now widely accepted that glycoproteins are a common feature in eukaryal, archael and bacterial domains. The role of N-linked glycosylation of periplasmic proteins in immune cell evasion was briefly discussed earlier. A gene cluster in *C. jejuni* has been identified and denoted as the *pgl* locus for protein glycosylation (Szymanski et al., 1999). Since then, greater than 30 potential glycoproteins have been identified in *C. jejuni* and are thought to be modified with a glycan on an asparagine residue in the motif Asn-Xaa-Ser/Thr as seen in eukaryotes (Young et al., 2002). In comparison O-linked protein glycosylation is restricted to the flagellin in *C. jejuni*. Pseudaminic or legionaminic acid derivatives are attached to serine and threonine residues in the central domain of the flagellin protein accounting for up to 10% of the total mass (Szymanski et al., 2003). This modification is surface exposed. The role of glycosylation in *C. jejuni* remains elusive however it has been suggested that glycosylation could be a mechanism to generate antigenic diversity for immune evasions and/or in the function and assembly of polar flagellin (Schirm et al., 2003).

1.4.3 Acetylation

Protein acetylation in bacteria is carried out by N-acetyl transferase enzymes which transfer acetyl groups (CH₃CO) from acetyl-CoA to amino groups of proteins and small molecules. There are two modes of acetylation; N α -acetylation and N ϵ -acetylation. Typically, N α -acetylation is an irreversible signal for protein degradation and N ϵ -acetylation of lysyl

residues usually effects protein activity (VanDrisse & Escalante-Semerena, 2019). Nε-acetylation of lysyl residues is reversible by protein deacetylases allowing for rapid regulation and response to the environment. Acetylation was initially discovered in eukaryotes as a mode of transcription regulation. The acetylation of histones was shown to remove their positive charge and block interactions with the DNA backbone resulting in the relaxation of DNA providing access for the transcription machinery (Sterner & Berger, 2000). Since then, data has been published on over 50 bacterial acetylomes including *E. coli* (Christensen et al., 2019; Yu et al., 2008). Recent work has shown that over 70% of all proteins in *C. jejuni* are acetylated and a specific deacetylase could be responsible for the regulation of this modification (Puttick et al, unpublished).

1.4.4 Bacterial Protein Phosphorylation

In 1979 isocitrate dehydrogenase was the first bacterial protein to clearly show Ser/Thr/Tyr phosphorylation (Garnak & Reeves, 1979). Protein phosphorylation is the covalent attachment of a phosphate group to the functional groups of amino acid side chains. Phosphorylation commonly takes place on the hydroxyl groups of serine and threonine and less commonly on the phenol-based side chain of tyrosine, 69.5%, 21.8% and 7.7% respectively (Lin et al., 2015). However, phosphorylation has also been observed on His, Arg, Lys, Asp, Glu and Cys *in vivo* (Cain et al., 2014). Phosphorylation is orchestrated by specific kinases and phosphatases which recognise short consensus sequences within a protein structure (Kennelly & Krebs, 1991). Protein kinases covalently modify specific proteins by the attachment of a γ-phosphoryl group of a nucleoside triphosphate onto an amino acid hydroxyl group inducing a conformational change from an inactive to active form. Protein phosphatases reverse this covalent reaction converting the substrate back to its dephosphorylated state.

1.4.5 Two Component Systems

Serine, threonine and tyrosine residues can be modified by both bacteria and eukaryotes however, bacteria also possess two component systems (TCS). TCS rely on specific signals to activate the autokinase activity of the sensory kinase allowing the subsequent phosphotransfer of the phosphate group to an aspartate residue of a cognate response regulator. This response regulator is capable of eliciting an appropriate cellular response. Often the aspartate response regulator functions as a transcription factor capable of DNA

binding and transcriptional regulation. A feature of TCS unlike other modes of protein phosphorylation is the high fidelity between the sensory kinase and response regulator during phosphotransfer (Laub & Goulian, 2007). TCS are found in nearly every sequenced bacterial genome with some encoding up to 200 different systems. These pathways respond to a wide range of stimuli including nutrient status, osmolarity, antibiotics and quorum sensing.

1.4.6 Serine/Threonine Phosphorylation

Serine and threonine phosphorylation in bacteria is predominantly carried out by Hanks type kinases also known as eukaryotic-like Ser/Thr kinases (eSTK) (Kobir et al., 2011). A small subset of serine/threonine phosphorylation is performed by atypical bi-functional kinases/phosphorylases which do not exhibit any sequence similarity to eukaryotic protein kinases. For example, the *Escherichia coli* isocitrate dehydrogenase kinase/phosphatase (AceK) enzyme that can phosphorylate and dephosphorylate isocitrate dehydrogenase (ICDH) (Zheng & Jia, 2010). ICDH is involved in the regulation of the glyoxylate bypass within the Krebs cycle, an anaplerotic pathway which permits growth on substrates such as acetate (Kornberg, 1966). Many phosphoproteomic studies in a range of bacterial organisms have now identified a large number of proteins phosphorylated on serine and threonine residues. However very little is understood about the functional significance of Ser/Thr phosphorylation. eSTKs can be characterised by conserved motifs and their two-lobed structure composed of an N-terminal β -sheet lobe and a larger C-terminal lobe composed of α -helices (Hanks et al., 1988). eSTKs have been associated with a broad range of bacterial processes. For example, due to their remarkable structural homology with eukaryotic kinases eSTKs are associated with virulence via the phosphorylation of host signalling proteins (Cain et al., 2014). Other functional roles include the regulation of cell shape and division as seen by PknA and PknB in *Corynebacterium glutamicum* (Fiuza et al., 2008).

Protein phosphatases that specifically dephosphorylate phospho-serine or phospho-threonine belong to two families the PPM (Mg^{2+}/Mn^{2+} dependent) or PPP family (Deutscher & Saier, 2006). These eukaryotic-like serine/threonine phosphatases (eSTP) can directly dephosphorylate both eSTKs and eSTK substrates. Similar to tyrosine phosphorylation eSTPs and eSTKs can be paired and co-transcribed in the genome however, there is often

far fewer eSTPs than eSTKs in bacterial genomes (Dworkin, 2015). For example, *Mycobacterium tuberculosis* possesses 11 known eSTKs but only 1 eSTP (Av-Gay & Everett, 2000). Interestingly *M. tuberculosis* also possesses 11 TCS (Prisic et al., 2010), this potentially suggests these two modes of phospho-signalling may be biologically linked (see figure 1.5). Phosphorylation via TCS causes changes in gene expression. eSTKs have also been shown to cause global changes in gene expression. It is thought eSTKs can phosphorylate non-TCS DNA binding proteins but also interact with TCS. Some evidence for this comes from the CovRS TCS from group A and B streptococci. Lin et al. (2009) report that changes in expression of genes associated with CovRS are also seen in knockout mutants for eSTK Stk. It was found that Stk could phosphorylate the response regulator of the CovR system inhibiting DNA binding. A non-TCS example of S/T phosphorylation includes GTPase elongation factor Tu (EF-Tu) observed to be phosphorylated in nearly all bacterial phosphoproteomes. PknB of *M. tuberculosis* can phosphorylate EF-Tu inhibiting protein synthesis at the ribosome.

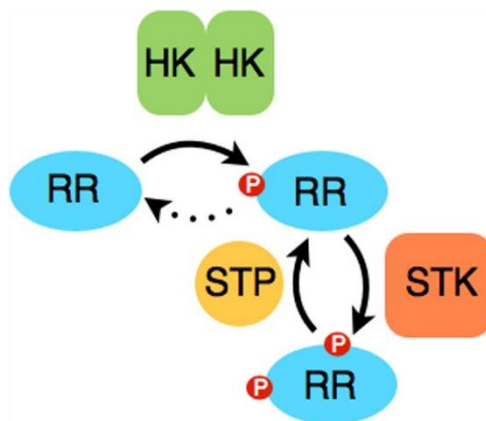


Figure 1.5 Interaction between eSTK/eSTP protein phosphorylation and TCS. Response regulators (RR; blue) can be phosphorylated by sensor histidine kinases (HK; green) on aspartate residues and then subsequently on Ser/Thr residues by Ser/Thr kinases (STK; red). This reaction is reversible by serine/threonine phosphatases (STP).

1.4.7 Tyrosine Phosphorylation

Tyrosine phosphorylation is ubiquitous among prokaryotes, catalysed by auto-phosphorylating ATP-dependent bacterial tyrosine kinases (BY-Kinase). The first example of which was discovered in *Acinetobacter johnsonii* (Duclos et al., 1996). Eukaryotic-like tyrosine phosphatases and/or low molecular weight protein tyrosine phosphatases (LMW-PTP) catalyse the dephosphorylation of tyrosine residues. Tyrosine phosphorylation is

associated with a range of cellular processes such as growth, proliferation, migration, stress response, flagellin export and polysaccharide synthesis (Whitmore & Lamont, 2012). BY-kinases and their cognate phosphatases are often found together in large operons involved in the production of exopolysaccharides (EPS) or capsular polysaccharides (CPS) such as for Wzc (BY-kinase) and Wzb (LMW-PTP) involved in the production of colanic acid in *E. coli* (Carole Vincent et al., 1999). Both EPS and CPS are important virulence factors in bacteria and hence tyrosine phosphorylation is biologically linked with bacterial pathogenicity (Cozzone et al., 2004). Some important substrates phosphorylated on tyrosine residues include flagellin a/b required for motility in *Pseudomonas aeruginosa* (South et al., 1994), as well as UDP-glucose dehydrogenase involved in the formation of precursors for acidic polysaccharide synthesis in *E. coli* (Grangeasse et al., 2003). Tyrosine phosphorylation has also been implicated in cellular localisation, for example DNA exonucleases in *Bacillus subtilis* can be phosphorylated to govern their cellular localisation (Jers et al., 2010).

BY-kinases possess a cytoplasmic catalytically active domain attached to a transmembrane domain which can function as an anchor and sensor. The BY-kinase catalytic domain lacks eukaryotic kinase motifs but can be defined by the presence of both Walker A and B motifs (Whitmore & Lamont, 2012). Autophosphorylation occurs at tyrosine rich clusters in the C-terminal region and the level of phosphorylation determines the strength of interaction between BY-kinases and their substrates (Grangeasse et al., 2007). Protein-tyrosine phosphatases possess a common catalytic mechanism involving a conserved C-aa₅-R motif in the active site within the phosphate binding loop. The active site is flanked at some distance by an essential D residue (Whitmore & Lamont, 2012). The cysteine residue in the conserved motif is essential for function and acts as a nucleophile by attacking the phosphorus atom of phosphotyrosine. This is potentially an explanation as to why mutation of this cysteine residue to serine abolishes activity against pNPP (p-Nitrophenyl Phosphate), a phosphotyrosine analogue (Ahmad et al., 2018). There are two main protein-tyrosine phosphatase families the first is the eukaryotic-like protein-tyrosine phosphatases (ePTP) and dual specific phosphatases capable of Ser, Thr and Tyr dephosphorylation. The second family are small acidic enzymes found in both eukaryotes and prokaryotes known as the low molecular weight protein-tyrosine phosphatases (LMW-PTP). The two families differ in the consensus sequence of the active site, the number of amino acid residues between the active site and the flanking D residue and finally the location of the active site along the polypeptide chain (Cozzone et al., 2004). Morona et al. (2002) have recently characterised a third class of protein-tyrosine phosphatase in *Streptococcus pneumoniae*.

They have suggested capsule biosynthesis protein CpsB to be a novel manganese-dependent phosphotyrosine-protein phosphatase belonging to the PHP (polymerase and histidinol phosphatase) family found predominantly in Gram-positive bacteria.

1.4.8 Other modes of Phosphorylation

Phospho-arginine has also been identified in bacteria with a role in protein degradation. In *Bacillus spp.* McsB has been shown to phosphorylate CtsR inhibiting its functions as a transcriptional repressor of ClpC resulting in the positive regulation of ClpC-mediated degradation (Fuhrmann et al., 2009). Phosphorylation of cysteine has also been reported in bacteria. For example, in *E. coli* phosphorylation of Cys421 of the phosphotransferase-type glucose transporter subunit IIBC is essential for the uptake of glucose as phosphorylated IIBC is a phospho- donor in the first step of glycolysis (Meins et al., 1993). Cysteine phosphorylation has also been associated with the phosphorylation of transcriptional regulators abolishing interactions with the promoters of transcriptional targets (Cain et al., 2014).

Recently Nguyen et al. (2017) have discovered a novel conserved protein kinase without any resemblance to eukaryotic counterparts. YdiB of *Bacillus subtilis* previously denoted as an ATPase is now suggested to be a member of the ubiquitous bacterial Kinase (ubK) family. This family is thought to be widespread in prokaryotes and can be identified by conserved motifs including the Walker A ATP-binding motif (SPT/S, HxDxYR, EW and Gx₄GKT). YdiB has been shown to phosphorylate Ser, Thr and Tyr residues with a HxD motif reminiscent of hanks type protein kinases. A knockout mutant suggests YdiB to have a role in sensitivity to paraquat treatment as well as a role in the chemical modification of some tRNAs. Interesting $\Delta YdiB$ cells exhibit a decrease in growth rate and altered cell morphology potentially suggesting another role in cell wall morphogenesis. YjeE a potential ubK in *E. coli* has been shown to be essential for growth under aerobic conditions suggesting a possible role in aerobic metabolism (Mangat & Brown, 2008). Finally, a potential protein tyrosine kinase lacking BY-kinase signatures has been identified in *Mycobacterium tuberculosis*. Currently no BY-kinase has been identified in *M. tuberculosis* however PtkA, previously denoted as a putative haloacid dehydrogenase has been shown to phosphorylate secreted protein tyrosine phosphatase A (ptpA) in vitro (Bach et al., 2009).

1.4.9 Phosphorylation in *Campylobacter jejuni*

The annotated 1.6 Mb genome of *C. jejuni* currently includes 15 TCS genes, two putative serine/threonine protein phosphatases, a LMW-PTP and the kinase and phosphatase for polyphosphorylation (Parkhill et al., 2000). Currently no cytoplasmic Ser, Thr or Tyr kinases have been identified and research into phosphorylation in *C. jejuni* is generally very limited. A study by Voisin et al. (2007) used mass spectrometry techniques on in-gel tryptic digests to identify 36 phosphopeptides from 1-D gel bands by nano-LC-MS/MS in *C. jejuni*. The major phosphopeptides identified were elongation factors, chaperonins, bacterioferritin and superoxide dismutase. However, the enzymes responsible for this phosphorylation still remain uncharacterised.

1.4.10 The use of mass Spectrometry in the Characterisation of Bacterial Phosphoproteomes

Mass spectrometry can be used alongside enrichment techniques such as Immobilized Metal Affinity Chromatography (IMAC) to enrich for phosphopeptides in a tryptic digest. This is a highly sensitive technique in the detection of phosphorylation sites which naturally exist at a relatively low abundance in bacteria. This method of phosphopeptide identification provides far more coverage of the phosphoproteome than traditional techniques involving 2D-gel separation, ³²P-radiolabelling and immunodetection. Gel-free phosphoproteomics has now been performed on a number of bacteria including *E. coli* (Macek et al., 2008), *Helicobacter pylori* (Ge et al., 2011) and *Bacillus subtilis* (Macek et al., 2007). Typically, in bacteria these studies identify 50-100 phosphoproteins however techniques such as methanol and chloroform precipitation of cell lysates has proved effective in the removal of inhibitors of phosphopeptide enrichment. These inhibitors include phospholipids, peptidoglycan and lipids. This pre-treatment method in *E. coli* coupled with liquid chromatography-tandem mass spectrometry (LC-MS/MS) resulted in the identification of 392 phosphoproteins (Lin et al., 2015). Alternatively, a study by Prisic et al. (2010) has shown the use of multiple growth conditions and stressors can increase the number of phosphosites identified; in this study 516 sites were discovered in 301 *M. tuberculosis* proteins. The identification of phosphopeptides in LC-MS/MS is based on a +79.9663 Da shift in the mass of a peptide ion compared to the unmodified peptide; site localization of phosphorylation on the peptide can be determined by the fragmentation pattern (Breitkopf & Asara, 2012). This shift in mass is due to the addition of a phosphate group on an amino acid side chain. Unfortunately, due to the acidic conditions during sample preparation it is not possible to extensively study acid-labile phosphoramidates such as histidine, arginine and lysine (Cieřla et al., 2011).

1.5 Project aims and objectives

The overall aim is to comprehensively characterise the *C. jejuni* phosphoproteome using Orbitrap mass spectrometry on cell free extracts of wild type and isogenic deletion mutants for kinase and phosphatase genes.

The specific objectives formulated at the start of the project included:

- Identification of putative kinases and phosphatases in *C. jejuni* NCTC 11168 using bioinformatic search techniques.
- Constructing deletion mutants of identified kinase and phosphatases in *C. jejuni* NCTC 11168 for phenotypic characterization.
- Development of gel staining and immunodetection techniques against phosphoproteins in order to identify phenotypic changes between wild type and mutant cells.
- Enrichment of cytoplasmic fractions of wildtype and mutants for phosphopeptides and use of mass spectrometry to analyse the phosphoproteome of *C. jejuni*.
- Identification of pathways linked to specific kinases and phosphatases revealing their biological role.
- Adhesion, invasion and colonisation assays with mutants to reveal *in vivo* phenotypes.

As the project developed, a possible link between phosphorylation and glutamine transport was pursued and this led to new insights into the mechanism of glutamine uptake in *C. jejuni*.

Chapter 2: Materials and Methods

2.1 Stocks and Strains

All strains were stored at -80 °C in Brain Heart Infusion (BHI) broth (Sigma) with 20% v/v glycerol. Before culture *C. jejuni* strains would be incubated overnight on Columbia agar (CA) (Sigma) before growth in culture. All strains used in this study are listed in sections 2.4 and 2.5.

2.2 Growth of *C. jejuni*

2.2.1 Routine growth of *C. jejuni*

Routine growth of *C. jejuni* NCTC 11168 was performed at 42 °C under microaerophilic growth conditions (10 % v/v O₂, 5 % v/v CO₂ and 85 % v/v N₂) in a MACS-VA500 incubator (Don Whitley Scientific Ltd, UK). Colonies were grown on Columbia agar (CA) (Sigma) containing 5 % v/v lysed horse blood and 10 mg ml⁻¹ of both amphotericin and vancomycin. Liquid cultures of *C. jejuni* were inoculated from plates in Brucella, Tryptone and Serine (BTS) broth containing 10 mg ml⁻¹ of both amphotericin and vancomycin shaking at 160 rpm. BTS broth was sterilised by autoclaving using steam autoclave (Astell).

2.2.2 Growth of *C. jejuni* in minimal media

C. jejuni was grown routinely in BTS to seed minimal media cultures. Cells were washed twice to remove all media by centrifugation at 12,000 xg at 4 °C and resuspended in minimal media. Minimal media cultures were inoculated to 0.1 or 0.01 OD_{600nm} for day or overnight growth, respectively.

Table 2.1 Batch Culture Minimal Media Formulation

Minimal Media Components (Batch)	Concentration ((mM) 5 s.f.)
Amino Acids	
L-Arginine hydrochloride	0.5972
L-Cystine 2HCl	2.0000
L-Histidine Hydrochloride-H ₂ O	0.2000
L-Isoleucine	0.3969
L-Leucine	0.3969
L-Lysine hydrochloride	0.3989
L-Methionine	1.1007
L-Phenylalanine	0.1939
L-Threonine	0.4034

L-Tryptophan	0.0490
L-Tyrosine	0.1992
L-Valine	0.3932
Sodium Pyruvate	0.2500
Vitamins	
Choline chloride	0.0071
D-Calcium pantothenate	0.0020
Folic Acid	0.0023
Niacinamide	0.0082
Pyridoxal hydrochloride	0.0049
Riboflavin	0.0003
Thiamine hydrochloride	0.0030
i-Inositol	0.0111
Vitamin B12	0.0010
Ascorbic Acid	0.1000
Inorganic Salts	
Calcium Chloride	1.8018
Magnesium Sulphate	0.8139
Potassium Chloride	5.3333
Sodium Bicarbonate	26.190
Sodium Chloride	117.24
Sodium Phosphate Monobasic	1.0145
Sodium Metabisulphite	0.0500
Ferrous Sulphate	0.0500
Sodium Molybdate	0.0050

Table 2.2 Continuous culture minimal media formulation

Minimal Media Components (Continuous)	Concentration (mM)
Amino Acids	
L-Alanine	0.2
L-Arginine hydrochloride	0.6
L-Asparagine	0.6
L-Aspartic Acid	4
L-Cystine 2HCl	2.0
L-Histidine Hydrochloride-H ₂ O	0.2
L-Isoleucine	0.4
L-Leucine	0.4
L-Lysine hydrochloride	0.4
L-Methionine	1.0
L-Phenylalanine	0.2
L-Proline	0.9
L-Serine	10
L-Threonine	0.4
L-Tryptophan	0.2
L-Tyrosine	0.2
L-Valine	0.4
Sodium Pyruvate	0.5
Vitamins	Concentration (uM)

Biotin	0.5
Calcium Chloride	5.0
D-Calcium pantothenate	2.0
Folic Acid	2.0
Niacinamide	10
Pyridoxal hydrochloride	5.0
Riboflavin	1.0
Thiamine hydrochloride	3.0
i-Inositol	11
Vitamin B12	1.0
Ascorbic Acid	100
Sodium Formate	1000
Vancomycin HCl	5.0
Inorganic Salts	Concentration (mM)
Sodium Chloride	117.2
Sodium Bicarbonate	26.2
Sodium Phosphate Monobasic	1.02
Potassium Chloride	5.3
Magnesium Sulphate	1
Sodium Metabisulphite	0.066
Ferrous Sulphate	0.050
Metals	Concentration (uM)
EDTA disodium .2H ₂ O	150
Boric Acid	3
Copper Sulphate	10
Zinc Chloride	5
Manganese Chloride	5
Cobalt Chloride	5
Nickel Chloride	5
Sodium Molybdate	5
Sodium Selenite	1

2.3 Growth of *E. coli*

E. coli was grown at 37 °C on Luria-Bertani (LB) (Oxoid) agar or in LB broth shaking at 200 rpm. LB media was made following manufacturers guidelines and sterilised by autoclave (Astell benchtop steam autoclave).

2.4 *E. coli* Strains used in this study

Table 2.3 *E. coli* strains used in this study in order of appearance

<i>Escherichia coli</i> strain	Genotype/Description	Source
DH5 α	F- Φ 80lacZ Δ M15 Δ (lacZYA argF) U169 recA1 endA1 hsdR17 (rK-, mK+) phoA supE44 λ - thi-1 gyrA96 relA1	Invitrogen
BL21 (DE3)	F- ompT hsdSB(rB-, mB-) gal dcm (DE3)	Invitrogen
Top10	F- mcrA Δ (mrr-hsdRMS mcrBC) Φ 80lacZ Δ M15 Δ lacX74 recA1 araD139 Δ (araleu)7697 galU galK rpsL (StrR) endA1 nupG	Invitrogen
BL21 (pET21a_Cj1258)	BL21 cells containing pET21a. C-terminal His-tagged Cj1258.	This study
BL21 (pET28a_Cj0184c)	BL21 cells containing pET21a. N-terminal His-tagged Cj0184c.	This study
BL21 (pET28a_Cj0184cE)	BL21 cells containing pET21a. N-terminal His-tagged Cj0184c (E – additional 10 amino acid extended form).	This study
BL21 (pET21a_Cj0184cNB)	BL21 cells containing pET21a. C-terminal His-tagged Cj0184c (NB - Nucleoside/nucleotide binding domain only).	This study
BL21 (pET-21a_Cj0184cPPP)	BL21 cells containing pET21a. C-terminal His-tagged Cj0184c (PPP – protein phosphatase domain only).	This study
BL21 (pET21a_Cj0817)	BL21 cells containing pET21a. C-terminal His-tagged Cj0817.	This study

2.5 *C. jejuni* Strains used in this study

Table 2.4 *C. jejuni* strains used in this study in order of appearance

<i>C. jejuni</i> strain	Description	Antibiotics	Plasmid	Source
Wild-type 11168	Human clinical isolate (genome sequenced)	Amphotericin B and Vancomycin	-	Parkhill et al., 200
11168Δ1258	11168 cj1258::kan	Amphotericin B, Vancomycin and Kanamycin	pGEM3Zf	This study
11168Δ0184c	11168GS cj0184c::kan	Amphotericin B, Vancomycin and Kanamycin	pGEM3Zf	This study
11168Δ0846	11168 cj0846::kan	Amphotericin B, Vancomycin and Kanamycin	pGEM3Zf	This study
11168Δ0184c+0184c	11168 cj0184c::kan/ cj0184c metK complement	Amphotericin B, Vancomycin, Kanamycin and chloramphenicol	pGEM3Zf pC46 (metK)	This study
11168Δ0901-0902	11168 cj0901-0902::kan	Amphotericin B, Vancomycin and Kanamycin	pGEM3Zf	This study
11168Δ0469	11168 cj0469::cat	Amphotericin B, Vancomycin and Chloramphenicol	pGEM3Zf	This study
11168Δ0901-0902Δ0467-0469	11168 cj0901-0902::kan, cj0467-0469::cat	Amphotericin B, Vancomycin, Kanamycin and chloramphenicol	pGEM3Zf	This study
11168Δ0903c	11168 cj0903c::kan	Amphotericin B, Vancomycin and Kanamycin	pGEM3Zf	This study

11168Δ0935c-0934c	11168 cj0935c- 0934c::hyg	Amphotericin B, Vancomycin and Hygromycin	pGEM3Zf	This study
11168Δ0552-0554	11168 cj0552-0554::apr	Amphotericin B, Vancomycin and Hygromycin	pGEM3Zf	This study
11168Δ0903c+0903c	11168 cj0903c::kan/ cj0903c metK complement	Amphotericin B, Vancomycin, Kanamycin and chloramphenicol	pGEM3Zf pC46 (metK)	This study
11168Δ0901-0903c Δ0467-0469	11168 cj0901- 0903c::kan, cj0467-0469::cat	Amphotericin B, Vancomycin, Kanamycin and chloramphenicol	pGEM3Zf	This study
11168Δ0903cΔ0817	11168 cj0903c::kan, cj0817::cat	Amphotericin B, Vancomycin, Kanamycin and chloramphenicol	pGEM3Zf	This study
11168Δ0817	11168 cj0817::cat	Amphotericin B, Vancomycin and Chloramphenicol	pGEM3Zf	This study
11168Δ0467-0469	11168 cj0467-0469::cat	Amphotericin B, Vancomycin and Chloramphenicol	pGEM3Zf	This study
11168Δ0940c	11168 cj0940c::apr	Amphotericin B, Vancomycin and Apramycin	pGEM3Zf	This study
11168Δ0940c+0940c	11168 cj0940c::apr/ cj0940c metK complement	Amphotericin B, Vancomycin, Apramycin and chloramphenicol	pGEM3Zf pC46 (metK)	This study

2.6 Antibiotics

Antibiotics were dissolved in distilled water and passed through a 0.45 µm filter. A few drops of 10 M NaOH was added to the water help dissolve amphotericin B and ethanol was used instead of water to dissolve chloramphenicol. Stocks were made at 1000x concentration and used at the following concentrations.

Table 2.5 Antibiotic concentrations used in this study

Antibiotic	Working Concentration (µg ml⁻¹)
Vancomycin	10 µg ml ⁻¹
Amphotericin B	10 µg ml ⁻¹
Kanamycin	50 µg ml ⁻¹
Chloramphenicol	20 µg ml ⁻¹
Carbenicillin	50 µg ml ⁻¹
Apramycin	50 µg ml ⁻¹
Hygromycin	100 µg ml ⁻¹

2.7 DNA Manipulation

2.7.1 Isolation and purification of DNA

The GenElute (Sigma) genomic extraction kit was used to for genomic DNA extraction. Plasmid DNA was purified using the QIAprep miniprep kit (Qiagen) and the QIAquick PCR purification kit (Qiagen) was used to clean up PCR products and DNA gel extractions. All kits were used according to manufacturer's instructions.

2.7.2 Polymerase Chain Reaction

High fidelity cloning was performed in 20 µL reactions using Phusion (Thermo) polymerase. MyTaq (Bioline) was used for the screening of mutants in a 12.5 µL reaction. Both reactions were performed using primers purchased from Sigma. The PCR reactions were performed in 0.2 µL PCR tubes in a Proflex PCR system (Applied Biosystems). The reaction components and PCR conditions are shown below.

Table 2.6 PCR reaction mix

Component	Phusion PCR Volume (μL)	MyTaq PCR Volume (μL)
2x Polymerase	10	6.25
Forward Primer (10 μM)	1	0.5
Reverse Primer (10 μM)	1	0.5
Template DNA (10 ng)	1	1/Colony
dH ₂ O	7	3.75/4.75

Table 2.7 PCR reaction steps

Step	Temperature ($^{\circ}\text{C}$)	Time (min/sec)	Cycles
Initial Denaturation	98	1min	1
Denaturation	98	10sec	30
Annealing	55	10sec	
Extension	72	1min kb ⁻¹	
Final Extension	72	5min	1
Hold	10	-	-

2.7.3 Primers used in study

Table 2.8 Primers used to construct mutants and expression vectors

<i>C. jejuni</i> 11168 mutant primers (knockout)	
ISA1258F1	GAGCTCGGTACCCGGGGATCCTCTAGAGTCCACTTATAGAAGCCGT AGAAA
ISA1258R1	AAGCTGTCAAACATGAGAACCAAGGAGAATTTGCCTAAGCATATAA AGAGTA
ISA1258F2	GAATTGTTTTAGTACCTAGCCAAGGTGTGCCTTATAAAATTTTATCC CTAGCTT
ISA1258R2	AGAATACTCAAGCTTGCATGCCTGCAGGTCTGAAGTTATCAGCTAT AGCAG
ISA0668F1	GAGCTCGGTACCCGGGGATCCTCTAGAGTCATACTCATCTTGAAGC CATT
ISA0668R1	AAGCTGTCAAACATGAGAACCAAGGAGAATAACACCTTCTTTAGGC ATT

ISA0668F2	GAATTGTTTTAGTACCTAGCCAAGGTGTGCAATTAGCATTAAAGAT GACAAA
ISA0668R2	AGAATACTCAAGCTTGCATGCCTGCAGGTCAACTTAGGTTACACACAT CAAG
ISA0184cF1	GAGCTCGGTACCCGGGGATCCTCTAGAGTCTTGCTCAAGATGTAAC CAT
ISA0184cR1	AAGCTGTCAAACATGAGAACCAAGGAGAATTTGCCTGCGTAATAA TTC
ISA0184cF2	GAATTGTTTTAGTACCTAGCCAAGGTGTGCTACGCGTAGTTACACTA GATG
ISA0184cR2	AGAATACTCAAGCTTGCATGCCTGCAGGTACGCTCTCATACTGCAT TA
ISA0846F1	GAGCTCGGTACCCGGGGATCCTCTAGAGTCTTTAAGACGGATAACA AAGG
ISA0846R1	AAGCTGTCAAACATGAGAACCAAGGAGAATTAACATTTGCTAAGC CAA
ISA0846F2	GAATTGTTTTAGTACCTAGCCAAGGTGTGCCTCCGAGTGAAATAGT GATT
ISA0846R2	AGAATACTCAAGCTTGCATGCCTGCAGGTGCGACTCCACTTGTGTAA GT
ISA0467F1	GAGCTCGGTACCCGGGGATCCTCTAGAGTCATTATCCTGCTAATGCT GTT
ISA0467R1	AAGCTGTCAAACATGAGAACCAAGGAGAATCAGGAGCTTGAGCTA ATATAA
ISA0467F2	GAATTGTTTTAGTACCTAGCCAAGGTGTGCTTGTATGGGATATTT ATGC
ISA0467R2	AGAATACTCAAGCTTGCATGCCTGCAGGTGCGATGCACTTTCATACTG ATG
ISA0469F1	GAGCTCGGTACCCGGGGATCCTCTAGAGTCGTAAGTGCAGCTATTA TTGTTTT
ISA0469R1	AAGCTGTCAAACATGAGAACCAAGGAGAATGATGCGAACCATAAAT ACTTT
ISA0469F2	GAATTGTTTTAGTACCTAGCCAAGGTGTGCCGAAAGAGCAAAGAAA TTT

ISA0469R2	AGAATACTCAAGCTTGCATGCCTGCAGGTCGACAACAAAACTCTT AAATGG
ISA0901F1	GAGCTCGGTACCCGGGGATCCTCTAGAGTCTAAGATTCATCATAACC TTCAAA
ISA0901R1	AAGCTGTCAAACATGAGAACCAAGGAGAATTTTTAATATTTCTATC GGGAA
ISA0901F2	GAATTGTTTTAGTACCTAGCCAAGGTGTGCAAACCTGAACTTAGGA TGAATAA
ISA0901R2	AGAATACTCAAGCTTGCATGCCTGCAGGTCTGAAGTAGGTTCATCA AATAAA
ISA0902F1	GAGCTCGGTACCCGGGGATCCTCTAGAGTCTTACTTTTATAGACAAC CTTTATGC
ISA0902R1	AAGCTGTCAAACATGAGAACCAAGGAGAATATAGCTATTACATCGC CTTTT
ISA0902F2	GAATTGTTTTAGTACCTAGCCAAGGTGTGCAGATTGAGAGAATTTTT AAACAA
ISA0902R2	AGAATACTCAAGCTTGCATGCCTGCAGGTCCAGTTTTAATTGATGTT GTTGT
ISA0940cF1	GAGCTCGGTACCCGGGGATCCTCTAGAGTCTTGGTTGCAAGTTTAA ATATAG
ISA0940cR1	AAGCTGTCAAACATGAGAACCAAGGAGAATTCTATCAAAGTCAAAA ATAATCAC
ISA0940cF2	GAATTGTTTTAGTACCTAGCCAAGGTGTGCACATATCTTGTTTTGAC TTTACC
ISA0940cR2	AGAATACTCAAGCTTGCATGCCTGCAGGTCAAGACTCGAACTTATG ACATC
ISA0817F1	GAGCTCGGTACCCGGGGATCCTCTAGAGTCAAGATGGAAGCTATTC TAAAGA
ISA0817R1	AAGCTGTCAAACATGAGAACCAAGGAGAATGCACTCAAATTTAAAG CAA
ISA0817F2	GAATTGTTTTAGTACCTAGCCAAGGTGTGCGACATTAAGAAGTTTT TAAGCA
ISA0817R2	AGAATACTCAAGCTTGCATGCCTGCAGGTCAAAGAATTACTAAGG CTGTTC

ISA0903cF1	GAGCTCGGTACCCGGGGATCCTCTAGAGTCATAGGTAGAATGTGCT TTAATG
ISA0903cR1	AAGCTGTCAAACATGAGAACCAAGGAGAATAATATCAGACGCTTTA TTGG
ISA0903cF2	GAATTGTTTTAGTACCTAGCCAAGGTGTGCTTAATGCTAGCAA ACTTGG
ISA0903cR2	AGAATACTCAAGCTTGCATGCCTGCAGGTCAAATTACTTCTGCTAA GGTG
ISA0903cF2 (antisense strand)	GAATTGTTTTAGTACCTAGCCAAGGTGTGCTTATTAGCTATAATAT CAGACGC
ISA0903cR2 (antisense strand)	AGAATACTCAAGCTTGCATGCCTGCAGGTCAAATTCATATTGTTAA ACCAA
ISA0552F1	GAGCTCGGTACCCGGGGATCCTCTAGAGTCAATTGCCAATTTATGG ATAC
ISA0552R1	AAGCTGTCAAACATGAGAACCAAGGAGAATAAACAATCAAAGGTA TAGAAGC
ISA0554F2	GAATTGTTTTAGTACCTAGCCAAGGTGTGCATATAGAAGATGATTA TCTTGGG
ISA0554R2	AGAATACTCAAGCTTGCATGCCTGCAGGTCCATAATTTATAGCCATA GCTCC
ISA0935cF1	GAGCTCGGTACCCGGGGATCCTCTAGAGTCAAGGATTTGCGTAAAG TG
ISA0935cR1	AAGCTGTCAAACATGAGAACCAAGGAGAATTACCGCTAAAATGAA ACC
ISA0934cF2	GAATTGTTTTAGTACCTAGCCAAGGTGTGCATTGTTTTATATCGCC TATAG
ISA0934cR2	AGAATACTCAAGCTTGCATGCCTGCAGGTCCGATCCATTAAGG TAATAGC
Kan cassette F	ATTCTCCTTGGTTCTCATGTTTGACAGCTTAT
Kan cassette R	GCACACCTTGGCTAGGTACTAAAACAATTCAT
Cat cassette F	ATTCTCCTTGGTTCTCATGTTTGACAGCTTGAATTCCTGCAGCCCGG GGG
Cat cassette R	GCACACCTTGGCTAGGTACTAAAACAATTCAGTAGTGGATCCCGGG TACC

Apr/Hyg cassette F	ATTCTCCTGGTTCTCATGTTTGACAGCTTCGTAACAAGGTAACCGT AGG
Apr/Hyg cassette R	GCACACCTTGGCTAGGTAATAACAATTCTACTTTGACTCTAGG GCC
<i>C. jejuni</i> complementation primers	
metKfwd0184c	AATATTCGTCTCACATGCGAATCTTACTTGTTTTAAGAG
metKrev0184c	AATATTCGTCTCACATGTTCTATAGAGCGTGTTAAGGT
metKfwd0903c	AATATTCGTCTCACATGAATTTAGATATTATGCTAGATTTTG
metKrev0903c	AATATTCGTCTCACATGTTTGAAAATCCTAGCAATG
metKfwd0940c	AATATTCGTCTCACATGTCTTTGTTTACTCAAAAAAATAAG
metKrev0940c	AATATTCGTCTCACATGGCTAACGAGACATTTTCTG
Protein expression primers	
NdeI1258fwd	TATATTCATATGAAAAAATACTCTTTATATGCTTAGG
XhoI1258rev	ATTTATCTCGAGTTTTGATAAAAAACAAGTAAATTT
NdeI0184cfwd	TATATTCATATGCGAATCTTACTTGTTTTAAGAG
XhoI0184crev	ATTTATCTCGAGTACACACTCAAACCTTTTTT
XhoI0184cEfw	TATATTCATATGCGAATCTTACTTGTTTTAAGAG
NdeI0184cErev	ATTTATCTCGAGTTATTTCTTTTTGTAAATTTGGT
XhoI0184cTfw	TATATTCATATGCGAATCTTACTTGTTTTAAGAG
NdeI0184cTrev	ATTTATCTCGAGCTATACACTCAAACCTTTTT
XhoI0184cNBfw	TATATTCATATGCGAATCTTACTTGTTTTAAGAG
NdeI0184cNBrev	ATTTATCTCGAGTTTGTATTTGCTTAAATTTGG
XhoI0184cPPPfw	TATATTCATATGCCAAAAAATACCAATTT
NdeI0184cPPPprev	ATTTATCTCGAGTTTCTTTTTGTAAATTTGGTTT
NdeI0817fw	TATATTCATATGAAAGATTTGGTTGTAGGAATG
XhoI0817rev	ATTTATCTCGAGCAAGAAAAAGTGATATTATTTG

2.7.4 Agarose gel electrophoresis

1% agarose was dissolved in 40 mM Tris-Acetate (pH 8), 1 mM EDTA and 0.1 µg ml⁻¹ ethidium bromide. DNA samples with 6X loading buffer (Bioline) were loaded and then separated with a constant voltage of 120V for 25 minutes. A 1kb hyperladder (Bioline) was used as a reference for band size. DNA was visualised using a Gene Flash gel documentation system (Sygene).

2.7.5 Restriction Digestion of DNA

DNA digestion was performed according to the manufacturer's instructions provided by NEB. Typically digests were incubated for 2-12 hours at 37 °C and then inactivated by incubation at 65-80 °C for 20 minutes or purification by gel extraction. Where appropriate 1 µl of rSAP (NEB) was added to the reaction for simultaneous phosphate treatment.

2.7.6 Ligation of DNA

Ligation reactions were performed in a 20 µL reaction volume containing 0.5 µL T4 ligase (Thermo), 1 µL T4 DNA ligase buffer (Thermo) and insert, vector and water up to 10 µL. DNA was quantified using a Genova Nano Spectrophotometer (Jenway) and a 3:1 insert:vector ratio was used. T4 ligase activity was inactivated by heating at 65 °C for 10 minutes.

2.7.7 DNA Sequencing

DNA and relevant primers were sent to an external sequencing service (GATC-Biotech) for sequencing. Approximately 1 kb reads were generated following GATC protocol.

2.7.8 Plasmids used in this study

Table 2.9 Plasmids descriptions

Plasmid	Description	Antibiotic resistance	Source
pGEM3ZF (-)	Cloning vector used for <i>C. jejuni</i> mutagenesis (knockout).	Amp	Promega
pJMK30	Cloning vector encoding kanamycin resistance.	Amp and Kan	Van Vliet <i>et al.</i> , 1998
pAV35	Cloning vector encoding chloramphenicol resistance.	Amp and Cat	Van Vliet <i>et al.</i> , 1998

pC46 (MetK)	Complementation vector which allows gene insertion at the cj0046 pseudogene locus in <i>C. jejuni</i> .	Cat	Gaskin <i>et al.</i> , 2007
pRRA	Complementation vector which allows gene insertion at the cj0046 pseudogene locus in <i>C. jejuni</i> .	Apr	Cameron <i>et al.</i> , 2014
pET21a (+)	Expression vector with restriction sites allowing the overexpression of proteins with a C-terminal His-tag. T7 IPTG inducible promoter.	Amp	Novagen
pET28a	Expression vector with restriction sites allowing the overexpression of proteins with a N-terminal His-tag. T7 IPTG inducible promoter.		
pBADHisA	Expression vector to over-express proteins with an N-terminal His-tag. AraBAD promoter responsible for L-arabinose inducible expression	Amp	ThermoFisher

2.8 *E. coli* mutagenesis

2.8.1 Preparation of chemically competent *E. coli*

To prepare 8ml of chemically competent *E. coli* cells an overnight culture (10 ml) was grown from glycerol or plate in LB broth shaking at 37 °C. The ON culture was seeded into fresh LB (100 ml) at 0.1 OD_{600nm} and grown in the same conditions until the culture has reached 0.6 OD_{600nm}. Cells were pelleted by centrifugation at 6000 xg for 20 minutes at 4 °C. The supernatant was discarded, and the pellet resuspended in 50 ml of RF1 buffer (100 mM KCl, 50 mM MnCl₂.4H₂O, 30 mM CH₃COOK, 10 mM CaCl₂.2H₂O, 15 % [_{v/v}] glycerol, adjusted to

pH 5.8 with 0.2 M acetic acid) and incubated on ice for 15 minutes. The cells were pelleted again by centrifugation as above and resuspended in 8 ml of RF2 buffer (10 mM MOPS, 10 mM KCl, 75 mM CaCl₂·2H₂O, 15 % [v/v] glycerol, adjusted to pH 6.8 with NaOH) and incubated for 20 minutes at 4 °C. The chemically competent cells were then stored in aliquots of 400 µl at -80 °C.

2.8.2 Transformation competent *E. coli*

10ng of plasmid DNA was added to thawed 50 µl aliquots of chemically competent cells. The cells were incubated on ice for 20 minutes, heat shocked at 42 °C for 45 seconds and returned to ice for a further 2 minutes. 750 µl of LB was then added to the cells and incubated at 37 °C for 45-60 minutes. After incubation cells were pelleted by centrifugation at 13000 rpm for 3 minutes (room temperature). Finally, cells were resuspended in 100 µl of LB and spread onto selective LB agar. Plates were incubated overnight at 37 °C and transformants selected by colony PCR.

2.9 *C. jejuni* mutagenesis

2.9.1 HiFi DNA assembly mutagenesis

Mutant vectors were constructed with pGEM3ZF as the backbone, flanking regions of the gene of interest (GOI) and an appropriate antibiotic cassette. The mutant vectors were transformed into *C. jejuni* where the flanking regions of the GOI performed a double crossover with homologous regions in the genome replacing the GOI with a resistance cassette. The flanking regions were approximately 500 bp upstream and downstream of the GOI. These regions were amplified from *C. jejuni* NCTC11168 genomic DNA using primers with adapters homologous to the ends of HincII linearised pGEM-3ZF or the resistance cassette. The resistance cassettes were also amplified using PCR, the template DNA was selected from section 2.7.8 dependent on the selection required. pGEM3ZF was linearised with HincII according to the manufacturers protocol. The 4 components mentioned above were combined in a HiFi DNA assembly reaction containing 2.5 µl 2x master mix, 12.5 ng of HincII linearised pGEM3ZF, a 2.5 µl mix of resistance cassette at a 2:1 and flanking DNA regions at a 4:1 ratio (cassette:pGEM3ZF, Flanking region:pGEM3ZF). This 5 µl reaction was then incubated at 50 °C for 1 hour in a thermocycler before immediate transformation or storage at -20 °C.

2.9.2 Complementation Vector Construction

The construction of complementation vectors was based on the pRRA/H and PC46 systems. The GOI including the promoter region for native promoter expression or excluding the promoter for constitutive expression was amplified by PCR with restriction site adapters. Both the amplified insert region and appropriate backbone were digested before ligation according to sections 2.7.5 and 2.7.6.

2.9.3 Preparation of chemically competent C. jejuni

C. jejuni NCTC11168 were grown for 24 hours on a nonselective blood agar plate. Cells were harvested from plate into 1 ml of wash buffer (15% v/v glycerol, 9% w/v sucrose) and pelleted by centrifugation at 12,000 xg for 5 minutes at 4 °C. The supernatant was discarded, and the resuspension and centrifugation step repeated 2 further times for a total of 3 washes. After the final wash the pellet was resuspended in 300 μ l of wash buffer and split into 3 100 μ l aliquots for immediate use or storage at -80 °C.

2.9.4 Transformation of competent C. jejuni

Plasmid DNA (~2000 ng) was added to an aliquot of competent *C. jejuni* cells. The cells plus plasmid DNA were transferred into prechilled electroporation cuvettes (Cell Projects 2mm gap - red). Using a BioRad Electroporator the cells were shocked at 2.5 kV and returned to ice. 100 μ l of BHI broth was added to the cells and the suspension was plated on a non-selective blood agar plate and incubated overnight. Cells were then harvested and resuspended in 300 μ l of BHI broth and 100 μ l aliquots were plated onto selective blood plates and incubated for 2-4 days until colonies appear. Colonies could then be screened using PCR before being stocked in glycerol and stored at -80 °C.

2.10 Protein Work

2.10.1 Cell free extracts

Cells were harvested by centrifugation and resuspended in buffer (500 mM NaCl, 20 mM NaPO₄, 20 mM C₃N₂H₄). Approximately 30 ml suspensions were then lysed using a French press (SIM Aminco) or by 4 x 20 sec sonication at 16 amplitude using a Soniprep 150 ultrasonic disintegrator (SANYO). Cell debris was then removed by centrifugation at 12,000 xg for 2 x 10 minutes at 4 °C. The supernatant containing the cell free extract was transferred to a fresh falcon tube between spins. After the final centrifugation the remaining supernatant was passed through a 0.45 μ m filter and immediately used or stored at -80 °C.

2.10.2 Protein concentration determination

The Biorad assay was used to determine the protein concentration of cell free extracts. Samples were diluted in 1/5 BioRad solution at a range of concentrations and compared against BSA standards. 10 µl samples were loaded onto a 96-well plate and 190 µl of 1/5 BioRad solution was added to each well before incubation at room temperature for 5 minutes. The optical density was measured in a 96-well plate reader at 600 nm and compared against the BSA control slope ($y = Ax + B$).

For the determination of pure protein concentration following purification absorbance at 280 nm and 320 nm was measured using a Shimadzu UV-2401PC spectrophotometer. The following equation was used to calculate the protein concentration:

$$M = \text{Abs}_{280\text{nm}} - \text{Abs}_{320\text{nm}} / \epsilon$$

M = Molar concentration

ϵ = Extinction coefficient (Derived from the complete amino acid sequence using the Expasy ProtParam service (<http://web.expasy.org/protparam/>)).

2.10.3 SDS-Polyacrylamide gel electrophoresis

12% SDS-polyacrylamide gels (1.00mm) were used with mini- PROTEAN II gel apparatus (Bio-Rad) to resolve the protein samples by SDS- PAGE. Prepared gels were immersed into a tank with freshly diluted 1x SDS running buffer (0.25 M Tris-HCL, 1.92 M Glycine pH 8.3, 1% SDS). Protein Samples (20ug) were mixed at a 1:1 ratio with 2X sample loading buffer (1M Tris HCL pH 6.8, 2% SDS, 10% glycerol, 0.02% bromophenol blue, 1/20 β -mercaptoethanol) and heated for 10 minutes at 100°C. Samples (20µl/20ug) were loaded onto gels with 5ul of EZ-Run Protein Ladder and run for 30 minutes at 80 volts followed by 160 volts for 40 minutes. Gels were then stained with Coomassie Blue (2.5 g Coomassie Blue R250, 200ml methanol, 720ml H₂O, 80ml acetic acid) for 1-2 hours. Gels were destained with multiple doses of destain (20% methanol, 8% glacial acetic acid, 72% dH₂O) for 2 hours and then left in water overnight. Gels were imaged using the Epson Perfection V550 Scanner.

2.10.4 Rapid Pro-Q Diamond Staining

Following protein separation by SDS-polyacrylamide gel electrophoresis Pro-Q diamond staining was used to visualise phosphorylated proteins. Protected from light the gel was immersed in fix solution (50% methanol, 10% acetic acid, 40% H₂O) at room temperature for 30 minutes agitating. The fixing step was repeated for a total of 1 hour and then the gel was immersed in water for 10 minutes agitating to remove methanol. This wash step was

repeated for a total of 3 washes. The gel was then immersed into 25 ml of Pro-Q diamond stain and heated in a microwave for 40 seconds and allowed to cool for approximately 7 minutes agitating at room temperature. The gel was heated for a further 20 seconds and allowed to cool for another 7 minutes before immersion in de-stain (20% acetonitrile, 50mM sodium acetate. pH 4.0) and agitation for 30 minutes repeated twice. Finally, the gel was washed once in water for 5 minutes at room temperature before visualisation using Image Lab software on a Chemidoc gel imager.

If required a SYPRO Ruby post stain could be applied in order to visualise total protein and compare against phosphorylated proteins. The gel was immersed in 25 ml of SYPRO Ruby gel and then heated in a microwave and allowed to cool at room temperature agitating. The heating and cooling steps were alternated in the following pattern; 30 sec, 30 sec, 20 sec, 5 min, 30 sec, 23 min. Finally, the gel was washed in 30 ml SYPRO Ruby wash solution for 30 minutes and then rinsed with water twice for 5 minutes before visualisation using Image Lab software on a Chemidoc gel imager.

2.10.5 Western Blotting

After separation by SDS-PAGE protein samples were transferred to a nitrocellulose membrane (Hybond-C Extra, Amersham Biosciences) in ice cold transfer buffer (25 mM Tris, 190 mM glycine, 20% [v/v] methanol) stirring using a Mini Trans-Blot Electrophoretic Cell (Bio-Rad, USA). The transfer of protein was carried out at 60 volts for 30 minutes followed by 100 volts for 1 hour. After transfer the nitrocellulose membrane was washed in 25 ml TBS (Tris-buffered saline) for 5 min at room temperature. The membrane was then incubated in 25 ml of blocking buffer (1x TBST (Tris-buffered saline with Tween[®] 20) with 5% w/v non-fat dry milk) agitating for 1 hour at room temperature. The membrane was then washed 3 times for 5 minutes each with 15 ml of TBST. The membrane and primary antibody were then incubated (at the recommended dilutions according to the product datasheet) in 10 ml primary antibody dilution buffer with gentle agitation overnight at 4°C. The membrane was washed three times for 5 min each with 15 ml of TBST. After wash the membrane was incubated with Anti-rabbit IgG, HRP-linked Antibody (1:2000) and anti-biotin, HRP-linked Antibody (1:1000–1:3000) to detect biotinylated protein markers in 10 ml of blocking buffer with gentle agitation for 1 hr at room temperature. Finally, the membrane was washed three times for 5 min each with 15 ml of TBST. 1X ECL Reagent was prepared by diluting one part 2X Reagent A and one part 2X Reagent B. The 1X ECL reagent

was then incubated with membrane for 1 minute, the excess solution removed and then visualized using Image Lab software on a Chemidoc gel imager.

2.10.6 His-tagged protein purification

An N-terminal or C-terminal his-tag could be purified by cloning a complete GOI into either L-arabinose inducible pBAD28 vector (Invitrogen) or the IPTG inducible pET21a vector (Novagen), respectively. The expression vector was then transformed in to either BL21 (DE3) cells (pET21a) or TOP10 cells (pBAD28). Overexpression strains were grown in LB containing 50 µg ml⁻¹ carbenicillin at 37 °C. Cultures were induced during the log phase (~0.6 OD_{600nm}) with either 0.002-0.2 % L-arabinose (pBAD28) or 0.2-0.4 mM IPTG (pET21a) and incubated for up to 24 hours depending on the level of expression required.

Cells were harvested by centrifugation and a cell free extract produced using a French Press (Section 2.10.1). DNase and a Protease-inhibitor cocktail was added to the cell suspension before lysis using the French Press. Cell free extracts were passed down a 5 ml HisTrap column (GE Healthcare, UK). The column was then washed in 30 ml binding buffer (500 mM NaCl, 20 mM NaPO₄, 500 mM C₃N₂H₄) and the bound fraction eluted in elution buffer over a 40 ml linear gradient. Fractions of interested were analysed by SDS-PAGE and if suitable concentrated to a final volume of 1-2 ml in Vivaspin 20 columns at 4 °C according to the manufacturers protocol (GE Healthcare, UK).

2.11 Assays

2.11.1 P-Nitrophenyl Phosphate Phosphatase Activity

The phosphatase activity of LMW-PTPs was measured by the dephosphorylation of the chromogenic substrate p-Nitrophenyl phosphate. The phosphatase activity of 1 µg of purified enzyme was measured across a range of pNPP concentrations (0.05 mM – 50 mM) in 1 ml total volume of 100 mM Tris-HCl (pH 6.5). The buffer and substrate were incubated at 37 °C and the absorbance (405 nm) was measured for 30 seconds (drift) in a Shimadzu UV-2401PC spectrophotometer. 1 µg of enzyme was added to initiate the reaction and absorbance was recorded every second until a linear rate was achieved.

2.11.2 Serine/Threonine Phosphatase Assay

The RediPlate™ 96 EnzChek® Serine/Threonine Phosphatase Assay Kit was used as a fluorescence-based assay for detecting serine/threonine phosphatase activity. The assay

was performed as described in the manufacturer's protocol using the 96- well microplate preloaded with 50 μ m 6,8-difluoro-4-methyl-umbelliferyl phosphate (DiFMUP). The reaction buffer contained 50 mM TrisHCl (pH 7.0), 0.1 mM CaCl₂, 125 μ g/ml BSA, 2 mM DTT, 200 μ m MnCl₂, and 0.05% Tween[®] 20 specifically formulated for PP-1 phosphatase activity. A control strip containing a series of DiFMU reference standards (0-5000 picomoles) was used to calculate the enzyme activity. The reaction was performed at 37 °C protected from light. Fluorescence was measured every 5 minutes for 30 minutes after the addition of 0.01-10 μ m PPase in a plate reader at excitation/emission of 358/452 nm. Background fluorescence was corrected by subtracting a PPase-negative control.

2.11.3 Thermofluor Binding Assay

In triplicate SYPRO™ Orange protein was used to measure changes in protein fluorescence after the addition of potential substrates. The 50 μ l reactions contained 5 μ m of purified protein, 500 μ m substrate, 1X SYPRO™ Orange and 1 mM sodium phosphate buffer (pH 7.4). Reactions were protected from light and measured at 280/340 nm (Excitation/emission) at every 1 °C ranging from 25°C to 95°C.

2.11.4 Disc Diffusion Assay

Overnight *C. jejuni* cells were grown to approximately mid log phase (0.6 OD_{600nm}). Lukewarm Muller Hinton agar was inoculated to 0.1 OD_{600nm} and allowed to set in plates. A sterile disc (soaked in an appropriate toxin e.g., H₂O₂) can then be placed in triplicate on each plate and incubated for 2 days. The zones of inhibition were then recorded for each strain and compared to wildtype.

2.12 Phosphoproteomics by LC-MS

2.12.1 Sample preparation

Cell free extracts were produced as described in 2.10.1 except for the following changes. The cells were harvested by centrifugation and then resuspended into a lysis buffer (100 mM Tris HCl (pH 8.5), 7 M urea, 1 mM MgCl₂, 1 mM sodium orthovanadate, 5 mM TCEP, 100 μ g/ml DNase I, PhosSTOP and pierce protease Inhibitor tablets). Samples were then sonicated as described in 2.10.1. After sonication 1% Triton X-100 was added and then samples were alkylated with 15mM iodoacetamide. Cell debris was then removed by centrifugation as described in 2.10.1. The cell free extract was then treated with benzonase (250 units) for 1 hour agitating at room temperature to remove all DNA and RNA.

2.12.2 Methanol/Chloroform precipitation

Cell pellets for LC-MS analysis were cleansed of lipids by extraction using chloroform methanol precipitation. 4 volumes of methanol, followed by 1 volume chloroform and then 3 volumes of ultrapure H₂O were added to the cell free extract. The sample was mixed intensely between each addition. The sample was then centrifuged at 12,000 xg for 5 minutes at 4 °C. The upper aqueous phase was removed and the mid-layer protein precipitate resuspended in 3 volumes of methanol. The methanol was removed by centrifugation at 14,000 xg for 5 minutes at 4 °C. The protein pellet was then air dried and stored at -80 °C or immediately processed.

2.12.3 Reduction, Alkylation and Trypsin Digestion

Air dried protein pellets were resuspending 100 mM TrisHCl (pH 8.5) plus 1% SDC. TCEP and Iodoacetamide were added to a final concentration of 5 mM and 30 mM, respectively. Trpsin (Pierce) was then added at a 1:20 ratio (w/w) and incubated overnight at room temperature.

2.12.4 Peptide desalting with sepPAK cartridges

Salt and urea were removed from digestion buffers using reverse-phase tC18 SepPak solid-phase extraction cartridges from Waters. The SepPak cartridge was selected so that the sample concentration did not exceed 5% of the packing materials weight. A vacuum manifold was used to perform the peptide desalting. The cartridge was washed with 10 ml of acitronitrile (ACN) followed by 5 ml 50% ACN 0.1% TFA. The cartridge was then equilibrated with 0.1% TFA, meanwhile samples were acidified (approximately pH 3) by adding 10% TFA to a final concentration of approximately 0.4% TFA. Samples were loaded into the cartridge 3 times before being washed with 10 ml of 0.1% TFA and then eluted slowly with 2 ml of 50% ACN 0.1% TFA. The eluted samples were then dried in a speedvac almost to completion.

2.12.5 IMAC enrichment of phosphopeptides

A 50 ul bed volume PHOS-Select resin was used for the enrichment of phosphopeptides. Desalted peptides were resuspended in 50% CAN/0.1% TFA, meanwhile the PHOS-select resin was washed in 1 ml 50% CAN/0.1% TFA by centrifugation for 30 seconds at 1000 rpm. The resin was washed 3 times and buffer completely removed after each wash. The peptide sample was transferred to the resin and incubated for 45 minutes at 700 rom in a thermomixer at 25 °C. The resin was then washed 3 times with 50% ACN/0.1 TFA, followed by 1% acetic acid and the water. The resin was then incubated in ammonia water (pH 11.3)

for 5 minutes at room temperature and eluted into a fresh Eppendorf. A second elution was performed, and the final sample neutralised with 50% formic acid and dried for analysis by LC-MS.

2.12.6 LC-MS Analysis

The enriched phosphopeptides were analysed by LC-MS in single 2h acquisitions per replicate, using an Orbitrap Elite coupled to an RSLCnano chromatography system. Data was processed using MaxQuant (Cox and Mann, 2008) and filtered to a 1 % false discovery rate (FDR) at the peptide and protein level, and phosphorylation sites were localised with a false localisation rate of 1 %. Significantly altered phosphorylation sites were identified using Perseus (Tyanova et al., 2016). All phosphorylation site data was normalised to protein abundance levels.

2.13 Chemostat Culture and RNA-seq

NCTC11168 was grown overnight and used to inoculate an 885 ml chemostat. The chemostat culture was grown for 6 hours without turning over in order for the *C. jejuni* cells to reach exponential growth phase. After 6 hours the pump was turned on at a rate of 0.18 volume per hour (2.66 ml/min). 4 volumes were passed through the chemostat and then the first time point was taken (T0). At T0 the chemostat was spiked with glutamine to reach a final concentration of 10 mM, a second pump was then switched on to maintain glutamine concentration. 4 ml samples were harvested at 5, 20 and 45 minutes, samples were immediately pelleted by centrifugation at 12,000 xg for 3 minutes at 4 °C. The supernatant was removed and the cell pellet flash frozen in liquid nitrogen and stored at -80 °C. Samples were sent to Genewiz for standard RNA-Seq involving RNA isolation, rRNA depletion, transcript library preparation and paired-end sequencing on an Illumina Hi-Seq. Differential gene expression was analysed using the Galaxy web based platform (Afgan et al., 2018). Bowtie 2 was used to align trimmed reads to the *Campylobacter jejuni* NCTC 11168 reference genome (Langmead & Salzberg, 2012). Numbers of mapped reads aligned to each gene were counted using HTSeq (Anders et al., 2014). Raw counts were converted to log2 counts per million using the LIMMA voom transformation (Law et al., 2014), and further differential expression analysis was performed using the LIMMA package in R.

2.14 Glutamine transport assay

Day cultures were grown in BTS (30 ml) and used to inoculate overnight MEM cultures (serine 20 mM + 5 mM glutamine). Overnight cultures were harvested and washed twice with 1 ml MEM media (minus glutamine) and normalised to 1 OD_{600nm} in a final volume of 1ml, stored on ice. 100 ul was then transferred into fresh MEM + 0.5% sodium lactate and incubated at 42°C for 3 minutes. 1 uCi (1.78 μ m) of C14 labelled glutamine and a final volume of 50 μ m cold glutamine was added to the 1 ml reaction at 42 °C. Every minute for 10 minutes 100 ul samples were taken from the reaction. Glutamine was added to the sample to achieve a 10 mM final concentration acting as a stop buffer to prevent further uptake of radiolabelled glutamine. Samples were then centrifuged and washed 3 times in 1ml stop buffer (10 mM Gln) before finally being resuspended in 10 ul of stop buffer and spotted onto Whatman paper. Spots were exposed for 2 days and the IP imaged using phosphorimager. The immediate local background of each spot was normalised using an adapted DRaCALA equation (Roelofs et al. 2012).

2.15 High resolution magic angle spinning (HRMAS) nuclear magnetic resonance (NMR) spectrometry

NMR analysis using HRMAS was performed in collaboration with the University of Lille via their Plateforme Analyses glycoconjugués (PAGés) service. *C. jejuni* cultures (30 ml) were grown overnight in BTS and pelleted by centrifugation. Cell pellets were frozen in liquid nitrogen and posted to the University of Lille in dry ice. ³¹P and ¹H-³¹P HSQC NMR was performed using the PAGés standard protocols to quantify the O-methylphosphoramidate modification in *C. jejuni*.

Chapter 3: Protein phosphorylation in *C. jejuni*

3.1 Introduction

The study of protein phosphorylation in bacteria was originally neglected due to the dated belief that bacteria were simple organisms devoid of complex regulatory networks based on post-translational modifications. However, since the discovery of a variety of post-translational modifications in bacteria, phosphorylation has arguably become the most extensively studied PTM. Currently, there are relatively few publications covering the phosphoregulatory pathways in *C. jejuni* and Voisin et al. (2007) have provided the most comprehensive analysis of the *C. jejuni* phosphoproteome. Their initial findings using 1-D gels and radiolabelled thio-ATP revealed that in the presence of magnesium a substantial number of proteins incorporated the ³⁵S label whereas in the presence of EDTA the level of incorporation was significantly reduced. This finding supports the theory that protein kinases must exist in the *C. jejuni* genome despite currently being unidentified. This can therefore explain the presence of phospho-Ser, -Thr and -Tyr identified by blotting with specific antibodies. 2-D gel proteome analysis using cytoplasmic extracts fractionated by Fe³⁺ IMAC identified 58 proteins including bacterioferritin, superoxide dismutase, a probable thiol reductase and two other proteins known to be phosphorylated in other organisms; elongation factor Tu and GroEL (Voisin et al., 2007). Mass spectral analyses of in-gel peptide digests revealed definitive proof of 57 phosphopeptides from 36 proteins whereby tyrosine modification was the rarest and serine sites were the most common followed by threonine. This study shows that phosphopeptides can be identified from bacterial extracts using simple metal ion affinity methods. No protein kinases have been annotated in the *C. jejuni* genome, however a low-molecular weight protein-tyrosine phosphatase (LMW-PTP) has been identified and partially characterised, Cj1258. Tolkatchev et al. (2006) showed Cj1258 to possess phosphatase activity using *p*NPP as a substrate. A *K*_m of 1.4 mM was determined consistent with other LMW-PTPs in bacteria. Incubation with phospho-Ser and phospho-Thr did not affect the dephosphorylation of *p*NPP suggesting Cj1258 to be tyrosine specific. A putative BY-kinase cannot be found within the same operon as that encoding Cj1258. Organisation of LMW-PTPs and BY kinases in the same operon is often found in other bacteria, where a role in capsular polysaccharide (CPS) and/or extracellular polysaccharide (EPS) biosynthesis has been implicated (Whitmore & Lamont, 2012). Other examples of LMW-PTPs with no cognate BY-kinase identified include Spd1837 in *Streptococcus pneumoniae* with potential substrates involved in metabolic

regulation such as ATP-dependent-6-phosphofructokinase and Hpr kinase/phosphorylase (Ahmad et al., 2018). Another example from *Bacillus subtilis* is YfkJ shown to dephosphorylate pNPP and undergo sigmaB dependent transcriptional upregulation in response to ethanol stress (Musumeci et al., 2005).

Given the very limited previous research on protein phosphoregulation in *C. jejuni* this study was developed to build upon the foundations laid by the Voisin et al. (2007) publication. Using metal-ion affinity methods, we set out to identify phosphopeptides directly from cytoplasmic extracts using LC-MS/MS without the need for 2-D gel analysis. Ultimately, this would provide a comprehensive global account of phosphorylated proteins in *C. jejuni*. Using the putative protein kinases and phosphatases identified by sequence homology analysis we also planned to compare the phosphoproteomes of wildtype to mutants lacking the putative enzymes; allowing us to identify potential substrates of specific kinases/phosphatases. The key enzymes of interest in this study were Cj1258, Cj0184c, Cj0668 and Cj0846. Cj0184c and Cj0846 are both annotated as S/T phosphatases and show homology to protein families containing protein phosphatases. Cj0668 was of particular interest based on its homology and conserved motifs from a novel family of protein kinases known as the Ubiquitous Bacterial Kinases (UbK) (Nguyen et al., 2017).

3.2 Results

3.2.1 Putative protein kinases and phosphatases for investigation

Cj1258 is a putative cytoplasmic phosphotyrosine protein phosphatase with experimental evidence from Tolkathev et al. (2006). Cj1258 has an amino acid length of 151 residues with 37.6% percent identity in a 149 amino acid overlap with LTP1, a LMW-PTP with PTPase activity in *Saccharomyces cerevisiae*. Cj1258 also has a percent identity of 27.7% in 148 amino acid overlap with PAP (YwIE) a protein-arginine-phosphatase from *Bacillus subtilis* as well as 24.5% percent identity in 143 amino acid overlap with Wzc a LMW-PTP from *E. coli*. Cj1258 possesses a conserved active site (V/I)CXGNXCRS from the LMW-PTP family, a family of soluble single domain enzymes widely distributed in prokaryotes and eukaryotes. As seen in figure 3.1 Cj1258 exists in a locus without its cognate kinase and a putative phosphotyrosine kinase is yet to be identified in *C. jejuni*.

Cj0668 is annotated as a putative ATP/GTP binding protein. It is 135 amino acids with 80 residues overlap and 33.8% identity to TsaE, suggested to be required for tRNA threonylcarbamoyladenosine synthesis in *E. coli*. Cj0668 also possesses multiple conserved nucleotide phosphate-binding motifs from the P-loop NTPase domain superfamily as well as motifs of the YdiB/YjeE family (UPF0079 UniprotKB database family) as seen in figure 3.2.

Cj0184c is annotated as a putative serine/threonine protein phosphatase, 384 amino acids in length with three conserved phosphoprotein phosphatase motifs, GD_XHG (partial), GD_XVDRG (partial) and GNHE involved in the dephosphorylation of phosphoserines and phosphothreonines on target proteins (figure 3.3). Blast analysis also revealed a specific hit with PF00149, a family of calcineurin-like phosphoesterases including protein phosphoserine phosphatases. Interestingly the N-terminal domain of Cj0184c has homology to a nucleotide/nucleoside kinase superfamily suggesting this protein could be bifunctional with both kinase and phosphatase activity (figure 3.3).

Finally Cj0846 is annotated as a membrane bound metallophosphatase in NCTC11168 however, in strain 81-176 it is annotated as a putative S/T phosphatase (Cj81176_0862). Cj0846 is 374 amino acids and predicted to have 4 transmembrane helices (predicted by TMHMM server v. 2.0). Blast analysis suggests residues 129-374 are homologous to members of the metallophosphatase superfamily (MPP). MPPs are a group of enzymes with a conserved domain containing an active site consisting of two metal ions. This family includes phosphoprotein phosphatases (PPPs). The protein sequence of Cj0846 contains the GD and GNHE conserved motifs from the MPP superfamily (figure 3.4).

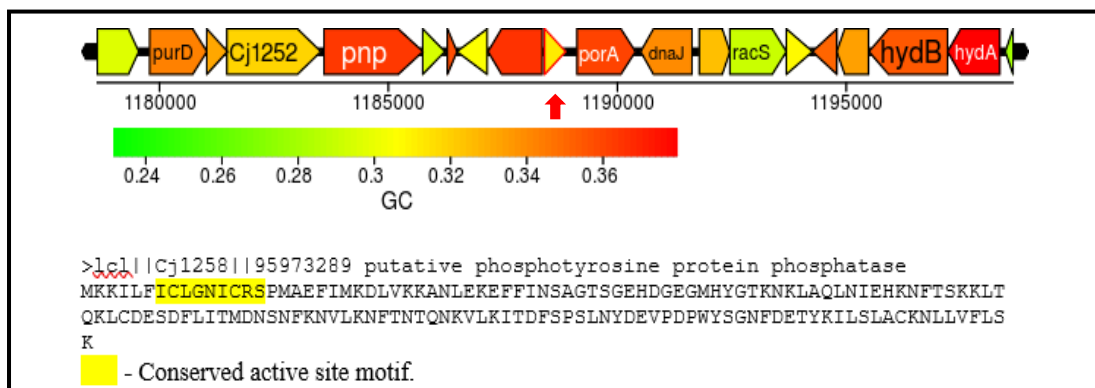


Figure 3.1 Cj1258 gene organisation and protein sequence. Red outline and arrow indicates position of Cj1258 in genome, yellow highlight shows LMW-PTP active site for PTPase activity.

```

>lcl||Cj0668||95942753 putative ATP/GTP-binding protein
MKEFI LAKNEIKTMLQ LMPKEGVVLLQ GDLASGKISLVQAWVKFLGLDVRVD SPTFSTMQKYENHDICIY HYDIY
QEGLEGLLANGLFENFFEKGLHLVWGGENLKKTLMKFGISTIQIKISIKDDKRKYEIE

    - Conserved UbK motifs
    - Walker A binding motif (GxxxxGK(S/T))
    - Walker B motif (hhhh(D/E)where h is a hydrophobic residue)

```

Figure 3.2 Cj0668 protein sequence. Yellow highlight shows conserved motifs found in the YdiB/YjeE family (UbK) (Nguyen et al., 2017). Green and purple highlight shows the walker A and B motifs, two highly conserved three-dimensional structures associated with ATP-binding proteins.

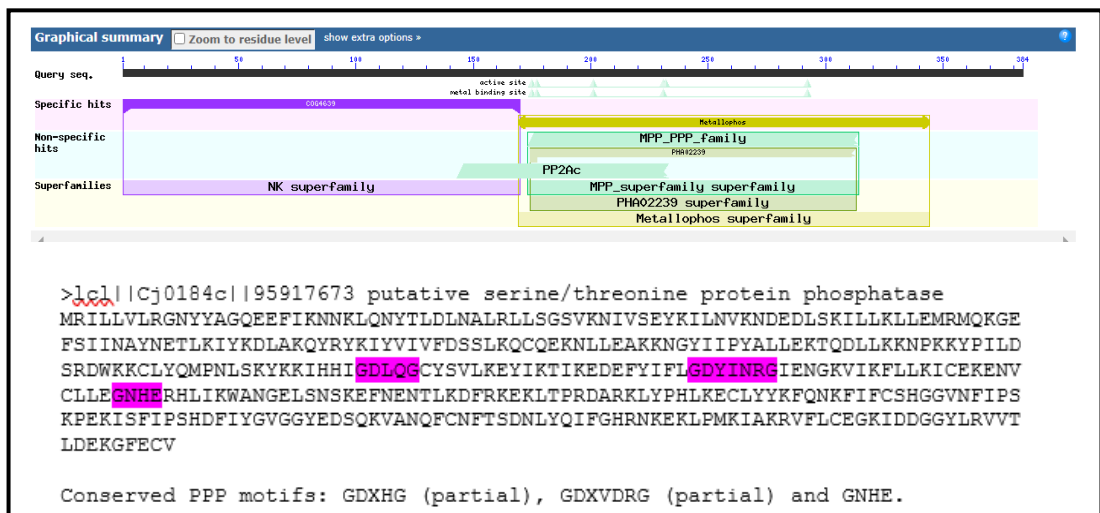


Figure 3.3 Cj0184c graphical protein blast output and protein sequence. Metallophos specific hit corresponds to pfam00149 entry the calcineurin-like phosphoesterase family, NK superfamily is short for nucleotide/nucleoside kinase superfamily. Metallophosphatase_Phosphoprotein phosphatase (MPP_PPP_Family) motifs highlighted in purple.

```

>FASTA Protein Sequence
MIFLIFSFIIVLLIFGLANVYIYKRLIKITLFRKYKIFSFIIVLFLAQAVFLIFRRDEYLSDTWYEILAMFYA
PTYCLFFMTLAWDFVVKLILALMGKRDKTYNLI LRLIFELSLIVLSVFLIYASINNALKTPEVKSVDVEIPNLKGD
LKIVMLTDIHLGKNLHENFLDKLITKVNLSQSPDMVVIV GD LIDTNPKDLKNIYISKLNDFNSTYGTFFYALGNHEYY
HGINEVLDLLRKHTNMKILVNQNLDLGFDIAGLDLGLDRGLYAPDLARIKVDLNTSKASILLTHQPKTALLY
DLSDFDLVLVSGHTGGQIFPFMFLVKLQQGFVHGLYDLGKTKLYVSSGAGFWGPSLRVFPAPSEIIVILNLKGGK

Conserved MPP_PPP motifs: GD and GNHE.

```

Figure 3.4 Cj0846 protein sequence. MPP_PPP superfamily motifs highlighted in yellow.

3.2.2 Kinase/phosphatase mutant construction

Deletion (knockout) mutants in the genes for the enzymes of interest were constructed by insertion of an antibiotic resistance cassette into the open reading frame by double homologous cross-over (fig 3.5a). Gibson assembly was used to construct the pGEM3Zf vector containing two flanking fragments from the gene of interest (~500 bp) separated by a resistance cassette (fig 3.5b). The vector was transformed into NCTC11168 using the methods in section 2.9.4. After transformation into NCTC11168 a selection of colonies were screened for the presence of the antibiotic cassette using the F1 and R2 flanking fragment amplification primers. The antibiotic cassette was identified by a change in gene size corresponding to the insertion (fig 3.5c). Successful mutant strains were stored in glycerol for future experiments. Unfortunately, no colonies were obtained after multiple attempts to knockout *Cj0668*. This suggests *Cj0668* may be an essential gene required for *C. jejuni* survival.

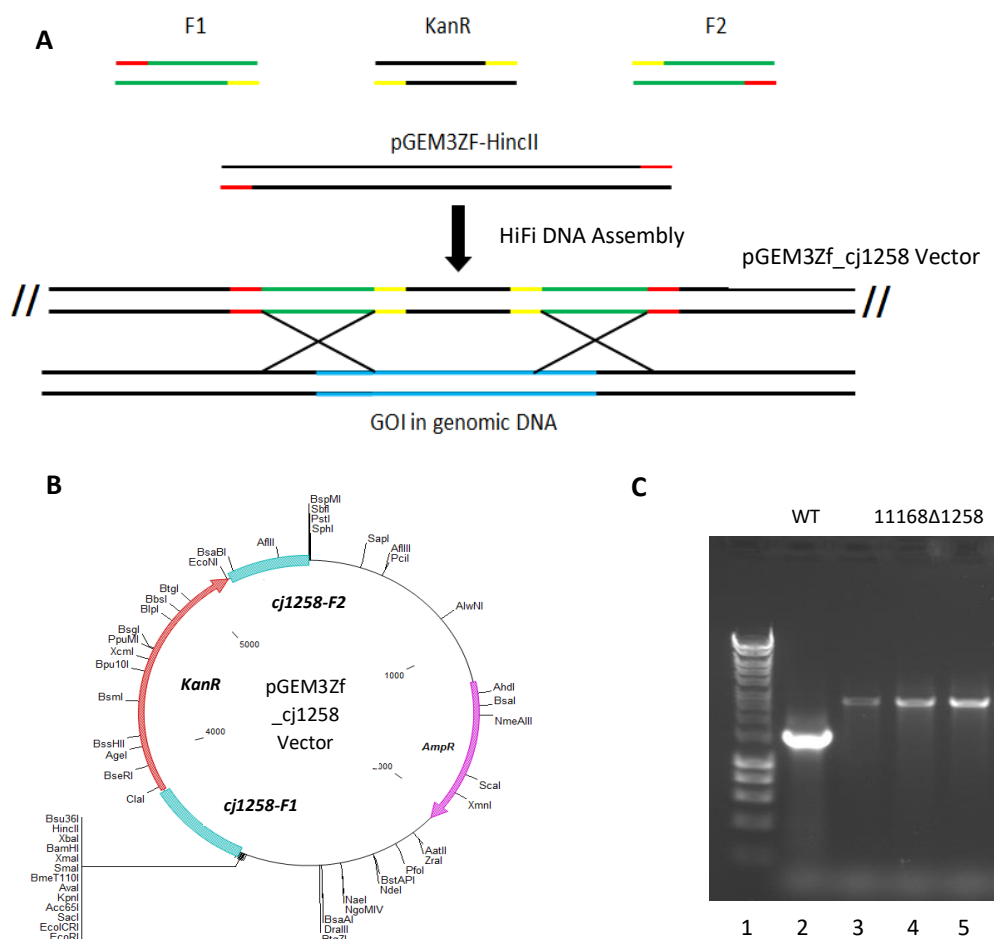


Figure 3.5 Gibson Assembly of deletion mutant strains. (A) Gene flanks and an antibiotic cassette were amplified with homologous adaptor regions to allow ligation of the gene fragments to the antibiotic resistance cassette and the *HincII* linearised pGEM3Zf vector in a HiFi DNA assembly reaction. (B) Plasmid map pGEM3Zf_cj1258_kan (C) Mutant colony screening results from using insert primers F1/R2. Lane 1 contains 1kb DNA hyperladder, Lane 2 shows WT *cj1258* gene, Lanes 3-5 *cj1258* with kanamycin cassette insertion (successful mutant colonies).

3.2.3 Cytoplasmic proteins are extensively phosphorylated in *C. jejuni*

A growth curve comparing wild-type and mutant strains was performed in BTS broth. All mutant strains discussed were compared against WT over 18 hours. All three mutant strains grew like WT as seen in figure 3.6. Samples were taken at each time point throughout the growth curve and total cell protein extracts resolved by SDS-PAGE. The protein gels were stained with the sensitive phosphoprotein stain Pro-Q diamond and counterstained with SYPRO ruby to show all proteins. As seen in figure 3.7 there was no significant change in any of the mutant phosphoproteomes compared to WT visible by eye. However, the Pro-Q diamond-stained gels reveal that cytoplasmic proteins in *C. jejuni* are extensively phosphorylated on serine, threonine and/or tyrosine residues. Therefore, it can be suggested that at least one kinase and phosphatase must exist in the genome despite none of the mutants currently exhibiting any phenotypic changes in phosphorylation. Potentially the sensitivity of the approach is not suitable to identify a change in phosphorylation on specific proteins. Further work was attempted using antibodies specific for different phosphorylated residues.

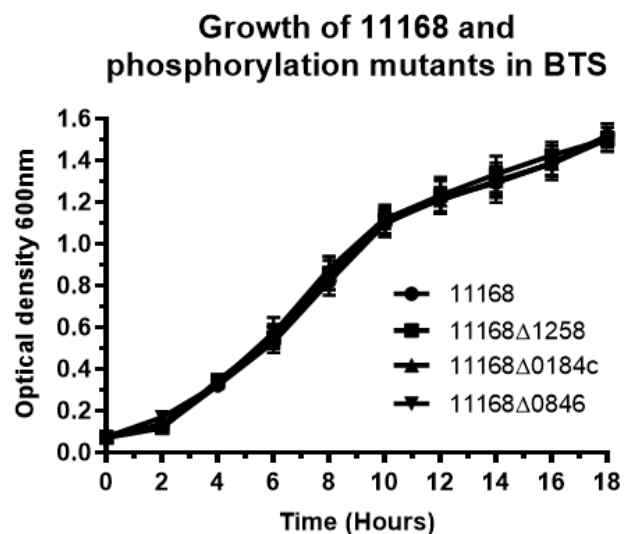
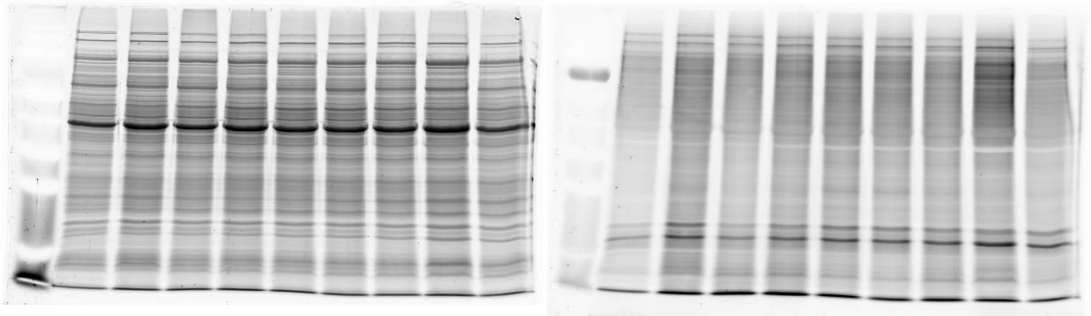


Figure 3.6 Growth in BTS unaffected by loss of putative kinase/phosphatase-enzymes. *C. jejuni* 11168 cells were grown overnight in BTS from agar plates and then fresh BTS broth was seeded with overnight cultures. Cells were grown for 18 hours and samples taken every 2 hours. Data points are the means of 3 independent replicates with error bars showing standard deviation.

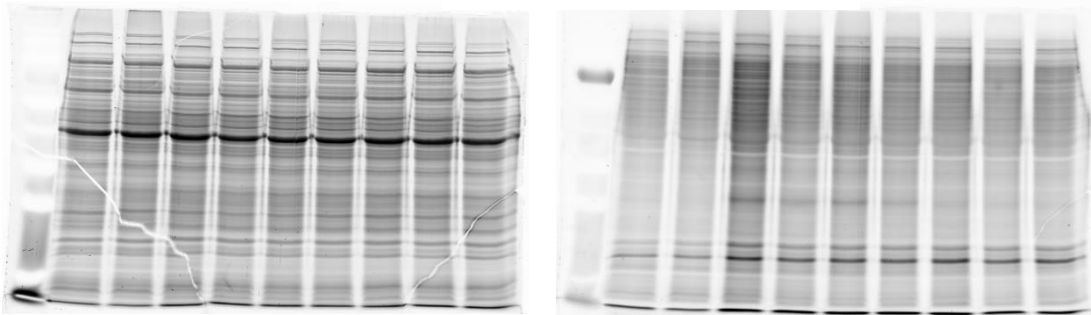
SYPRO Ruby

Pro-Q Diamond

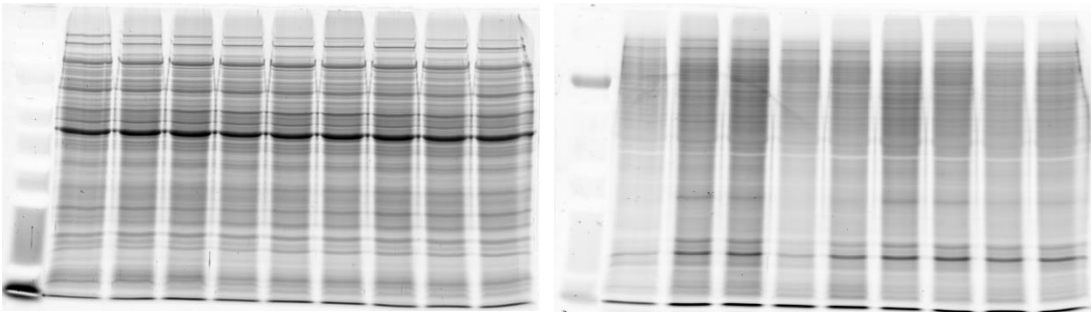
11168



11168Δ0184c



11168Δ0846



11168Δ1258

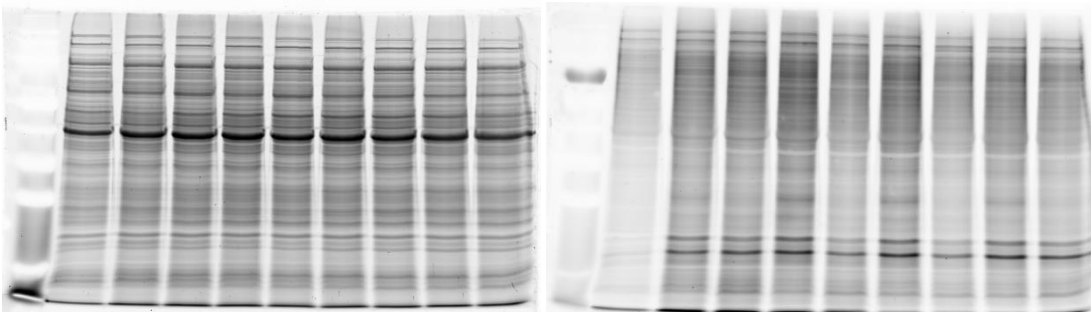


Figure 3.7 No changes in phosphoproteome visible after knockout of putative phospho-enzymes. Samples taken from figure 3.6 were harvested by centrifugation and a cell free extract produced by sonication. 12.5 ug of protein was added to each well and resolved by SDS-PAGE and stained with Pro-Q diamond phosphoprotein stain (right) before counterstaining with SYPRO ruby protein stain (left) (Staining protocol section 2.10.4). Lanes from left to right include DNA hyperladder 1kb and timepoints 2hr – 18hr.

3.2.4 Blotting with antibodies to phospho-amino acids to identify changes in phosphorylation

Phosphoprotein staining using commercial stains such as Pro-Q diamond was useful to show the abundance of phosphorylation occurring in the cytoplasm of *C. jejuni*. However, to identify individual phosphoproteins of interest a more specific approach was required. Anti-pT and anti-pY were used to try and identify key proteins with differential phosphorylation in mutant vs wildtype. As seen in the immunoblot in figure 3.8 a protein of approximately 30 kDa appears to be highly phosphorylated on tyrosine residues in wildtype however in the strain lacking Cj1258 - a tyrosine phosphatase - this protein appears to be dephosphorylated substantially. In contrast when comparing the levels of pT between 11168 and 11168 Δ 0184c, no observable differences in band pattern could be found (fig 3.9).

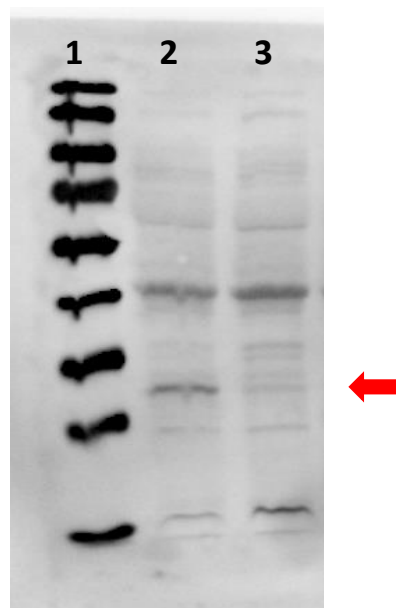


Figure 3.8 Anti-Phosphotyrosine Western Blot of 11168 and 11168 Δ 1258. 30 μ g of cell free extract was loaded into each well and resolved by SDS-PAGE. Western blot using 1/2000 anti-pY to detect phosphorylated tyrosine residues from 30ug cell free extracts. The ~30kDa tyrosine phosphoprotein of interest is highlighted with a red arrow.

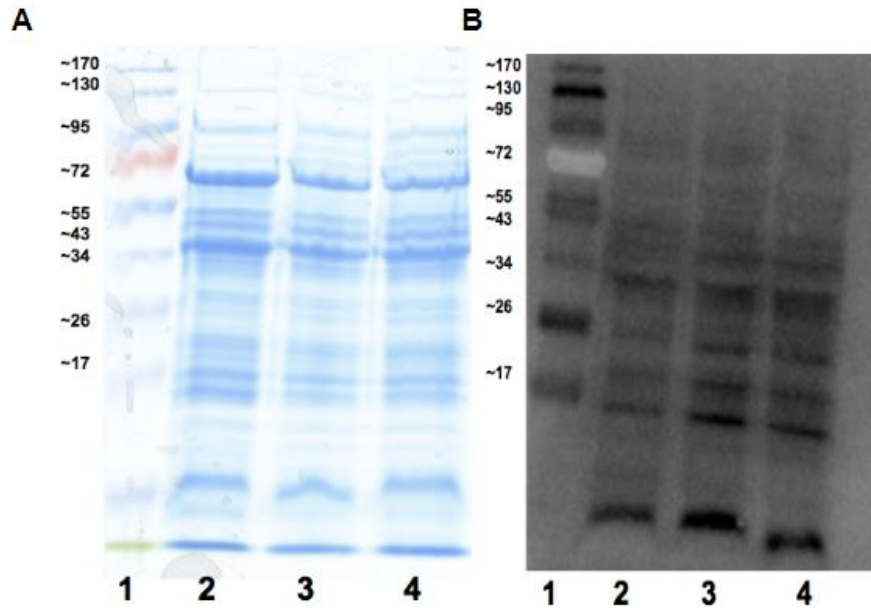


Figure 3.9 Anti-pT western blot of 11168 vs 11168 Δ 0184c. (A) SDS-PAGE comparing 30ug of 11168 (lane 2), 11168 Δ 0184c (lane 3) and 11168 Δ 0184c+0184c (lane 4). 5ul E/Z protein ladder (lane 1). (B) Western blot using 1/2000 anti-pT to detect phosphorylated threonine residues from 30ug cell free extracts.

3.2.5 Phosphatase activity of purified Cj1258

Enzymatic activity assays determining the phosphatase activity of Cj1258 were performed with purified his-tagged Cj1258 under predetermined optimal conditions in section 2.11.1. *p*-nitrophenyl phosphate is a phospho-tyrosine analogue and its hydrolysis can be measured at 405nm based on the formation of the yellow nitrophenyl anion. The determined K_m value was 1.7 (+/- 0.1) mM with a V_{max} of 22.1(+/- 0.4) $\mu\text{mol min}^{-1} \cdot \text{mg protein}^{-1}$. These values are consistent with LMW-PTPs in other organisms such as *E. coli* Wzb (Vincent et al., 1999).

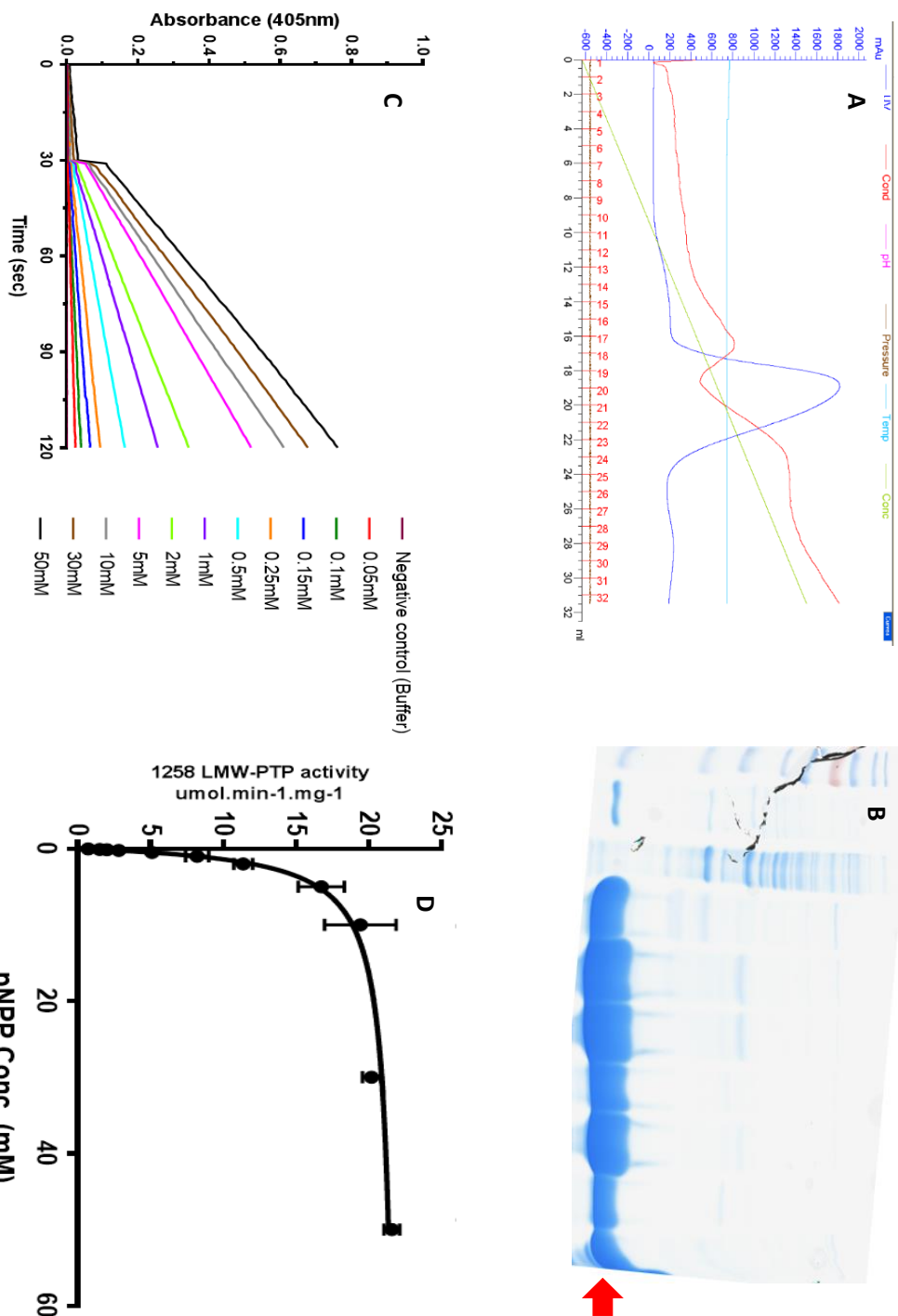


Figure 3.10 Overexpression, purification and phosphatase activity of Cj1258. (A) Elution profile of Cj1258 (peak at fractions 18-23) from ~25ml of *E. coli* pET21a_1258 cell free extract (CFE) from 2L of LB culture resuspended in binding buffer loaded on a HisTrap™ HP column (GE Healthcare). Elution took place over 40 ml along an imidazole gradient (50-500mM) (B) SDS-PAGE of Cj1258 peak fractions. Lane 1 (5µl of EZ-RUN™ pre-stained Rec protein ladder), lane 2 (10µl *E. coli* pET21a_1258 CFE), lane 3 (10µl of flow through from CFE loading onto AKTA), lane 4 (10µl of fraction 18), lane 5 (10µl of fraction 19), lane 6 (10µl of fraction 20), lane 7 (10µl of fraction 21), lane 8 (10µl of fraction 22), lane 9 (10µl of fraction 23), lane 10 (10µl of buffer exchanged and concentrated Cj1258 (fractions 18-23 pooled), Cj1258 ~17kDa (red arrow) (C) Cj1258 enzymatic activity in the presence of increasing concentrations of substrate pNPP. Enzyme activity of Cj1258 for pNPP in 100mM Tris-HCl buffer (pH 6.5) was measured when 1µg of Cj1258 was used in the assay and a linear rate achieved (30-120 seconds). (D) The graph represents the mean activity and non-linear fit of enzyme activity data to the Michaelis-Menton equation to determine the Km value for Cj1258.

3.2.6 Selection of *Cj0184c* for phosphoproteome analysis using LC-MS/MS

A preliminary experiment was performed with purified *Cj0184c* using DIFMUP (section 2.12.2) to explore threonine specific phosphatase activity. The results of this preliminary experiment indicated that *Cj0184c* did indeed possess phospho-threonine phosphatase activity (purification of *Cj0184c* and the activity data shown in chapter 4). The knowledge that *Cj0184c* possessed phosphatase activity combined with its novel two-domain structure potentially suggesting it to be a bi-functional enzymes made it an appealing candidate for further phosphoproteomic analysis. Additionally, serine and threonine are the most common phosphorylated residues in bacteria and tyrosine is often a rarer modification. Therefore, it was decided that *Cj0184c* would be our first candidate for phosphoproteome analysis using LC-MS/MS. The single *cj0184c* deletion mutant was chosen to be compared with WT due to the expensive nature of MS techniques. Initially we wanted to trial the experimental process before later performing a larger experiment with all mutants in this study.

3.2.7 Trial LC-MS/MS workflow

As seen in figure 3.11 the initial workflow devised was to culture both WT and mutant cells and harvest cells by centrifugation from mid log phase. Cytoplasmic proteins would be isolated by disruption using sonication and differential centrifugation. The cytoplasmic cell free extract samples could then be subjected to conventional mass spectrometry peptide preparation including reduction, alkylation, trypsin digestion and desalting. Finally the resulting peptide sample were enriched for phosphopeptides using Fe(3+) Immobilized metal affinity chromatography (IMAC) based on the affinity of negatively charged phosphate groups towards the positively charged Fe(3+) metal ions. The enriched phosphopeptide samples were then analysed by LC-MS/MS and significant changes in phosphorylation due to the deletion of *Cj0184c* explored.

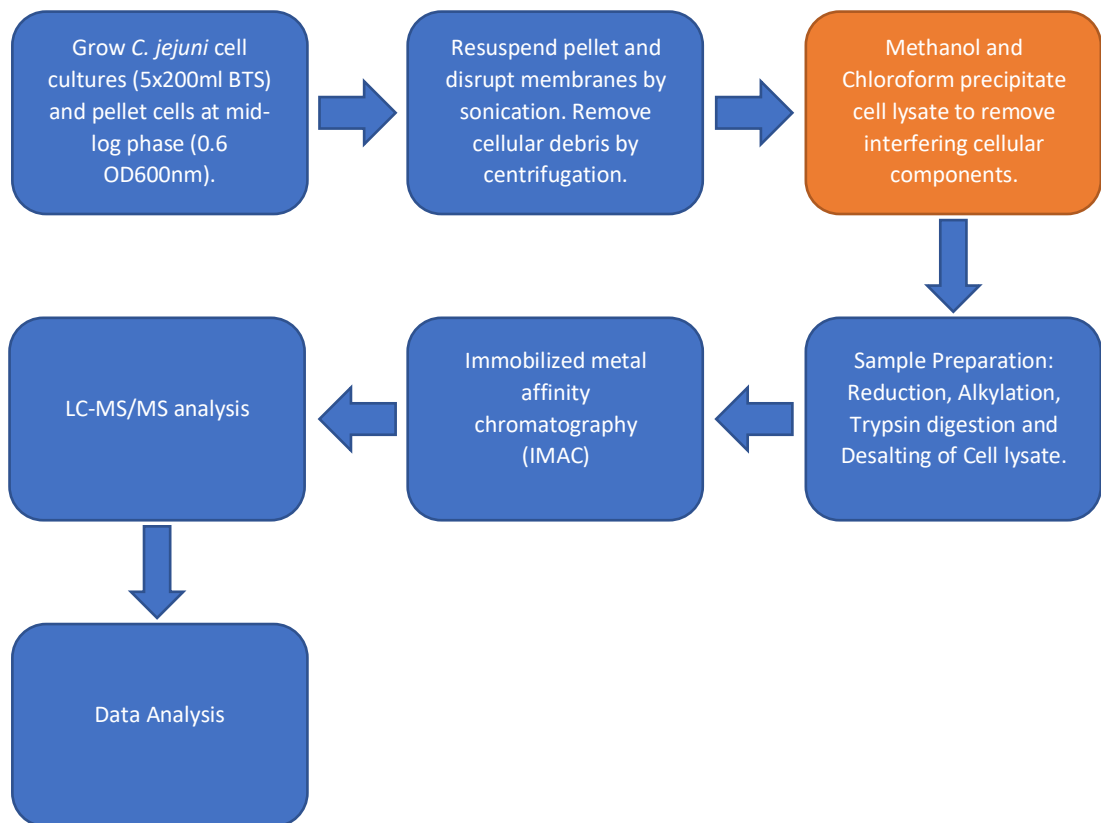


Figure 3.11 LC-MS/MS Workflow. Experimental procedure in order to identify phosphopeptides from cytoplasmic peptide samples. Orange box was an additional step implemented to improve sample purity.

After multiple attempts to produce a comprehensive phosphoproteome data set a methanol, chloroform precipitation step was introduced to the workflow in order to reduce any potential contaminants and increase the sensitivity and reproducibility of the data. To ensure this step did not affect the protein concentration or phosphorylation status of proteins an anti-pT western blot was performed as seen in figure 3.12. There was no identifiable change in phosphorylation between samples pre and post methanol, chloroform precipitation. The protein concentration of each sample remained consistent between replicates as seen by SDS-PAGE analysis in figure 3.12.

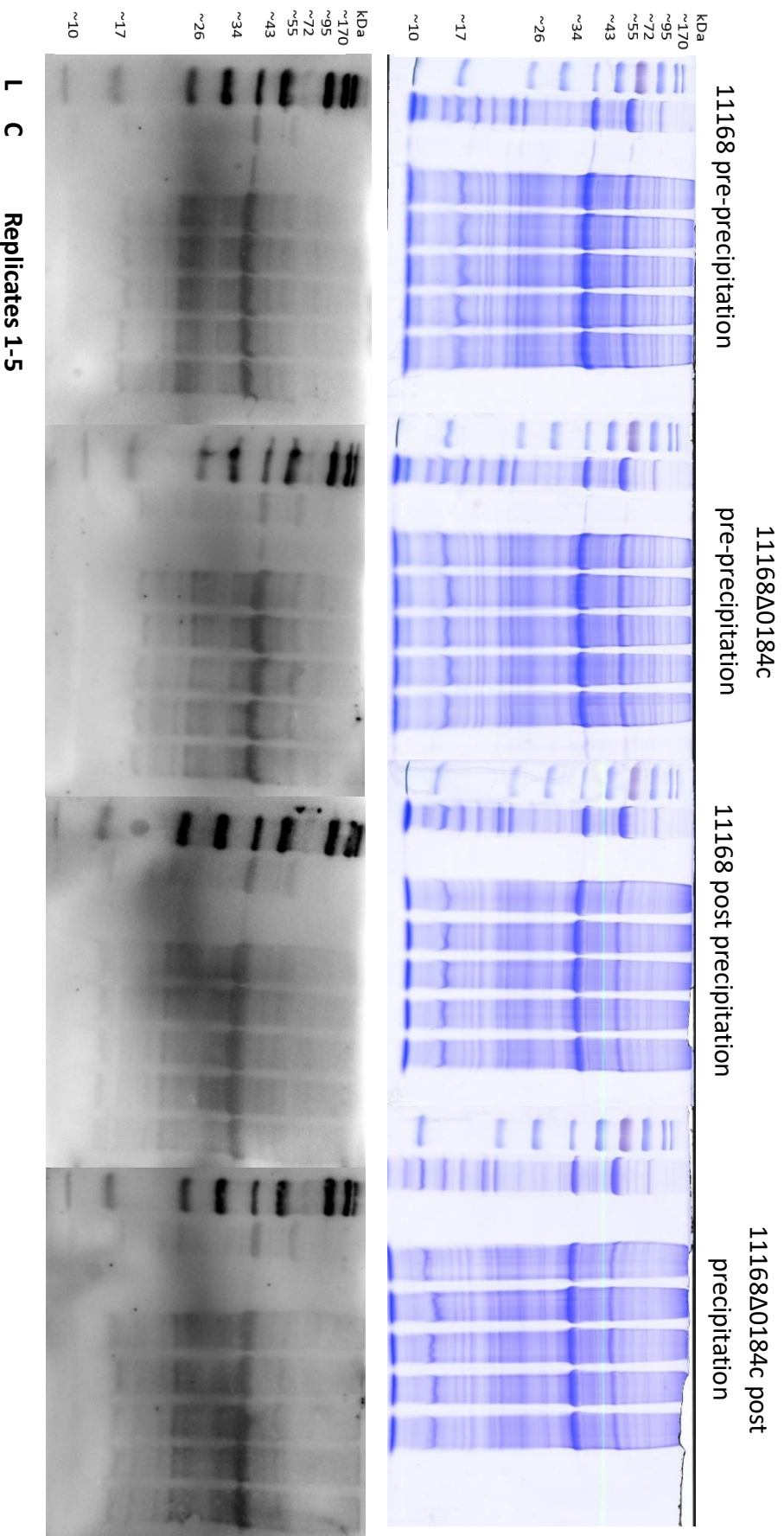


Figure 3.12 1 SDS-PAGE and Anti-pT Western blot of pre and post Methanol, chloroform treated cytoplasmic samples. *C. jejuni* was grown to 0.1 OD_{600nm} in 5x200 ml cultures. Cells were pelleted by centrifugation and lysed by sonication. Cellular debris was removed by centrifugation to produce a cell free extract. Methanol, chloroform precipitation was performed on 5x WT and 5x mutant CFE samples to compare to 5x WT and 5x mutant samples pre-precipitation. These samples were resolved by SDS-PAGE to ensure no loss in concentration. A western blot using 1/2000 anti-pY to detect phosphorylated tyrosine residues was also carried out on 30 ug samples to ensure that the additional methanol, chloroform step did not result in a loss in phosphorylated threonine residues. Lane 1 (DNA hyperladder 1kb), lane 2 (*C. jejuni* CFE positive control), lanes 4-8 (*C. jejuni* CFE).

3.2.8 Deletion of *Cj0184c* has a significant impact on protein expression

Prior to the identification of phosphorylated residues our peptide samples were analysed for abundance in both WT and *Cj0184c* deficient strains. As seen in figure 3.13 the total protein concentrations according to LFQ intensity data is uniform and there are no statistically significant differences between samples and replicates. A total of 1312 proteins were identified in the *C. jejuni* cytoplasmic samples; which were to be enriched and analysed for phosphorylation status. The proteome profile also confirmed the absence of *Cj0184c* in the mutant strain and its presence in the WT strain. Peptides covering up to 11.7% of the *Cj0184c* protein were found in the WT samples whereas in the mutant strain no *Cj0184c* peptides were identified in 4/5 replicates. A single *Cj0184c* peptide was identified in mutant replicate 2 however the coverage was only 2.7% and considering we were working at a false discovery rate (FDR) of 1% this is most likely a false positive. The data allowed us to identify proteins differentially expressed between the two strains. Figure 3.14 shows a volcano plot with the proteins of interest that are significantly up or down regulated in response to the deletion of *Cj0184c* (FDR=0.01). Tables 3.1 and 3.2 show all the protein and gene names of the significantly down- and up-regulated proteins, respectively. Interestingly these hits show changes in enzymes associated with capsule biosynthesis: *Cj1422*, *Cj1419* and *Cj1429* as well as glutamate and glutamine metabolism: *GltB*, *GltD* (glutamate synthase) and *GlnA* (glutamine synthase). As seen in fig 3.15 bacterial chemotaxis proteins are also differentially expressed. Multiple methyl-accepting proteins are increased in abundance in the mutant as well as the flagella motor protein *MotA*.

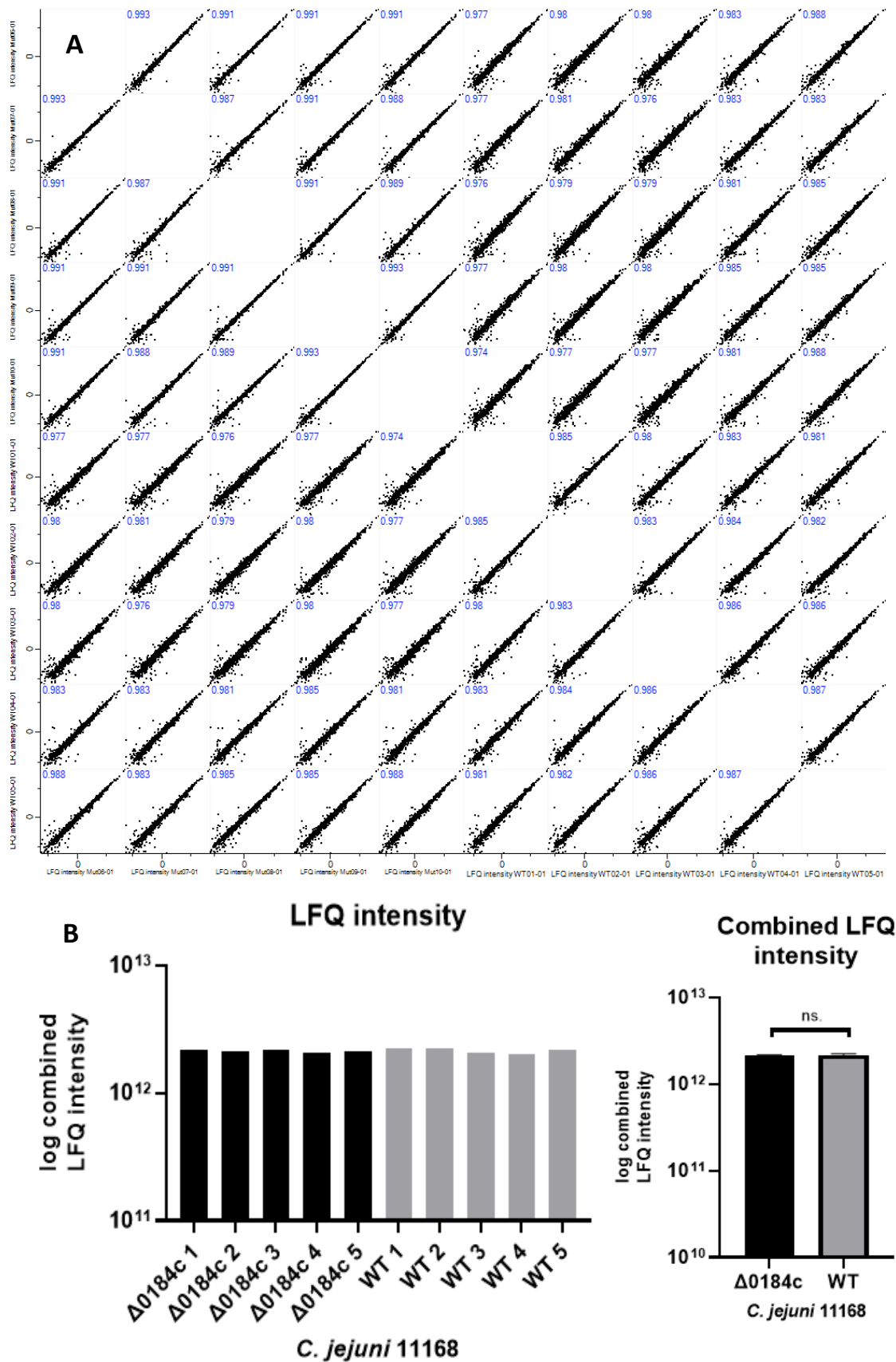


Figure 3.13 Proteome profile LFQ intensity data. Trypsin digested peptides were subjected to LC-MS/MS and analysed at the protein level using Perseus. (A) Individual comparisons between replicates with R2 value displayed, Mut refers to mutant strain 11168 $\Delta 0184c$. (B) Combined LFQ intensity of each strain.

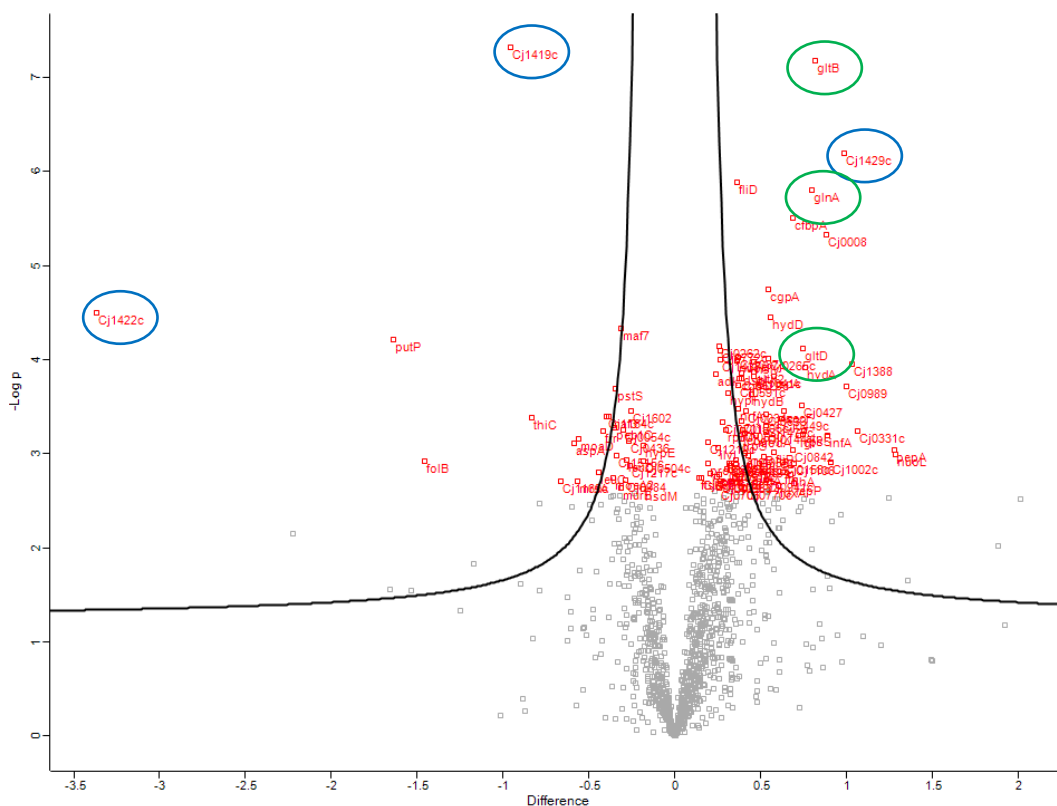


Figure 3.14 Volcano plot showing the statistically significant proteins differentially expressed in WT/ $\Delta 0184c$. Log students T-test values were plotted against the difference in p value between WT/ $\Delta 0184c$ protein samples. Proteins highlighted in red above the significance lines are those significantly different in abundance (FDR=0.01)

Table 3.1 Proteins with significantly reduced abundance in 11168 $\Delta 0184c$ compared to 11168

Protein name	Gene name	Student's T-test Difference Mut/WT (FDR=0.01)
Putative sugar transferase	Cj1422c	-3.3648
Putative sodium/proline symporter	putP	-1.6367
Putative dihydroneopterin aldolase	folB	-1.4581
Putative methyltransferase	Cj1419c	-0.9557
Phosphomethylpyrimidine synthase	thiC	-0.8322
Putative periplasmic protein	Cj1169c	-0.6598
Aspartate ammonia-lyase	aspA	-0.5826
Peptide methionine sulfoxide reductase MsrA	mrsA	-0.5676
Putative molybdopterin converting factor, subunit 1	moaD	-0.5574
3-isopropylmalate dehydratase large subunit	leuC	-0.4408
Ribosome-recycling factor	frr	-0.4175

Uncharacterized protein	Cj1164c	-0.3961
Uncharacterized protein	maf3	-0.3841
Putative molybdopterin biosynthesis protein	moeA2	-0.3547
Probable ABC transporter ATP-binding protein PEB1C	peb1C	-0.3517
Putative periplasmic phosphate binding protein	pstS	-0.3471
Carboxynorspermidine/carboxyspermidine decarboxylase	Cj1515c	-0.3368
UDP-N-acetylenolpyruvoylglucosamine reductase	murB	-0.3100
Uncharacterized protein	maf7	-0.3096
Cytokinin riboside 5-monophosphate phosphoribohydrolase	Cj0054c	-0.3007
Uncharacterized protein Cj0984	Cj0984	-0.2870
3-isopropylmalate dehydratase small subunit	leuD	-0.2787
Putative pyridoxamine 5-phosphate oxidase	Cj0436	-0.2661
Laccase domain protein Cj1217c	Cj1217c	-0.2591
Uncharacterized protein	Cj1602	-0.2563
Hydrogenase isoenzymes formation protein	hypE	-0.1850
Putative type I restriction enzyme M protein	hsdM	-0.1815
Putative oxidoreductase	Cj0504c	-0.1800

Table 3.2 Proteins with significantly increased abundance in 11168ΔO184c compared to 11168

Protein name	Gene name	Student's T-test Difference Mut/WT (FDR=0.01)
NADH-quinone oxidoreductase subunit L	nuoL	1.2845
Probable cytosol aminopeptidase	pepA	1.2791
Uncharacterized protein	Cj0331c	1.0658
Putative endoribonuclease L-PSP	Cj1388	1.0360
Putative membrane protein	Cj0989	1.0023
Uncharacterized protein	Cj1429c	0.9894
Putative phosphoglycerate/bisphosphoglycerate mutase	Cj1002c	0.9132
Translation initiation factor IF-1	infA	0.8920
Uncharacterized protein	Cj0008	0.8861
Glutamate synthase (NADPH) large subunit	gltB	0.8217
Glutamine synthetase	glnA	0.7977
Ni/Fe-hydrogenase small chain	hydA	0.7639
ATP synthase F0 sector B subunit	atpF	0.7534
30S ribosomal protein S19	rpsS	0.7488
Glutamate synthase (NADPH) small subunit	gltD	0.7446
Uncharacterized protein	Cj0427	0.7400
Prolipoprotein diacylglycerol transferase	lgt	0.7247
Signal peptidase I	lepP	0.6952
Putative periplasmic thioredoxin	Cj1106	0.6926
Putative iron-uptake ABC transport system, periplasmic iron-binding protein	cfbpA	0.6894
Putative lipoprotein	Cj0842	0.6881
Flagellar biosynthesis protein	flhA	0.6741
Protein-export membrane protein SecF	secF	0.6373

Bacterial non-heme ferritin	ftn	0.6336
Putative haem-binding lipoprotein	Cj0158c	0.6323
Uncharacterized protein	Cj0449c	0.6221
Ferredoxin	fdxA	0.6029
Geranyltranstransferase	ispA	0.5810
Flagellar biosynthetic protein FlIP	fliP	0.5764
Putative hydrogenase maturation protease	hydD	0.5598
Putative periplasmic protein	cgpA	0.5489
Putative cytochrome C-type haem-binding periplasmic protein	Cj0265c	0.5471
Putative methyl-accepting chemotaxis signal transduction protein	Cj0144	0.5356
Putative hydrolase	Cj1477c	0.5347
Putative periplasmic protein	Cj0633	0.5326
Putative permease	Cj0941c	0.5324
Homolog of E. coli rod shape-determining protein	mreC	0.5209
Two-component sensor (Histidine kinase)	dccS	0.4922
Putative molybdate-binding lipoprotein	modA	0.4719
ATP-dependent protease subunit HslV	hslV	0.4630
Putative periplasmic ATP/GTP-binding protein	Cj1041c	0.4628
Glutamate--tRNA ligase 2	gltX2	0.4613
Ni/Fe-hydrogenase large subunit	hydB	0.4464
Putative flagellar motor proton channel	motA	0.4432
Phosphate transporter	Cj1194	0.4376
Putative sulfatase family protein	Cj1055c	0.4320
Putative periplasmic protein	Cj0034c	0.4194
Cbb3-type cytochrome c oxidase subunit	ccoP	0.4082
Putative NLPA family lipoprotein	Cj0770c	0.4076
Acetylglutamate kinase	argB	0.4068
Putative periplasmic protein	Cj0530	0.3948
Disulphide bond formation protein	dsbl	0.3896
Tryptophan--tRNA ligase	trpS	0.3894
Putative MCP-type signal transduction protein	Cj1506c	0.3887
Putative aminodeoxychorismate lyase family protein	Cj0529c	0.3882
Cb-type cytochrome C oxidase subunit II	ccoO	0.3782
Cytochrome c-552	nrfA	0.3732
Putative lipoprotein	Cj0591c	0.3727
Putative peptidase	Cj1087c	0.3690
Flagellar hook-associated protein 2	fliD	0.3653
NADH-quinone oxidoreductase subunit H	nuoH	0.3632
Capsule polysaccharide export system inner membrane protein	kpsE	0.3590
N-acetylmuramoyl-L-alanine amidase	amiA	0.3573
Putative periplasmic protein	Cj1637c	0.3534
Molybdopterin containing oxidoreductase	Cj0264c	0.3323
Uncharacterized lipoprotein Cj0983	Cj0983	0.3301
Putative periplasmic protein	Cj0910	0.3271
Putative peptidase M23 family protein	Cj1275c	0.3267
Non-haem iron protein	rrc	0.3177

Carbamoyltransferase	hypF	0.3134
Putative NLP family lipoprotein	Cj0771c	0.3046
50S ribosomal protein L13	rplM	0.3023
Putative protease	Cj0701	0.2769
Putative NLP family lipoprotein	Cj0772c	0.2677
Aminotransferase	Cj1437c	0.2662
Putative lipoprotein	Cj0089	0.2639
Uncharacterized protein	Cj0706	0.2611
Putative methyl-accepting chemotaxis signal transduction protein	Cj0262c	0.2587
Polyphosphate kinase	ppk	0.2580
Acetolactate synthase	ilvI	0.2539
Pyruvate-flavodoxin oxidoreductase	Cj1476c	0.2462
Adenylate kinase	adk	0.2401
Uroporphyrinogen decarboxylase	hemE	0.2114
Proline--tRNA ligase	proS	0.1958
Putative periplasmic protein	Cj1219c	0.1943
Uncharacterized protein	Cj0621	0.1590
DNA translocase FtsK	ftsK	0.1432

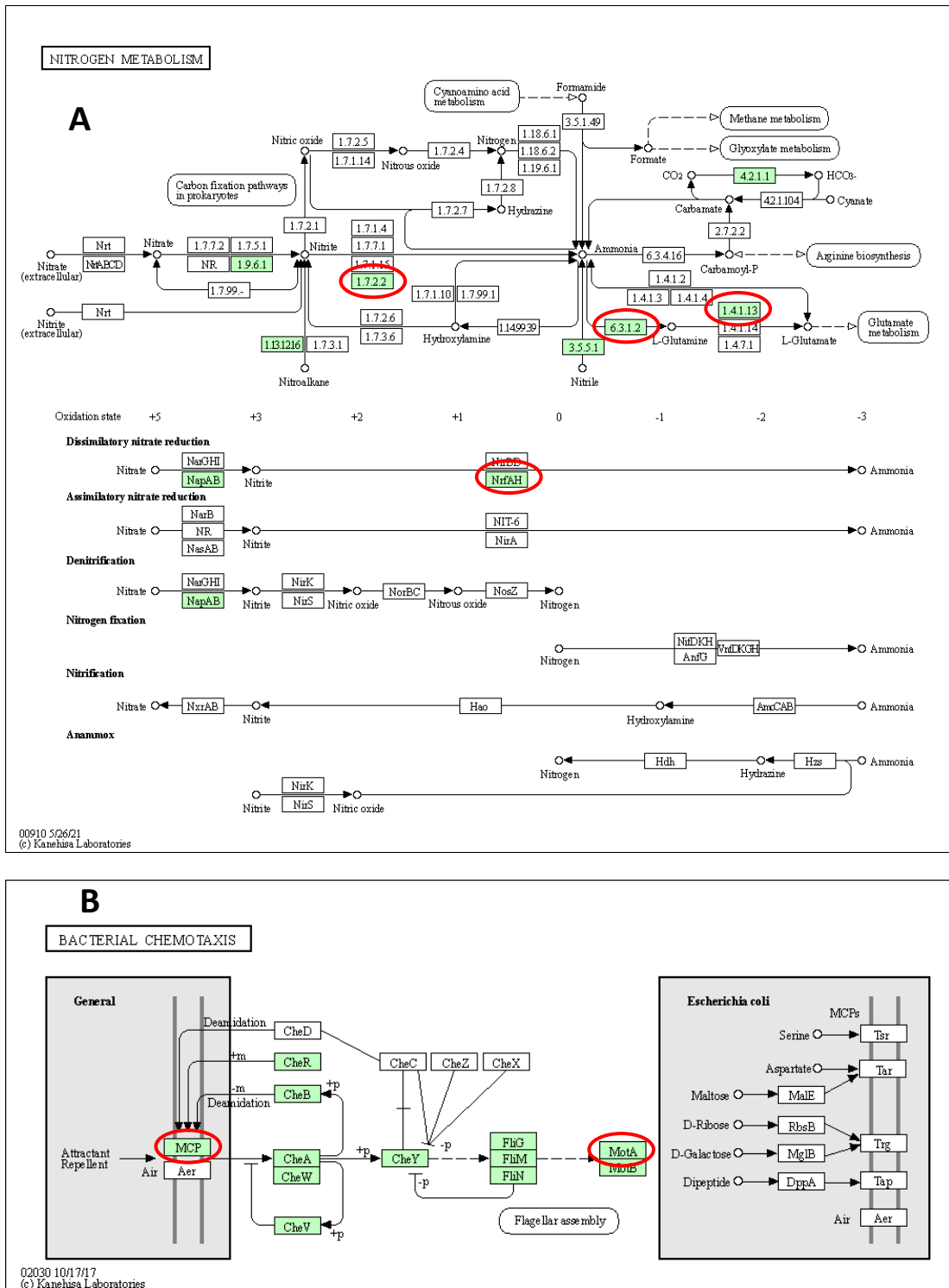


Figure 3.15 David functional annotations of cellular processes. Significant proteins from protein profiling WT/ Δ 0184c circled in red. A. Nitrogen metabolism pathways 1.7.2.2 = *nrfA*, 6.3.1.2 = *glnA* and 1.4.1.13 = *gltB/gltD*. B. Bacterial chemotaxis pathways MCP = *Cj1506c*, *Cj0144*, *Cj0262c*, *MotA* = *MotA*

3.2.9 Deletion of Cj0184c has a specific impact on the *C. jejuni* 11168 phosphoproteome

Following the peptide profiling, the trypsin digested peptide samples were enriched for phosphopeptides using Fe(3+) IMAC. Using LC-MS/MS and analysis in Perseus a comprehensive data set of the *C. jejuni* 11168 and 11168Δ0184c phosphoproteomes was produced. These two data sets could be compared to identify significant changes in the phosphorylation of specific peptides and thus potentially identify likely substrates of Cj0184c subject to dephosphorylation. Firstly, all contaminants which did not map to the 11168 genome were removed, and the FDR was set to 1%. 852 phosphosites and 349 phosphorylated proteins were identified between the two strains, 679 and 320, respectively were identified as class I sites. A class I site is defined by a localization probability of 0.75 and a probability localization score difference greater than or equal to 5. The majority of phosphorylation events were observed on serine (49%), followed by threonine (30%) and tyrosine (21%). This distribution generally agrees with a similar study in *E. coli* however tyrosine appears to be overrepresented and serine underrepresented in *C. jejuni* (fig 3.16).

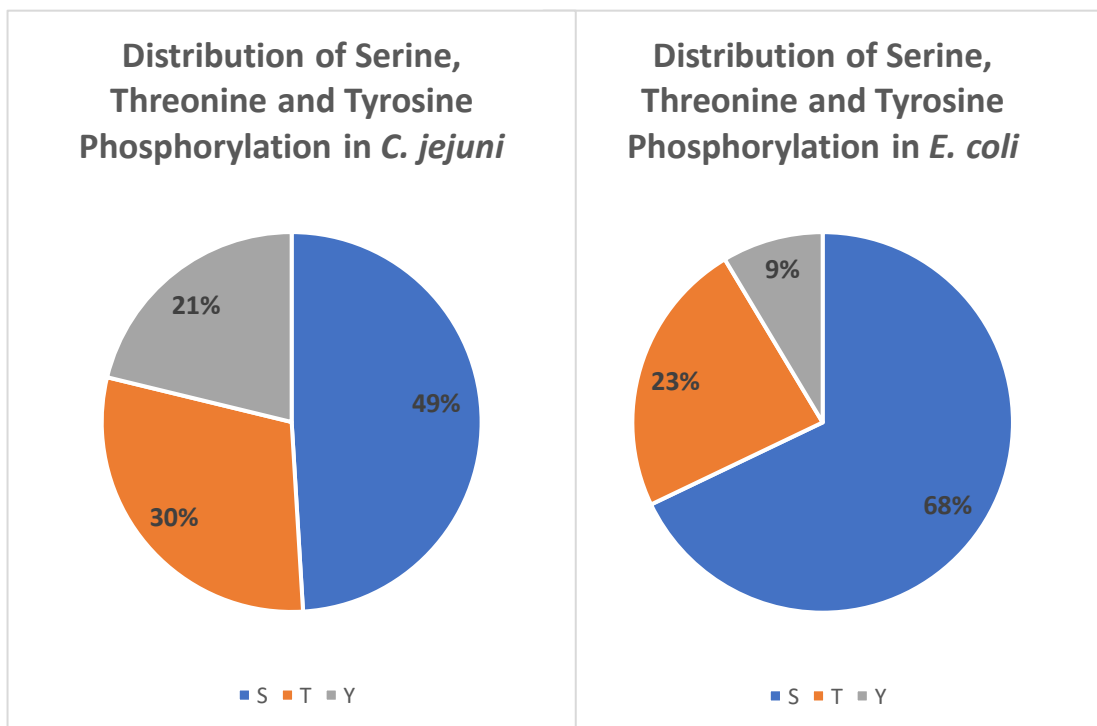


Figure 3.16 Distribution of phosphorylation on serine, threonine and tyrosine residues in *C. jejuni* and *E. coli*. Data taken from (Sultan et al., 2021).

Unfortunately, whilst comparing the variability of each individual dataset from WT and the Cj0184c mutant it was discovered that the peptide intensity data of only 3/5 WT replicates and 4/5 mutant replicates followed normal distribution and were comparable. For this reason, the other datasets were omitted from analysis to prevent missing potentially significant targets for further analysis. Using the remaining samples, we carried out statistical analysis in the form of T-testing. In the Cj0184c mutant we found 9 and 7 phosphopeptides with a significantly higher or lower abundance than WT. These phosphopeptides corresponded to 7 and 4 proteins with an increased or decreased abundance, respectively (figure 3.17).

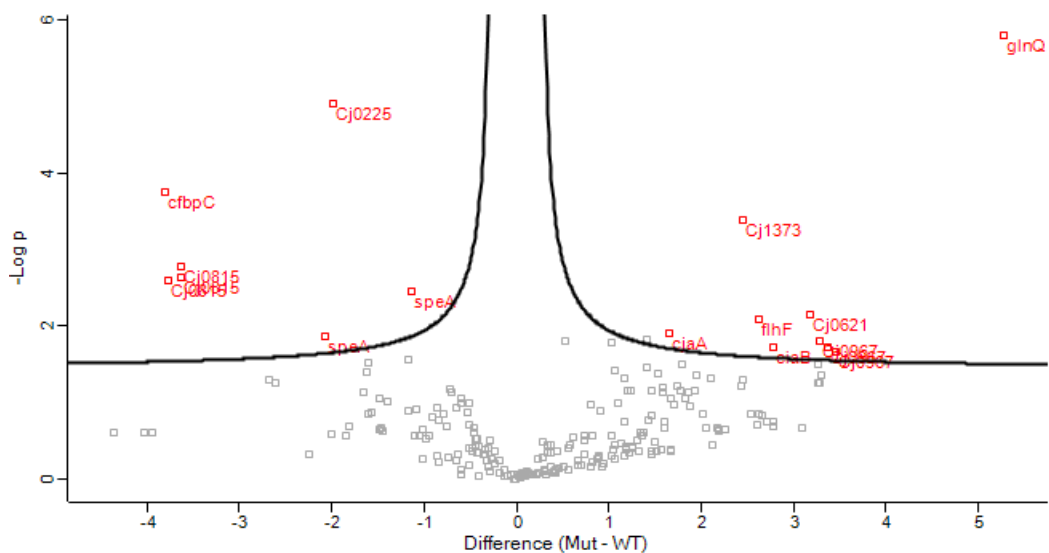


Figure 3.17 Volcano plot showing statistically significant phosphorylated peptides. Log students T-test values were plotted against the difference in p value between $\Delta 0184c$ and WT peptide samples. Proteins highlighted in red above the significance lines are those significant different in abundance (FDR=0.01).

As seen in table 3.3 the function of the significant proteins varied greatly and using multiple analytical tools no common pathways were identified. However, the most significant change in phosphorylation status occurred on glnQ, a putative ATP binding protein with homology to glnQ the ATPase in the ABC transport systems responsible for glutamine transport from other organisms. This is of interest based on the changes observed in the peptide profiling data where nitrogen metabolism pathways were significantly up regulated in the Cj0184c mutant strain. The predicted site of phosphorylation is at S80 with a score difference of 40.11.

Table 3.3 Proteins with a significant change in phosphorylation status in 11168Δ0184c vs WT

Protein names	Gene names	Student's T-test Difference Mut_WT
Putative glutamine transport ATP-binding protein	glnQ	5.2815
Putative periplasmic protein	Cj0967	3.4632
Uncharacterized protein	Cj0621	3.1844
CiaB protein	ciaB	2.7741
Flagellar biosynthesis protein FlhF	flhF	2.6220
Putative integral membrane protein	Cj1373	2.4469
Putative amino-acid transporter periplasmic solute-binding protein	cjaA	1.6612
Arginine decarboxylase	speA	-1.1333
Putative acetyltransferase	Cj0225	-1.9873
Uncharacterized protein	Cj0815	-3.7665
Putative iron-uptake ABC transport system ATP-binding protein	cfbpC	-3.8010

3.3 Discussion

The identification of the four putative kinases/phosphatases this study was based on homology to other characterised kinases and phosphatases as well as genome annotations. Preliminary experiments including the use of fluorescence based staining and western blotting methods were unable to show significant changes in the phosphorylation of proteins in cell free extracts resolved by SDS-PAGE. Growth data also showed all mutant strains grew like WT and the deletion of any of the four cognate genes, did not appear to reduce fitness in batch cultures. Therefore, any changes in phosphopeptide abundance are unlikely to be related to a growth rate phenotype and instead the result of the specific deletion. These preliminary experiments were designed to provide validation to select an enzyme candidate for further analysis using LC-MS/MS, a very expensive but sensitive technique. Whilst staining methods such as Pro-Q diamond are quick and inexpensive methods that can be readily performed, the sensitivity and specificity can be unreliable. It has been shown that non-phosphorylated proteins can be detected using stains such as Pro-Q diamond making interpretation difficult (Wang et al., 2014). An alternative method for observing phosphorylation is to use monoclonal antibodies (mAbs) against phosphorylated residues. However as seen in fig 3.8 and 3.9 our data did not reveal any obvious phosphatase targets in either anti-pY or anti-pT blots. Although, our results did indicate that a ~30kDa protein was dephosphorylated in the 11168 Δ 1258 strains. *Cj1258* encodes an LMW-PTP and therefore in theory deletion would result in an increase in phosphorylation. One explanation for this phenotype could be related to the functionality of BY-kinases. As discussed earlier BY-kinases and their cognate LMW-PTP are often found within the same operon, often directly downstream/upstream of one and other suggesting coordinated expression. This genomic organisation is common in gram negative bacteria (Cozzone et al., 2004). Typically, the operon also contains the proteins and enzymes involved in the production of exopolysaccharide or capsule. For example *wzb* and *wzc* are located together within a 19 gene operon responsible for the synthesis of colonic acid in *E. coli* (Stevenson et al., 1996). It has been shown that some protein-tyrosine kinases including *wzc* are much more active in polysaccharide synthesis in their dephosphorylated state (Vincent et al., 2000). Niemeyer & Becker (2001), have taken this one step further and shown that in *Sinorhizobium meliloti* the phosphorylation of one tyrosine residue in Wzc-like protein ExoP is affected by the phosphorylation state of other tyrosine residues effecting the levels of succinoglycan produced. This suggests that disruption of genes encoding either the kinase or phosphatase can disrupt the tightly regulated pathways BY-

kinases/phosphatase pairs belong to. Therefore, the phenotype seen in fig 3.8 could be explained by a reduction in kinase activity due to the absence of its cognate LMW-PTP, Cj1258. However, despite Cj1258 sharing 24.8% identity with Wzb the genomic organisation of *Cj1258* is dissimilar to LMW-PTP organisation in other organisms. No cognate kinase is found in the same operon and sequence analysis has not revealed any putative targets for a cognate kinase in the entire genome. Despite no obvious phosphatase phenotypes and unconventional genomic organisation, enzymatic assays using phospho-tyrosine analogue, *p*-nitrophenyl phosphate, confirmed Cj1258 to be tyrosine phosphatase. The determined K_m and V_{max} values are consistent with LMW-PTPs in other organisms such as *E. coli* Wzb (Vincent et al., 1999). At this point in the study Cj1258 could be suggested to be the ideal candidate for further investigation using the mass spectrometry approach described in figure 3.11. However, data that will be discussed in chapter 4 also indicated that another putative enzyme in the study possessed phosphatase activity. DIFMUP (section 2.12.2) was used as a substrate to explore phosphatase activity for other residues. The results of this preliminary experiment indicated that Cj0184c possessed phosphatase activity. As discussed Cj0184c also has a novel structure indicative of a potential dual function. The proven phosphatase activity of Cj0184c in combination with its novel structure made this an appealing candidate for further investigation. In addition, knowing that the typical distribution of phosphorylated serine, threonine and tyrosine residues in *E. coli* is 67.9%, 23.5% and 8.6%, respectively, a putative S/T phosphatase is likely to provide more significant changes in a phosphoproteome dataset. For this reason, Cj0184c was selected to be the first candidate for phosphopeptide analysis by LC-MS/MS against WT. If the mass spectrometry technique proved valuable and highly sensitive the approach would be repeated with Cj1258 to identify the likely smaller percentage of the proteome subject to regulation by phosphorylation on tyrosine residues.

The essentiality of *Cj0668* prevented the construction of a deletion mutant strain. For this reason it will not be possible to analyse the phosphoproteomes of this strain using LC-MS/MS. *Cj0668* is of particular interest due to its homology to the YdiB/YjeE family (UPF0079 UniprotKB database family). A recent study by Nguyen et al. (2017) suggests enzymes belonging to this family could act as ubiquitous bacterial kinases (UbK) and YdiB has been shown to phosphorylate Ser, Thr and Tyr residues with a HxD motif reminiscent of hanks type protein kinases. No putative kinases have been identified in the NCTC11168

genome and therefore it is plausible that phosphorylation in *C. jejuni* on Ser, Thr and Tyr could be solely performed by *Cj0668* acting as a UbK.

Unfortunately, due to the highly complex nature of the samples as well as the selectivity of metal ions we struggled with reproducibility and comparable replicates within our trial mass spectrometry data. One explanation of this could be contamination by DNA/RNA and/or non-specific binding of non-phosphorylated peptides. Therefore, we introduced a benzonase nuclease treatment step after sonication to degrade all forms of DNA and RNA with no proteolytic activity. A methanol, chloroform precipitation step was also introduced to help remove other potential contaminants such as lipids from the peptide samples. These steps were not previously implemented when performing a similar workflow studying acetylation in *C. jejuni* (Puttick et al., (unpublished)). A separate issue with the trial data was a decline in the number of phosphopeptides in samples in sequential processing order. This was most likely a methodological problem related to the order the samples were prepared. Originally the samples were desalted individually in order from sample 1-5. In order to attempt to prevent a loss of phosphopeptides during storage on ice all samples were simultaneously desalted using a vacuum manifold to prevent a sequential loss of phosphopeptides in the samples. Despite all the changes above the trial data remained unconvincing and no significant changes in phosphopeptide intensity were identified without omitting multiple replicates from the data set. However due to time constraints, expense and no further solutions for improving the issue a complete run was performed comparing 5 WT replicates against 5 mutant replicates.

The proteome profile for both the WT and 11168 Δ 0184c strain revealed the presence of 1312 proteins in the peptide samples for phosphopeptide enrichment. As seen the key changes in protein expression are in genes involved in glutamine/glutamate metabolism and capsule biosynthesis genes. The increase in glutamine and glutamate synthase suggests that deletion of *Cj0184c* could affect glutamine/glutamate metabolism and perhaps phosphorylation is therefore a key regulatory step in either the transport or metabolism of glutamine/glutamate. Additionally, the *C. jejuni* CPS is composed of complex heptoses and O-methyl phosphoramidate (MeOPN). MeOPN is a nitrogenous structure that is ultimately derived from glutamine (McNally et al., 2007) and therefore a link between glutamine metabolism is common in both these changes. *Cj1422* is known to encode a transferase

responsible for the addition of MeOPN to C-3 of β -D-GalNAc or to C-4 of D-glycero- α -L-gluco-Hep (McNally et al., 2007) and *Cj1419* and *Cj1429* could also have a role in capsule biosynthesis based on their predicted functions and locality to capsule biosynthesis genes in the genome. The phosphoproteome data further adds weight to these findings with the most significant hit being GlnQ, the ATPase in the GlnPQ ABC transport system. In the 11168 Δ 0184c mutant the abundance of GlnQ peptides phosphorylated at S80 is significantly increased compared to WT. One potential scenario could be that *Cj0184c* is a S/T phosphatase responsible for the dephosphorylation of GlnQ at S80. Therefore, the deletion of *Cj0184c* results in the permanent phosphorylation of GlnQ inhibiting glutamine transport causing an increase in expression of glutamine and glutamate synthase genes. In this scenario phosphorylation is a post-translational modification responsible for the regulation of glutamine transport. The relationship between *Cj0184c* and GlnQ will be explored further in chapter 4.

The current data set identified 679 and 320 phosphopeptides and phosphoproteins, respectively. This is much higher than published phosphoproteomes from other organisms such as *E. coli*. Only 127 phosphopeptides were identified in a recent study by Sultan et al. (2021), with a distribution of 67.7% occurring on serine, 28.31% on threonine and 3.94% on tyrosine. Our dataset had a similar trend with the majority of phosphorylation events being observed on serine (49%), followed by threonine (30%) and lastly tyrosine (21%). This perhaps suggests that phosphorylation is a major regulatory modification in *Campylobacter jejuni* with a higher than usual dependence on tyrosine phosphorylation. The *C. jejuni* genome is only 1.6 Mbp with a small number of known transcriptional regulators (Parkhill et al., 2000) therefore perhaps *C. jejuni* is reliant on extensive post-translational modifications such as phosphorylation to regulate and respond to stimuli in order to survive and thrive in multiple environmental niches. In comparison the *E. coli* genome is much larger and therefore more regulation can occur at the transcriptional level. However, the strength of the phosphorylation data is debatable. There was a lack of reproducibility between some replicates and a single replicate from the 11168 Δ 0184c strain and two replicates from the 11168 strain were removed from analysis in order to provide significant results which could be interpreted. The mass spectrometry process was performed multiple times introducing extra steps for purity however the data's reliability did not improve significantly. It is therefore a possibility that a proportion of this data could be non-specific binding during the IMAC or even chemical phosphorylation occurring. The time constraint

that this project needed to be completed by and the funds available restricted how much more time could be spent on mass spectrometry. It was decided that with the current data sets providing significant hits and patterns in relation to glutamine/glutamate metabolism and capsule biosynthesis that the project would progress to exploring these significant targets. Therefore, further work was focused on the relationship between Cj0184c and GlnQ.

Chapter 4: The relationship between Cj0184c and GlnQ

4.1 Introduction

Following the discovery that Cj0184c potentially dephosphorylates S80 on GlnQ an annotated glutamine transport ATPase in NCTC11168, we decided to investigate this relationship and the functions of both proteins. Firstly, we explored the current modes of glutamine transport in *C. jejuni*. As mentioned above, a study by Lin et al. (2009) has shown that the pathogenesis-associated glutamine (Paa) ABC transporter system is responsible for glutamine uptake in *C. jejuni* 81-176. The ABC transporter permease is encoded by *cj0467-68* and the ATPase by *cj0469*. These proteins are 43% and 60% identical to GlnP in *E. coli* and GlnQ in *Streptococcus pneumoniae*, respectively (Parkhill et al., 2000). The deletion of either the ABC transporter permease (*paqP*) or the ATPase (*paqQ*) resulted in glutamine transport levels <50% compared to WT. An intermediate glutamate transport phenotype was also observed. The mutants were also defective in the uptake of cysteine and aspartate to a lesser extent. Microarray analysis has also revealed that the levels of *Cj0467-69* mRNA are increased during INT407 cell infection suggesting a potential role for glutamine ABC transporters in pathogenesis (Gaynor et al., 2005). An increased resistance to limited CO₂ and selected reactive oxygen species is also seen in $\Delta paqP$ and $\Delta paqQ$ mutants, however no significant differences in adherence, invasion or intracellular survival (Lin et al., 2009). The increased resistance to the ROS generating agent, tert-butylhydroperoxide (t-BOOH), is comparable to *ggt*-deficient *C. jejuni* mutants which exhibit increased invasion efficiency associated with H₂O₂ resistance (Barnes et al., 2007). It is therefore plausible that ROS resistance could be linked to glutamine transport in *C. jejuni*. GGT is a periplasmic enzyme responsible for the hydrolysis of glutamine to glutamate followed by uptake via the Peb system. The glutamate can in turn be converted back to glutamine in the cytoplasm via the incorporation of ammonia catalysed by glutamine synthetase (GS) at the expense of one ATP molecule. A Δggt mutant has been shown to be defective in mouse colonization however no significant differences in colonization were observed in the $\Delta paqP$ and $\Delta paqQ$ mutants (Hofreuter et al., 2006; Lin et al., 2009). Despite the characterisation of the PaqPQ system a periplasmic amino acid binding protein for the ABC transporter system remains unidentified. One study has suggested that the putative cysteine binding protein, CjaA is PaqPQ amino acid binding protein. This is based on the orthologues of CjaA (*Cj0982*) and the PaqPQ system (*Cj0467 – Cj0469*) all being part of the same operon in *H. pylori* (Müller et al., 2005). The designation of CjaA as a cysteine binding protein despite its similar

structure to a glutamine binding protein from *E. coli* is based on the discovery of cysteine in the binding pocket of the CjaA crystal structure (Müller et al., 2005).

A second potential ABC transporter system for Gln exists in *C. jejuni* known as the GlnPQ system comprised of a permease (GlnP) and an ATPase (GlnQ). A potential amino acid binding protein has also been annotated as GlnH. This system has been annotated based on homology to GlnPQ systems in other organisms including *E. coli* GlnP (37.5%) and *Bacillus stearothermophilus* GlnQ (56.2%). The *Cj0467-69* operon which encodes the PaqPQ system also shares high identity to Cj0902 (GlnQ) and Cj0940 (GlnP). Cj0467 and Cj0468 share 33% identity with Cj0940 and Cj0469 share 55% identity with Cj0902 (Parkhill et al., 2000). The GlnPQ system in *C. jejuni* has not been characterised; however based on homology and unpublished observations by Lin et al. (2009) including competition assays which suggest a redundancy for glutamine transport in *C. jejuni* exists, it is plausible to suggest the annotated GlnPQ system is likely a glutamine transport system. Interestingly another annotated permease (Cj0901) exists in the same operon as GlnQ (Cj0902). Typical permeases are expressed from the same operon and therefore this permease was also investigated in this study despite sharing no significant similarity to *E. coli* GlnP.

As well as glutamine transport the phosphoproteomic analysis of $\Delta 0184c$ against WT also revealed a number of significant changes in proteins associated with capsule biosynthesis. The *C. jejuni* CPS is composed of complex heptoses and phase variable O-methyl phosphoramidate modifications present in up to 70% of *C. jejuni* isolates (Karlyshev et al., 2005; McNally et al., 2007). In this chapter we will be exploring the putative role of S/T phosphatase Cj0184c and how the dephosphorylation of GlnQ may regulate glutamine transport and capsule biosynthesis.

4.2 A model for the relationship between Cj0184c and GlnQ

Based on the phosphoproteomic and peptide profiling data from chapter 3 a model was devised that incorporated multiple significant clusters of proteins up/down regulated or significantly phosphorylated in response to deletion of *Cj0184c*. As seen in fig 4.1 we propose that both the PaqPQ and GlnPQ ABC systems are responsible for the transport of glutamine perhaps in a redundant manner or subject to regulation in response to different stimuli. For example, we suggest the phosphatase Cj0184c could be regulated by levels of cytidine diphosphate (CDP) in the cytoplasm. CDP is involved in the biosynthesis of MeOPN and could interact with the nucleotide/nucleoside binding domain in Cj0184c. Therefore, we suggest that binding of CDP nucleosides to the N-terminal domain could cause a conformational change in structure inhibiting the activity of the C-terminal phosphatase domain. However, when levels of these capsule specific nucleoside substrates are low the loss of binding to Cj0184c could activate the phosphatase domain triggering the dephosphorylation of S80 on GlnQ. The dephosphorylation of S80 could be essential to allow GlnQ to dock with GlnP and allow the ATP-dependent transport of glutamine into the cytoplasm. S80 is located within a looped region of the ATPase which interacts with GlnP. We also suggest GlnH could be a promiscuous amino acid binding protein capable of delivering glutamine to either system.

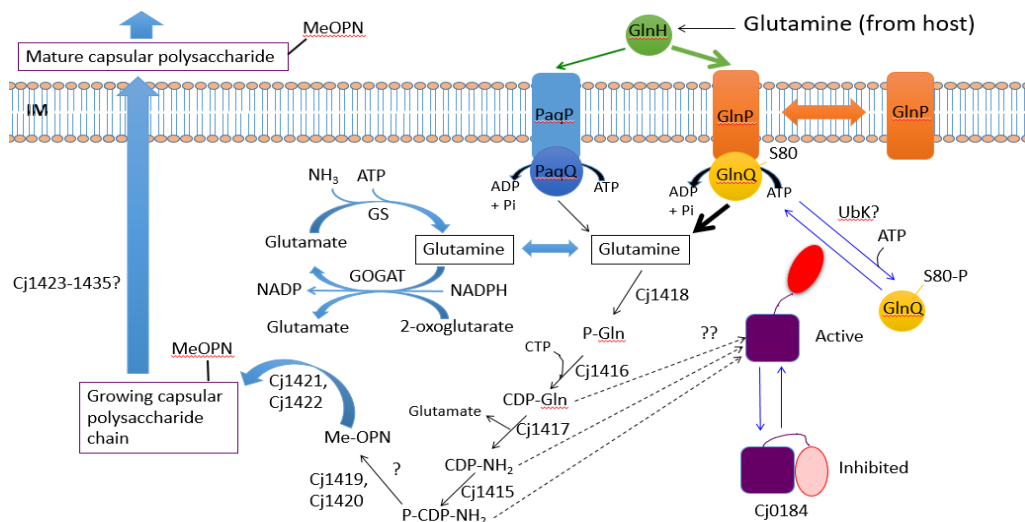


Figure 4.1 *C. jejuni* glutamine transport model. *GlnH* binds and delivers glutamine to *GlnP* (preferentially) and *PaqP* for active transport into the cytoplasm driven by *GlnQ* and *PaqQ*, respectively. *GlnQ* activity is regulated by the phosphatase *Cj0184c*. Phosphorylation of serine 80 in *GlnQ* prevents docking to *GlnP* and thus reduces glutamine uptake. However activated *Cj0184c* can dephosphorylate *GlnQ* allowing glutamine uptake. The activity of *Cj0184c* is regulated by CDP intermediates in the Me-OPN synthesis pathway derived from glutamine.

4.3 Results

4.3.1 Overexpression and purification of Cj0184c and S/T Phosphatase Assay

Several overexpression plasmids (using pET28a/pET21a vectors) containing Cj0184c with a terminal His₆ tag under an IPTG inducible promoter were constructed, to explore the phosphatase activity of both domains as well as the native protein. Additionally, Cj0184c is known to exist in two forms (1) a 384 aa protein and (2) a 394 aa extended protein. This extension exists in a range of isolates after *in vitro* and *in vivo* passage at a frequency ranging between 41.9-50.6% (Thomas et al., 2014). As seen in figure 4.2 a GT deletion induces a shift of the stop codon and results in the addition of ten amino acids (V* -> IEIKNQIYKKK). For this reason, four separate expression vectors were designed and constructed (1) pET28a_Cj0184c, native version (2) pET28a_Cj0184cE, extended version (3) pET21a_Cj0184cNB, N-terminal nucleotide/nucleoside binding domain only and (4) pET-21a_Cj0184cPPP, C-terminal phosphatase domain only (extended). Figure 4.3 shows all 4 constructs and the regions cleaved to isolate the N-terminal and C-terminal domains. In the C-terminal phosphatase domain version all 3 conserved motifs of the PPP family remained intact.



Figure 4.2 GT deletion induces a shift of stop codon and 10 amino acid extension in Cj0184c. Start codon (green), GT (yellow) and stop codon (red).

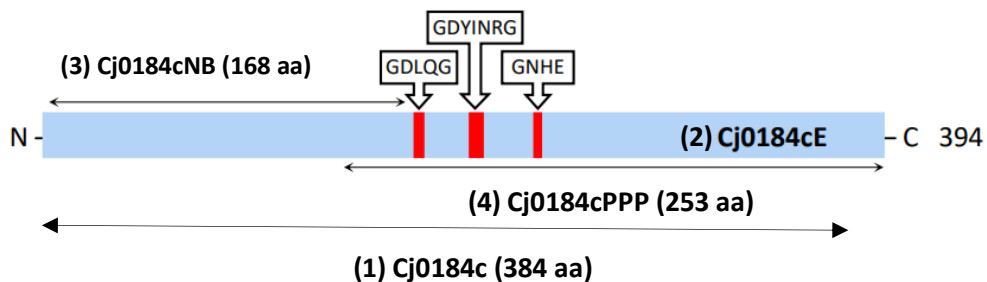


Figure 4.3 Cj0184c constructs and protein organisation. Conserved protein phosphatase (PPP) motifs are highlighted in red.

All constructs were transformed into *E. coli* BI21 (DE3) and induced as standard with IPTG. Cell-free extracts were applied to a HisTrap™ HP affinity column, which was used to purify Cj0184c fractions from a gradient of elution buffer from 50 - 500 mM imidazole. Unfortunately, as seen in figure 4.4 Cj0184c and Cj0184cE were eluted early in the elution gradient along with other non-specifically bound proteins. In an attempt to reduce non-specific interactions, the NaCl concentration in the binding and elution buffer was increased to 1 M and the imidazole concentration reduced to 300 mM in the elution buffer to extend the elution profile. Neither of these changes increased the purity of the eluted fractions or prevented early elution. This suggests that the position of the N-terminal His₆ tag could be partially inaccessible to the column. A C-terminal His₆ tag was trialled however it was found to interfere with the C-terminal phosphatase activity of the native Cj0184c version. Therefore, the impure fractions in figure 4.4 were assayed for phosphatase activity and those with significant activity were pooled and concentrated into 1 ml storage buffer. The CFE was used as a negative control for phosphatase activity.

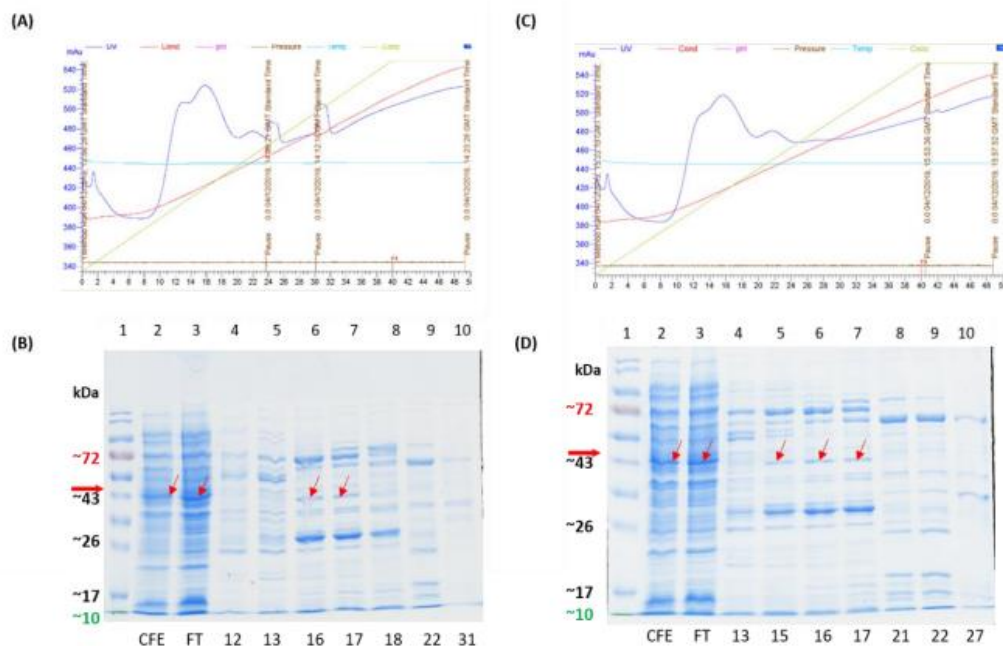


Figure 4.4 Purification of Cj0184c and Cj0184cE (A) Elution profile of Cj0184cE and (B) Cj0184c from ~25ml of *E. coli* pET21a_0184c/E cell free extract (CFE) from 4L of LB culture. Elution took place over 40 ml along an imidazole gradient (50-300mM) (B) SDS-PAGE of Cj0184cE and (C) Cj0184c peak fractions. Lane 1 (5µl of EZ-RUN™ pre-stained Rec protein ladder), lane 2 (10µl *E. coli* pET21a_0184c/E CFE), lane 3 (10µl of flow through from CFE loading onto AKTA), lane 4 - 10 (10µl of relevant fractions). Cj0184c/E (red arrow).

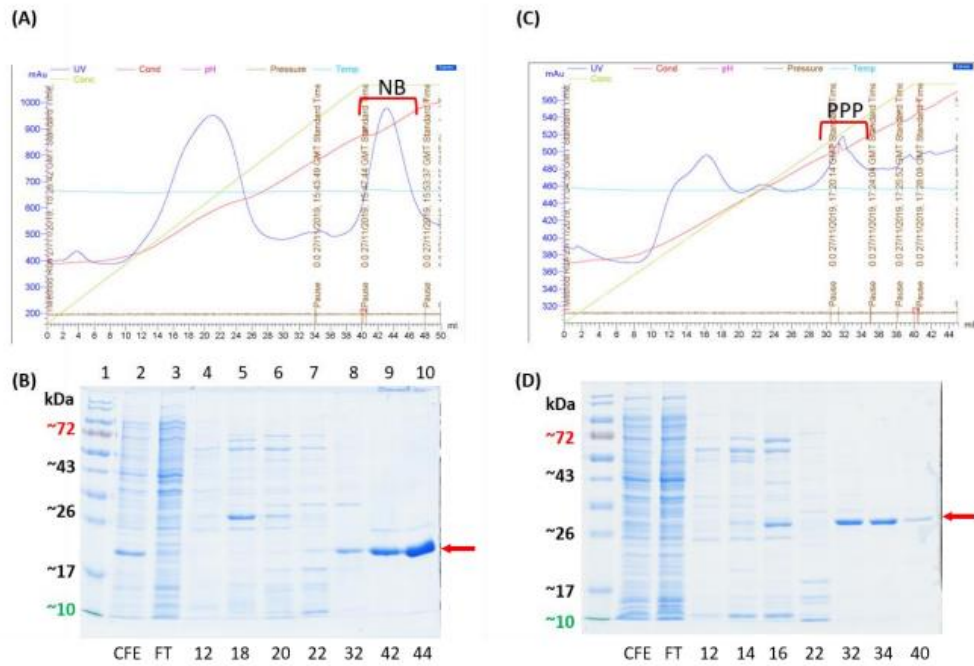
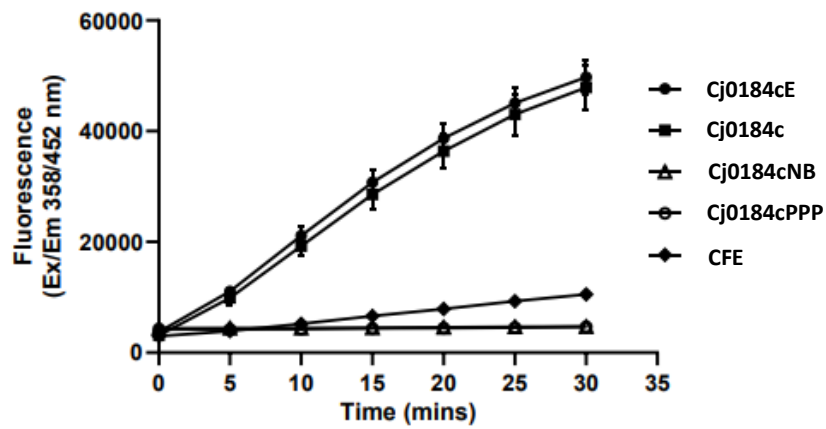


Figure 4.5 Purification of Cj0184cNB and Cj0184cPPP (A) Elution profile of Cj0184cNB and (B) Cj0184cPPP from ~25ml of *E. coli* pET21a_0184c/E cell free extract (CFE) from 4L of LB culture. Elution took place over 40 ml along an imidazole gradient (50-500mM) (B) SDS-PAGE of Cj0184cNB and (C) Cj0184cPPP peak fractions. Lane 1 (5 μ l of EZ-RUN™ pre-stained Rec protein ladder), lane 2 (10 μ l *E. coli* pET21a_0184cNB/PPP CFE), lane 3 (10 μ l of flow through from CFE loading onto AKTA), lane 4 - 10 (10 μ l of relevant fractions). Cj0184cNB/PPP (red arrow).

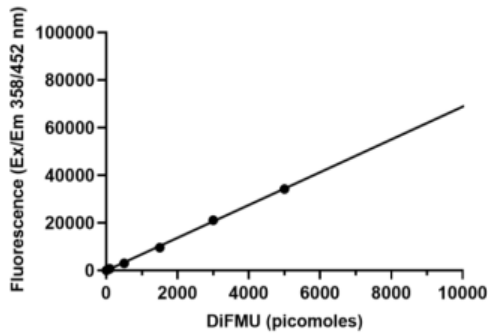
Cj0184cNB and Cj0184cPPP, both with a C-terminal His₆ tag, were purified from the CFE of *E. coli* BL21 (DE3) (figure 4.5). The proteins eluted far later in the elution gradient and therefore a much higher degree of purity was achieved with these constructs. The level of purity allowed us to concentrate purified fractions into storage buffer and determine the protein concentrations for specific enzyme kinetics.

The concentrations of the final purified protein samples were normalised and then used in a phosphatase assay using the fluorogenic substrate DiFMUP. The dephosphorylated product of DiFMUP can be measured using an excitation/emission maxima combination of 358/450 nm. As seen in figure 4.6 the specific activity of each Cj0184c version was calculated using linear regression analysis of data fitted to a DiFMU standard curve. The specific activity of the CFE from BL21 acting as a negative control was subtracted from the calculated specific activity of the impure Cj0184c and Cj0184cE samples. As seen in figure 4.6 the entire protein is required for phosphatase activity and the genomic GT deletion does not result in either a significant increase or decrease in phosphatase activity.

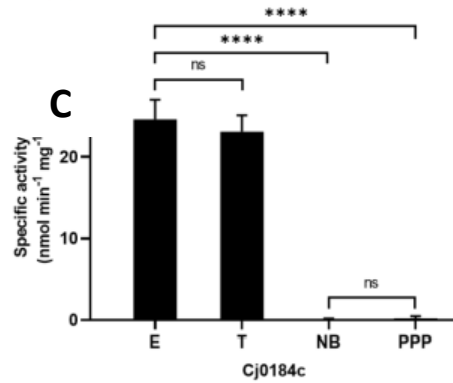
A



B



(B)



C

Name of Cj0184c protein	Specific activity (nmol min ⁻¹ mg ⁻¹)
Cj0184cE	24.61
Cj0184cT	23.11
Cj0184cNB	0.14
Cj0184cPPP	0.25

Figure 4.6 Phosphatase activity of Cj0184c proteins. (A) Enzyme activity was determined by monitoring the change in fluorescence every 5 minutes over 30 minutes. Cj0184c proteins (10 µg) were incubated with DiFMUP (100 µM) at 37 °C in 1x PP-1 reaction buffer, pH 5.0 (EnzChek®). (B) DiFMUP standard curve generated using control strip containing reference standards (0-5000 picomoles). (C) Specific activity of Cj0184c proteins calculated using reference standards. Data points are the means of 3 independent replicates with error bars showing standard deviation. **** $P \leq 0.0001$, ns indicates not statistically significant.

4.3.2 11168 Δ 0184c Sensitivity to Reactive Oxygen Species (ROS)

An assay for sensitivity to ROS was performed on the Δ 0184c mutant to try and establish a link between Cj0184c and known phenotypes of current glutamine transporter deletion mutants. In theory if dephosphorylation by Cj0184c was a regulatory step in glutamine transport by the GlnPQ system then it might be expected to observe similar phenotypes in the Δ 0184c mutant as those seen in Δ Cj0467 and Δ Cj0469 mutants (Lin et al., 2009). The assay performed was sensitivity to hydrogen peroxide (H_2O_2), as an increase in resistance to specific ROS was seen in the Δ Cj0467 and Δ Cj0469 mutants. As seen in figure 4.7 there was no significant difference in the sensitivity of Δ 0184c compared to WT suggesting the stress responses linked to H_2O_2 are not regulated by Δ 0184c.

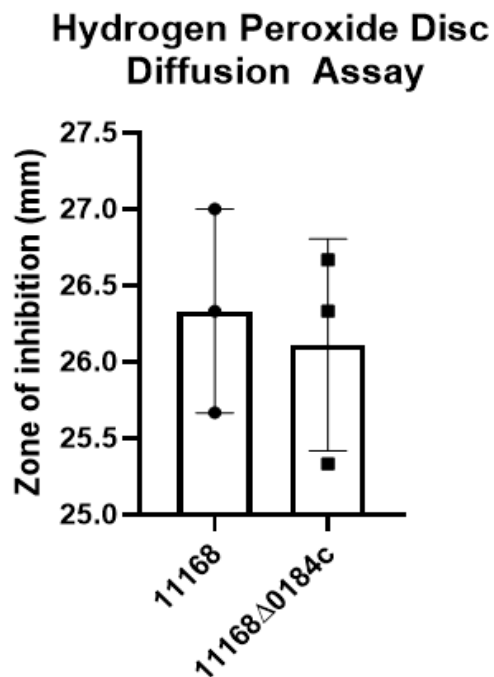


Figure 4.7 Disc Diffusion Assay with H_2O_2 . *C. jejuni* cells were grown in BTS broth to midlog phase and used to inoculate MH agar to 0.1 OD_{600nm} . Once set, sterile discs soaked in 2M H_2O_2 were placed in triplicate. Data points are the means of 3 independent replicates with error bars showing standard deviation.

4.3.3 Growth on glutamine

It is generally accepted that *C. jejuni* cannot grow on glutamine as a sole carbon source. However van der Stel et al. (2015) observed that a *ggt* mutant can reach higher OD_{600nm} when grown on DMEM plus glutamine compared to DMEM alone (Stel et al., 2015). This shift in optical density could therefore be used to measure growth on glutamine. As seen in figure 4.8 when NCTC11168 was grown on a variety of carbon sources (20 mM) alone and in combination with glutamine (5 mM), growth on glutamate as a sole carbon source was the most optimal perhaps due to glutamate's role in glutamine synthesis via the GS:GOGAT cycle. Serine as expected was also a good sole carbon source. As expected growth on glutamine was negligible however as reported by van der Stel et al. (2015), when glutamine was added to minimal media in combination with any one of the 5 alternative carbon sources a significant increase in the final optical density was observed.

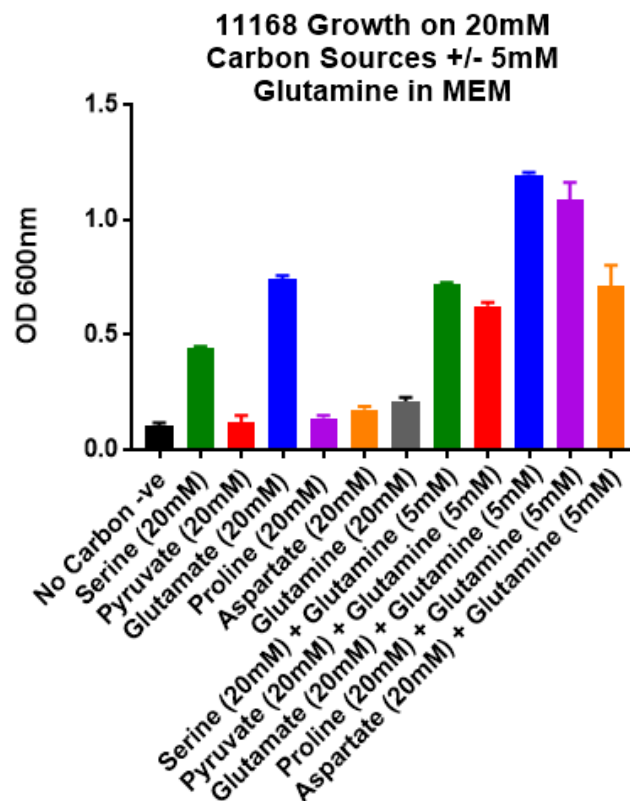


Figure 4.8 11168 growth on alternative carbon sources in combination with glutamine. *C. jejuni* cells were grown in BTS broth to mid-log phase and used to inoculate minimal media cultures to 0.1 OD_{600nm} in triplicate. Cultures were grown on carbon sources 20 mM +/- glutamine 5 mM. Data points are the means of 3 independent replicates with error bars showing standard deviation.

11168 and 11168 Δ 0184c were grown in minimal media with multiple carbon sources with and without glutamine to explore the putative role of Cj0184c in glutamine transport. As seen in fig 4.9 when grown on serine a shift in optical density is observed when 5 mM glutamine is present in the media. However, in the 11168 Δ 0184c strain this shift is also observed suggesting that glutamine transport systems are still functional in this strain. This same experiment was repeated using proline, glutamate and pyruvate. When grown on proline the shift in optical density was significantly reduced in the 11168 Δ 0184c strain and an intermediate phenotype was seen on glutamate. Importantly, these phenotypes were reversed in the complemented strains. Similar to growth on serine when grown on pyruvate no significant change in growth compared to wild-type was observed.

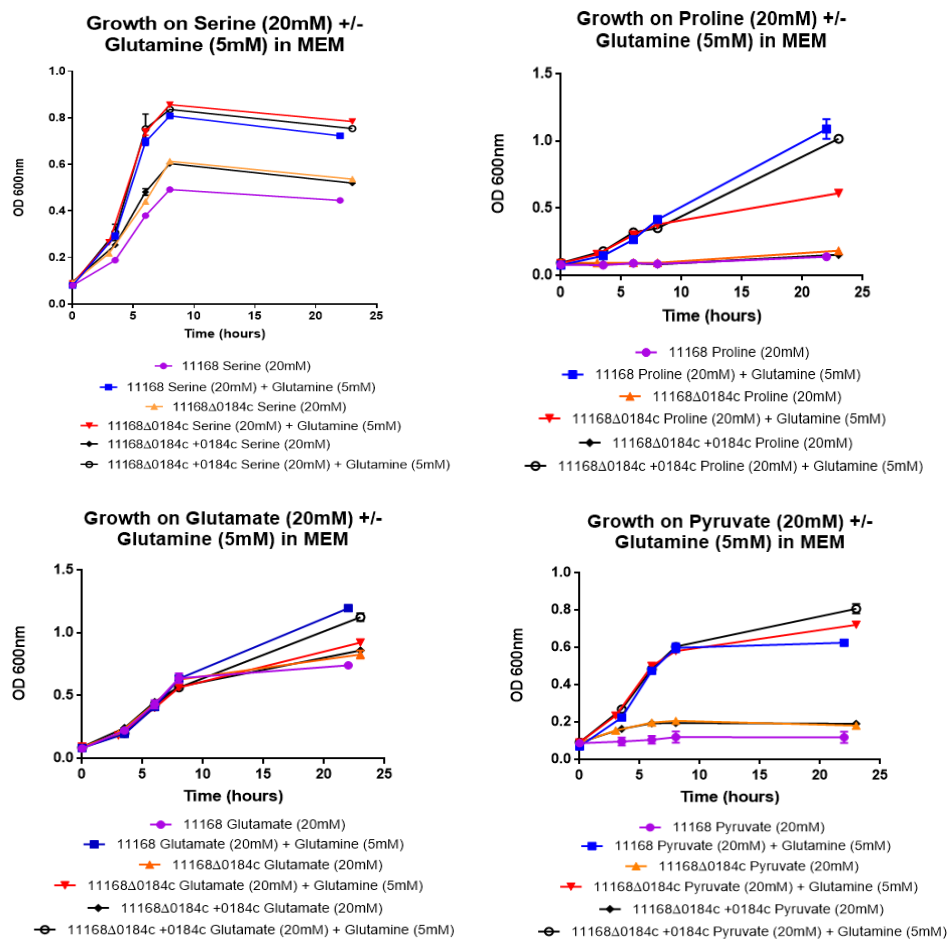


Figure 4.9 11168 Δ 0184c growth on glutamine. *C. jejuni* cells were grown in BTS broth to mid-log phase and used to inoculate minimal media cultures to 0.1 OD_{600nm} in triplicate. Cultures were grown on carbon sources 20 mM +/- glutamine 5 mM. Data points are the means of 2 independent replicates with error bars showing standard deviation.

4.3.4 *paqPQ* and *glnPQ* Mutant Construction

To test the role of GlnQ in glutamine transport directly rather than indirectly through the deletion of *Cj0184c*, deletion mutants were constructed in *glnP* and *glnQ*. The results in section 4.3.3 suggest that GlnQ potentially does have a role in glutamine transport based on the reduction in optical density shift when grown on proline plus glutamine compared to proline alone in the 11168 Δ 0184c strain vs 11168. Although, a shift in optical density is still observed. However, when grown on serine plus glutamine no difference in growth is observed between 11168 and 11168 Δ 0184c. These results suggest that (1) if the GlnPQ system is involved in glutamine transport it is only under certain conditions such as growth on proline and (2) another system must exist such as the PaqPQ system responsible for glutamine transport in conditions such as growth on serine. (3) finally, a redundancy in glutamine transport may be present even when the GlnPQ system is functional based on only a reduced phenotype when grown on proline plus glutamine and not a complete loss of phenotype as would be expected if the sole glutamine transport system was inactive. Based on the findings of Lin et al. (2009) the PaqPQ system is most likely to be the alternative route for glutamine to enter the cell in 11168. Therefore, deletion mutants were also constructed in *paqP* and *paqQ* as well as a double mutant deleting both ABC transport systems from 11168. In theory we would expect to observe a reduced shift in OD_{600nm} when grown on glutamine in either a *paqPQ* or *glnPQ* deletion mutant strain. However, in the double mutant removing both systems we would expect to observe a complete loss of OD shift when grown on glutamine.

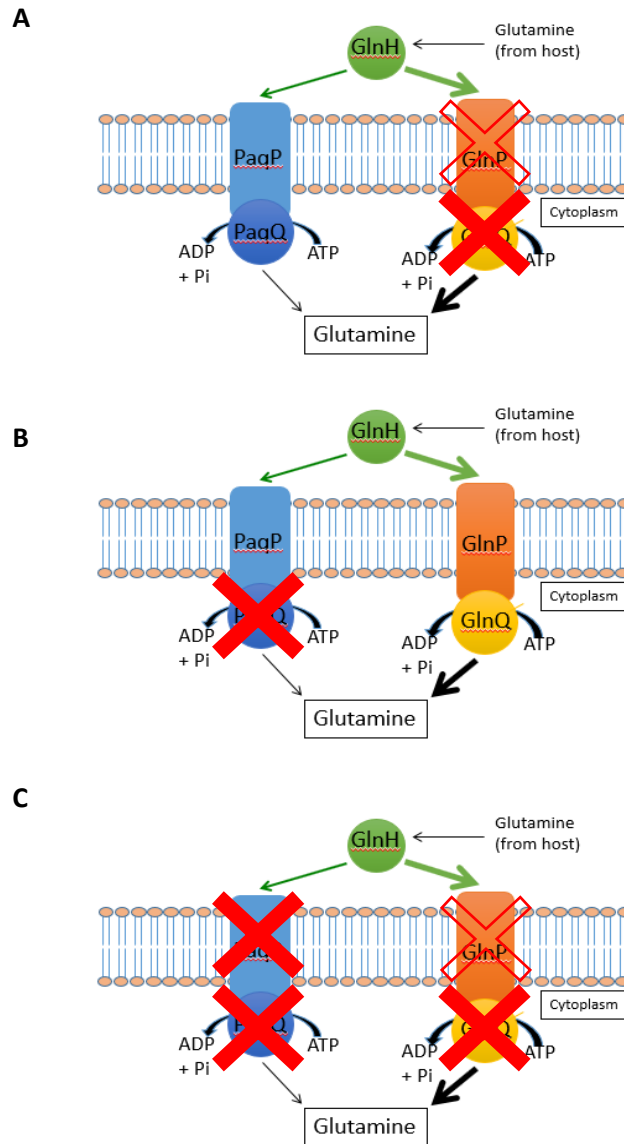


Figure 4.10 Glutamine transport mutant construction. Red filled cross indicates the deletion of gene, clear filled red cross indicates the deletion of *cj0901* a putative permease which could be a heterodimer to *glnP*. Deletion of *cj0901* was possible with one antibiotic cassette insertion and therefore deleted instead of *cj0940c* (annotated *glnP*) (A) 11168 Δ 0901-0902 ($\Delta glnPQ$) (B) 11168 Δ 0469 ($\Delta paqQ$) and (C) 11168 Δ 0901-0902 Δ 0467-0469 ($\Delta glnPQ\Delta paqPQ$).

4.3.5 Glutamine ABC Transporters and growth on glutamine

Both putative glutamine transport systems were individually deleted from the 11168 genome. The mutant strains were then grown on pyruvate (20 mM) with and without glutamine (5mM). As seen in figure 4.11 neither deletion resulted in a reduction in OD_{600nm} compared to WT when grown on glutamine. Interestingly we observed a small but significant increase in growth in the 11168 Δ 0469 strain when grown on glutamine. One explanation for the lack of growth defect when grown on glutamine in either mutant could be that the alternative system is acting in a redundant manner. When grown on glutamate no significant shift in optical density was observed. Growth on glutamate acts as a control as the glutamate can be converted to glutamine in the cytoplasm by glutamine synthetase. Therefore, we would not expect any changes in growth when grown on glutamate with or without glutamine.

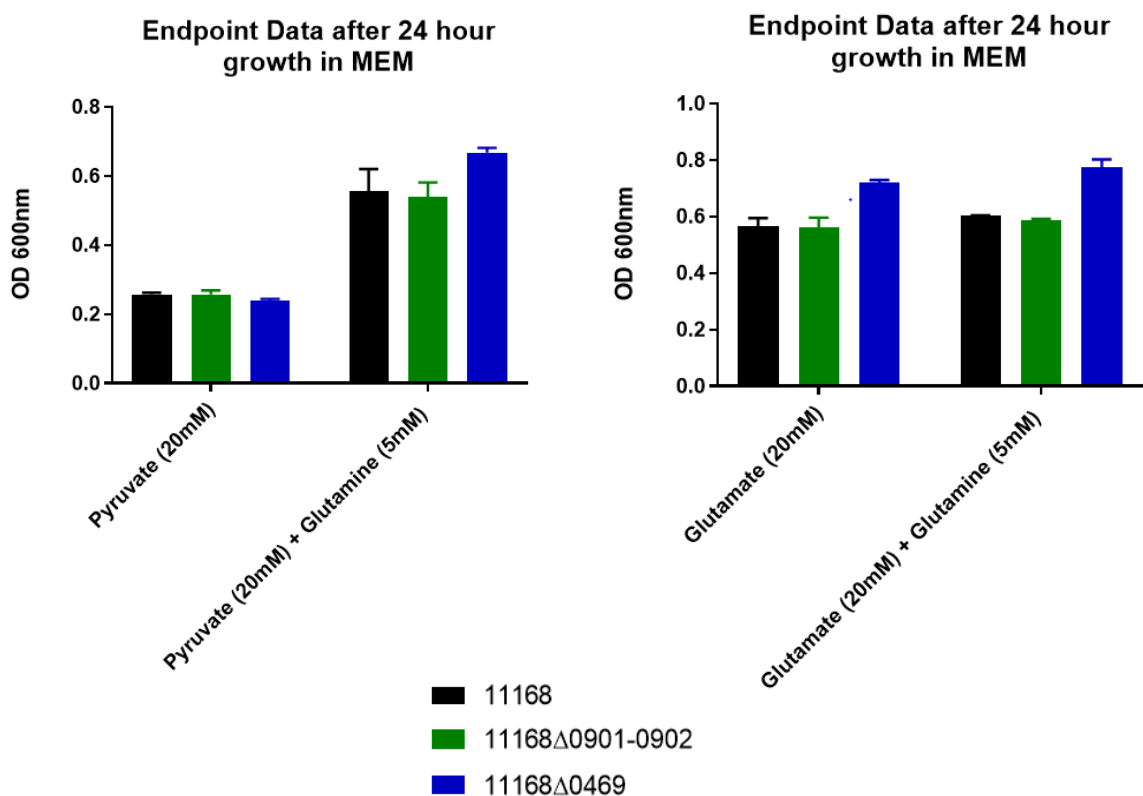


Figure 4.11 Glutamine transport mutant growth on glutamine *C. jejuni* cells were grown in BTS broth to mid-log phase and used to inoculate minimal media cultures to 0.1 OD_{600nm}. Cultures were grown on pyruvate 20 mM +/- glutamine 5 mM. Data points are the means of 2 independent replicates after 24 hours with error bars showing standard deviation.

As seen in figure 4.12 the mutant strain lacking both the GlnPQ and PaqPQ systems was also unaffected by growth on glutamine. This data suggests that neither system is involved in glutamine transport under these conditions. Whilst growth experiments are a routine and accessible method for measuring growth on a specific substrate, due to the complex nature of the media a more specific approach may be more appropriate to measure glutamine transport such as a glutamine uptake assay using radiolabelled glutamine.

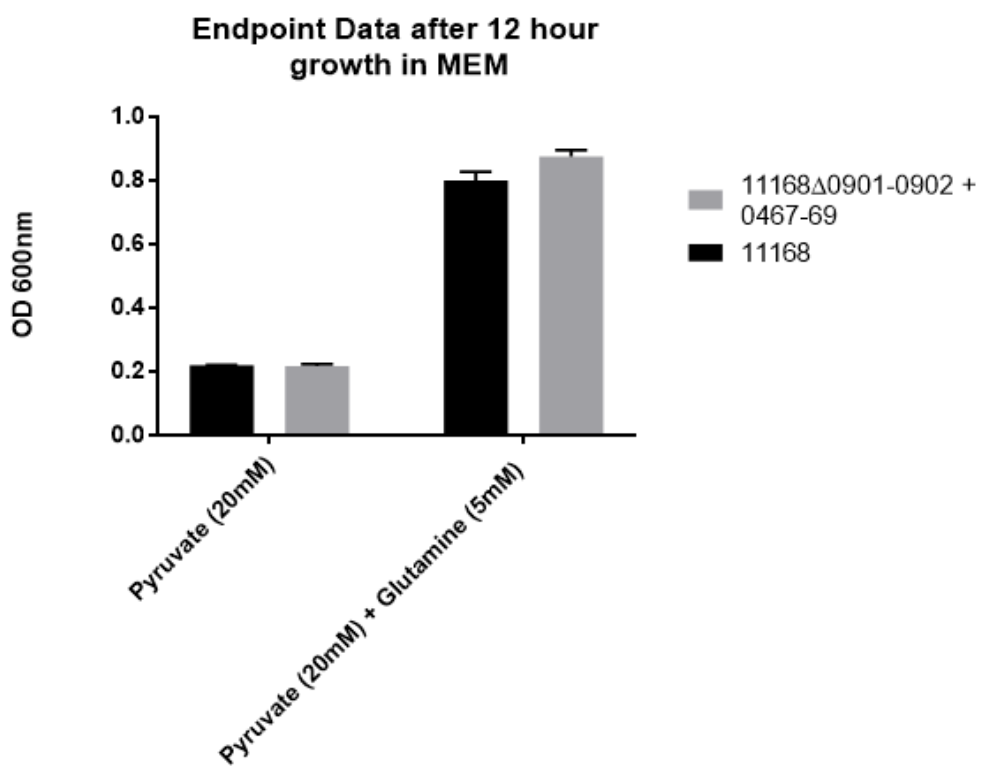


Figure 4.12 Δ glnPQ Δ paqPQ double mutant growth on glutamine. *C. jejuni* cells were grown in BTS broth to mid-log phase and used to inoculate minimal media cultures to 0.1 OD_{600nm}. Cultures were grown on pyruvate 20 mM +/- glutamine 5 mM. Data points are the means of 2 independent replicates after 24 hours with error bars showing standard deviation.

4.3.6 NMR analysis using HRMAS

In order to provide a link between the cluster of capsule biosynthesis genes involved in MeOPN modification identified in the peptide profiling data and the proposed model (section 4.2) we used NMR analysis using HRMAS to observe any variability of MeOPN on the surface of 3 strains; 11168, 11168 Δ 0184c and 11168 Δ 0184c+0184c. The ^{31}P spectra seen in figure 4.13 shows the presence of MeOPN in the three strains with a chemical shift at 13.5 ppm. From the peak heights, no significant difference in the quantity of MeOPN was observed.

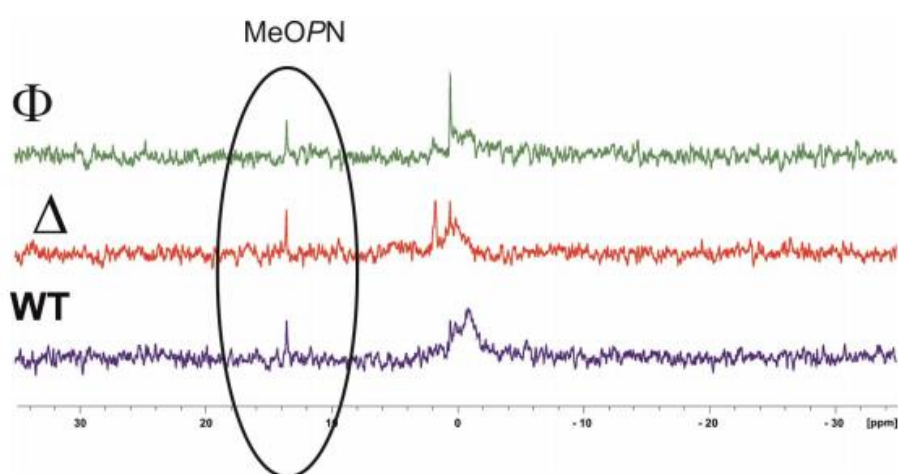


Figure 4.13 ^{31}P nuclear magnetic resonance spectra of *Campylobacter* strains. Φ = 11168 Δ 0184c+0184c, Δ = 11168 Δ 0184c, WT = 11168.

The ^1H - ^{31}P HSQC on crude samples of each strain shows two phosphorylation states (figure 4.14). The first state at δ ^1H = 4.04, 3.83 and δ ^{31}P = 0.3 correspond to a phosphorylated glycerol and the second one at δ ^1H = 3.69 δ ^{31}P = 13.3 corresponds to the O-methylphosphoramidate group. These signals are identical to those described in literature (McNally et al., 2005, 2007).

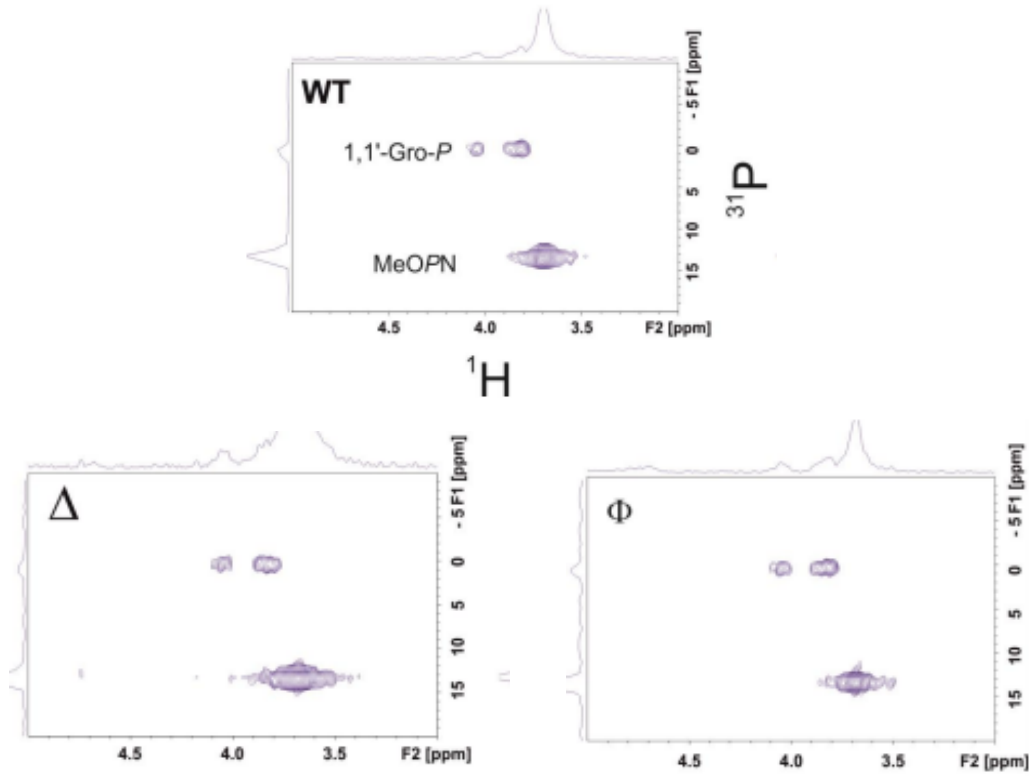


Figure 4.14 ^1H - ^{31}P -HSQC NMR experiment. $\Phi = 11168\Delta 0184c+0184c$, $\Delta = 11168\Delta 0184c$, WT = 11168.

4.4 Discussion

Cj0184c has a novel two-domain structure consisting of a nucleotide/nucleoside binding domain attached to a domain with phosphatase activity related to the PPP family. Additionally it is known that two forms of this protein exist, the native Cj0184c and an extended form due to a GT deletion (Thomas et al., 2014). This deletion was shown to occur at a frequency of 41.9-45.4% after human passage in a collection of isolates compared to a frequency of 50.6% without host passage. A difference of >15% was suggested to be significant genetic variation due to human passage. Therefore, this change in frequency was insufficient to be classified as a phenotype of human passage. However, the GT deletion induces a shift of the stop codon and results in the addition of ten amino acids (V* -> IEIKNQIYKKK). This extension is lysine rich, the primary charged amine on the ϵ -carbon of the lysine side chain usually results in lysine residues being solvent exposed. Therefore, this extension has the potential to affect substrate binding and interfere with phosphatase activity. Based on this change in structure and an observable change in frequency after passage we decided to explore whether this extension has any impact on phosphatase activity. In theory the GT deletion could act as another indirect regulator of glutamine transport at a transcriptional level changing the phosphatase activity of Cj0184c. As seen in section 4.2.2 there was no significant difference in the specific activity of either the native or extended Cj0184c versions. The impurity of the samples is an issue in this experiment however the cell free extract of BL21 was used as a control to account for background activity and was shown to have little phosphatase activity. Therefore, the activity in the fractions containing overexpressed Cj0184c is most likely due to the presence of Cj0184c. This observation was unsurprising due to the consistent frequency of the GT deletion pre and post passage (Thomas et al., 2014). Therefore, we propose this genomic variation to have no affect on the activity of Cj0184c as a phosphatase. In addition, the two domains of Cj0184c were isolated independently and purified to explore whether the PPP domain is the catalytic phosphatase domain and if both domains were required for functional phosphatase activity. As seen in section 4.2.2 a high degree of purity was achieved however neither domain possessed any phosphatase activity independently. This finding suggests that both the nucleotide binding domain and the domain containing the conserved PPP family motifs are required for functional phosphatase activity. However, there is a possibility that the cleavage point chosen to segregate the domains could have caused a loss of secondary structure and therefore rendered both domains non-functional.

The devised model in chapter 4 provided a testable hypothesis for glutamine transport whilst linking all the data collected from the phosphoproteomic data in chapter 3. Lin et al. (2009) have already suggested a glutamine ABC transport system exists in the *C. jejuni* genome however their findings suggest that the transporter does not exhibit specificity exclusively for a single amino acid. Another study suggests that the PaqPQ system is a cysteine transporter based on an orthologous system in *H. pylori* including CjaA, a cysteine binding protein in *C. jejuni* (Müller et al., 2005). Therefore, we hypothesised that the GlnPQ system could be the major glutamine transporter in *C. jejuni* and the PaqPQ system could be capable of transporting glutamine in a less specific manner. Initial experiments exploring growth on a range of carbon sources with and without glutamine confirmed the findings by van der Stel et al. (2015) that *C. jejuni* strain 81116 is capable of utilizing glutamine in a GGT independent manner. Van der Stel et al. (2015) have shown that a *ggt* mutant reaches higher OD_{600nm} when grown in DMEM plus glutamine compared to DMEM alone. Similarly, our findings in 11168, a naturally *ggt* deficient strain, show that 11168 reaches a higher OD_{600nm} when grown on minimal media containing a carbon source in combination with glutamine compared to the sole carbon source alone. This shift in OD_{600nm} provides us with a qualitative measure of glutamine transport. Interestingly our data and observations by van der Stel et al. (2015) show that *C. jejuni* cannot grow on glutamine as a sole carbon source in a GGT-deficient strain. It is currently unclear why *C. jejuni* cannot grow on glutamine despite the evidence of glutamine transport. *C. jejuni* is capable of growth on glutamate as seen in figure 4.8 and therefore it would be expected that growth on glutamine could occur via GOGAT converting glutamine to glutamate. A deeper understanding of the regulation of the GS:GOGAT cycle and the role of glutamine is needed to understand this phenomenon. One potential explanation is that glutamine acts as a nitrogen source in *C. jejuni* and less like a carbon source. Despite this uncertainty the transport of glutamine in a *ggt* independent manner has been shown in a range of *C. jejuni* strains including 11168, 81-176 and 81116.

Based on the model in figure 4.1, a decrease in OD_{600nm} would be expected in a Δ 0184c mutant strain when growing on glutamine if the phosphatase activity of Cj0184c was required for glutamine transport via GlnPQ. If the PaqPQ system is capable of transporting glutamine then a reduction in the glutamine dependent phenotype would be expected. Our data suggests glutamine transport is unaffected by a *Cj0184c* deletion when growing on serine or pyruvate. Interestingly a reduction in OD_{600nm} was observed when grown on

proline and an intermediate phenotype on glutamate. Proline is transported into the cytoplasm via PutP where PutA is responsible for the oxidation of L-proline to L-glutamate (Parkhill et al., 2000). Glutamate is transported into the cytoplasm via the Peb system (Leon-Kempis et al., 2006). Both glutamate and proline are therefore subject to entering the GS:GOGAT cycle. As seen in the peptide profiling data in figure 3.14 we know that the deletion of *Cj0184c* results in expression changes in key genes involved in the GS:GOGAT cycle, *glnA*, *gltB* and *gltD*. The upregulation of GS:GOGAT could in theory result in the dysregulation of GS:GOGAT and perhaps explain a reduction in OD_{600nm} due to an increase in glutamate being maintained within the GS:GOGAT cycle. Another potential explanation for the significant phenotype seen when grown on proline and glutamine could be that *Cj0184c* may regulate proline transport into the cell. The peptide profiling data suggests that deletion of *Cj0184c* results in a decrease in expression of *putP* with a student's T-test difference of -1.6367 compared to WT (FDR=0.01). The student T-test difference of -1.6367 is the second highest (*Cj1422c* = -3.3648) score for downregulated genes in response to *Cj0184c* deletion. Regardless, the preliminary growth experiments with 11168Δ*0184c* suggest that if *Cj0184c* is involved in the dephosphorylation and activity of GlnQ another system must exist that can transport glutamine. One hypothesis is that a redundancy exists between the GlnPQ and PaqPQ ABC transporters.

To explore this hypothesis mutants were constructed deleting both the GlnPQ and PaqPQ ABC transport systems independently and together. Mutants were grown on pyruvate with and without glutamine to explore growth on glutamine. Pyruvate was the chosen carbon source as it provides a measurable shift in OD_{600nm} and the transport and metabolism of pyruvate is independent of glutamine pathways within the cell. Serine also provides a significant shift in OD_{600nm} which could be used to test growth on glutamine. However, serine is converted to pyruvate in the cytoplasm producing a NH₃ molecule which can then be incorporated into glutamate via GlnA to produce glutamine. As seen in figure 4.11 the deletion of either system independently did not produce a glutamine phenotype. Similarly, the double mutant with a deletion in both the GlnPQ and PaqPQ systems was also unaffected by growth on glutamine. This suggests that neither system is involved in glutamine transport under these conditions.

The model depicted in figure 4.2 at this point had no evidence to support a link between *Cj0184c* and glutamine transport. It appears neither system proposed transports glutamine unless a third redundant system exists in the genome. It is possible that *Cj0184c* does indeed dephosphorylate GlnQ, however the role of GlnQ is unclear and we conclude it is

unlikely to be involved in glutamine transport. The only aspect of the model remaining to test was the link between Cj0184c and MeOPN modification of the capsule. Crude cell samples were sent for NMR analysis using HRMAS. No variability was observed between mutant and WT in regards to MeOPN modification. Therefore, the change in abundance of capsule biosynthesis enzymes in the peptide profiling data in fig 3.14 is currently unexplained.

The proposed relationship between Cj0184c and GlnQ is thus currently unresolved. Further investigation of the role of Cj0184c is required and perhaps proline transport via putP is the next best target from the peptide profiling and phosphoproteomics. However, the work on Cj0184c did reveal that *C. jejuni* is heavily dependent on glutamine transport for optimal growth. A high concentration of glutamine is found in the chicken gut and is suggested to be important in the maintenance of gut metabolism, structure, and function (Xue et al., 2018). From an evolutionary angle a highly accessible amino acid as a nitrogen source in the primary host of a pathogen is likely to be utilised. We have shown that glutamine is required for optimal growth but not as a carbon source. In the next chapter we will explore glutamine transport and metabolism in *C. jejuni* as a nitrogen source. Techniques such as RNA-seq will be employed to identify key transport proteins potentially developing on the current work on the GlnPQ and PaqPQ systems.

Chapter 5 Identification of a novel glutamine transporter

5.1 Introduction

Glutamine plays an important role in bacterial physiology. Glutamine is one of 20 standard amino acids in protein synthesis. However, it is also required for the biosynthesis of a variety of nitrogenous compounds. Similarly, glutamine is present in the gut and plays an important role in interactions with host microbiota and immunity. Glutamine is the most abundant free amino acid in the human body. Similarly in the chicken, glutamine can be synthesised in multiple organs including the liver, kidneys and brain (Newsholme et al., 1985). Further research has also shown that glutamine supplementation in the diet alleviates adverse effects of necrotic enteritis, improves body weight, villus heights in the duodenum and jejunum as well as serum IgA and IgG concentrations in birds (Bartell & Batal, 2007; Waldroup et al., 2012; Xue et al., 2018). Despite its designation as a non-essential amino acid there is growing evidence to suggest glutamine is conditionally essential during times of enteric challenge and critical illness (Lacey & Wilrnore, 1990). Therefore, it is unsurprising that glutamine appears to play such a significant role in the growth of enteric bacterial species such as *C. jejuni*.

Glutamine contributes to three major metabolic functions; (1) as a primary product of ammonium assimilation, (2) as a nitrogen donor in biosynthetic pathways and (3) in protein synthesis. As seen in figure 5.1, glutamine synthetase can catalyse the incorporation of ammonia into glutamate to produce glutamine. The GS reaction is considered the most efficient mode of ammonium assimilation and is universally conserved in all organisms able to utilise ammonium as a nitrogen source (Forchhammer, 2007). Glutamine synthesis via GS/GOGAT has two key functions; to provide enough glutamine for anabolic reactions such as protein and nucleic acid synthesis as well as ammonia assimilation. The regulation of GS gene expression and enzyme activity is complex and dependent on nitrogen status in bacteria. High activity of GS is required when cells are actively engaged in nitrogen assimilation, whereas lower activities are needed when nitrogen is well supplied in the cell, as only glutamine's role in other biosynthetic reactions is required. In "model" bacteria such as *E. coli*, the nitrogen regulatory system (Ntr) has been well characterised and consists of the sigma factor NtrA (RpoN), a histidine kinase, NtrB and its cognate response regulator, NtrC (Merrick & Edwards, 1995). Under nitrogen replete conditions NtrB is found

interacting with the PII protein, acting as a phosphatase. However, in nitrogen limiting conditions PII is uridylylated, blocking interactions with NtrB and thus allowing NtrB to function as a kinase to phosphorylate NtrC (Jiang & Ninfa, 1999). A low level of phosphorylated NtrC, along with an RNA polymerase containing the NtrA sigma factor, is sufficient to promote the expression of the *glnAntrBC* operon (encoding GS, NtrB and NtrC). However, an increase in activated NtrC is required for the expression of other Ntr-dependent genes including *amtB*, encoding a known ammonium transporter. Interestingly in *C. jejuni* no such Ntr system has been identified, and although a gene encoding a sigma factor similar to RpoN is present this does not seem to control genes involved in N-assimilation (Chaudhuri et al., 2011). Furthermore, although an *amt* homolog has been identified in *C. jejuni* NCTC11168, a frameshift has rendered the gene non-functional, existing in the genome as a pseudogene (Parkhill et al., 2000). Therefore in *C. jejuni* the regulation of GS and cellular nitrogen levels remains unclear.

Recently another role for glutamine has been discovered. Lu et al. (2013) have shown that L-glutamine provides acid resistance for *E. coli* via the enzymatic release of ammonia by YbaS. YbaS can convert intracellular glutamine to L-glutamate in an acid-activated manner releasing gaseous ammonia. The free ammonia is thought to neutralize protons increasing intracellular pH allowing survival in acid environments. Again, neither YbaS or an amino acid antiporter GadC, which exchanges intracellular glutamate with extracellular glutamine in acid conditions, have been identified in *C. jejuni*.

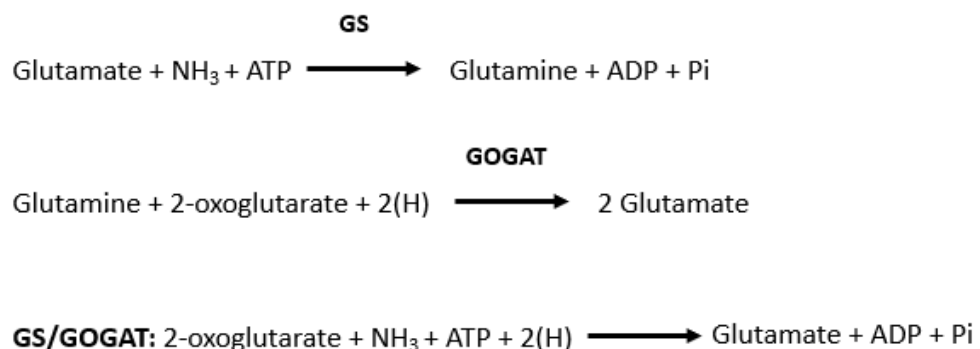


Figure 5.1 GS/GOGAT and nitrogen assimilation. GS catalyses the incorporation of ammonia into the γ -carboxyl of glutamate. The γ -carboxyl group is first phosphorylated by ATP which allows the incorporation of ammonia by amidation releasing inorganic phosphate. GOGAT reductively aminates 2-oxoglutarate using the amide group of glutamine to generate two molecules of glutamate. The overall GS/GOGAT reaction therefore synthesises a single molecule of glutamate from 2-oxoglutarate and ammonium, consuming one ATP and two electrons (derived from NADPH).

Glutamine transport in *C. jejuni* was extensively discussed in chapter 4 including the roles of ABC transporters GlnPQ and PaqPQ. However, after experimental investigation we suggest that in *C. jejuni* NCTC11168 at least, these systems may not function as glutamine transporters. This chapter will focus on improving our understanding of glutamine transport and metabolism in *C. jejuni*.

5.2 Results

5.2.1 Gene expression changes in chemostat culture during a transition from glutamine limitation to glutamine excess

To identify some potential candidates for genes involved in glutamine transport and nitrogen assimilation we performed RNA-seq analysis on samples from a glutamine-limited chemostat culture after the addition of excess glutamine. Cells were grown continuously in minimal media containing 10 mM serine as sole carbon and nitrogen source to support growth. After four volumes a T0 sample was taken. The culture was then immediately adjusted to 10 mM glutamine by bolus addition and maintained at the concentration by an external pump. Samples were taken at T0, T5, T20 and T45 min after glutamine addition. Standard RNA-seq was performed on all samples and differential gene expression was analysed using the Galaxy web based platform (Afgan et al., 2018).

As seen in figure 5.2 a range of genes were up and down regulated in response to glutamine. Specifically, the down regulated genes were of interest based on the theory that in an environment with excess glutamine, genes involved in the transport of glutamine would be downregulated as part of an inhibitory loop. All timepoint samples were consistent with 61% of significant hits found to be repeated at multiple timepoints. 23/51 and 27/56 hits were unique to the dataset at T5 and T45, respectively. No unique hits were identified at T20. 81 significant gene expression changes were identified across all 3 timepoints in response to excess glutamine. The genes encoding the GS/GOGAT enzymes are all downregulated in response to excess glutamine (*gltBD* and *glnA*). Interestingly trimmed reads were identified belonging to the pseudogene Cj0501, an ammonium transporter. This suggests although the ammonium transporter is non-functional in NCTC11168 due to a frame shift, the transcriptional regulatory pathways must still be acting on this operon in response to increased glutamine concentrations. Perhaps this

suggests a relatively recent loss of function in Cj0501. Three putative solute transport systems were identified to be downregulated in response to glutamine, encoded by *Cj0903c*, *Cj0552-54* and *Cj0935c-34c* (Table 5.1). These genes were selected for further investigation and mutagenesis to test their role in growth on glutamine. As seen in figure 5.3 a range of metabolic pathways and cellular processes were subject to regulation in response to glutamine including biosynthesis, degradation, ammonia assimilation, DNA metabolism and DNA repair. Table 5.2 shows all significant changes in gene expression after the addition of glutamine at T=45. Interestingly an iron uptake system operon (Cj1658-1663) is upregulated in response to glutamine at T=20 and T=45 along with some other genes related to iron assimilation (e.g., *tonB2*, *tonB3* and *cfrA*).

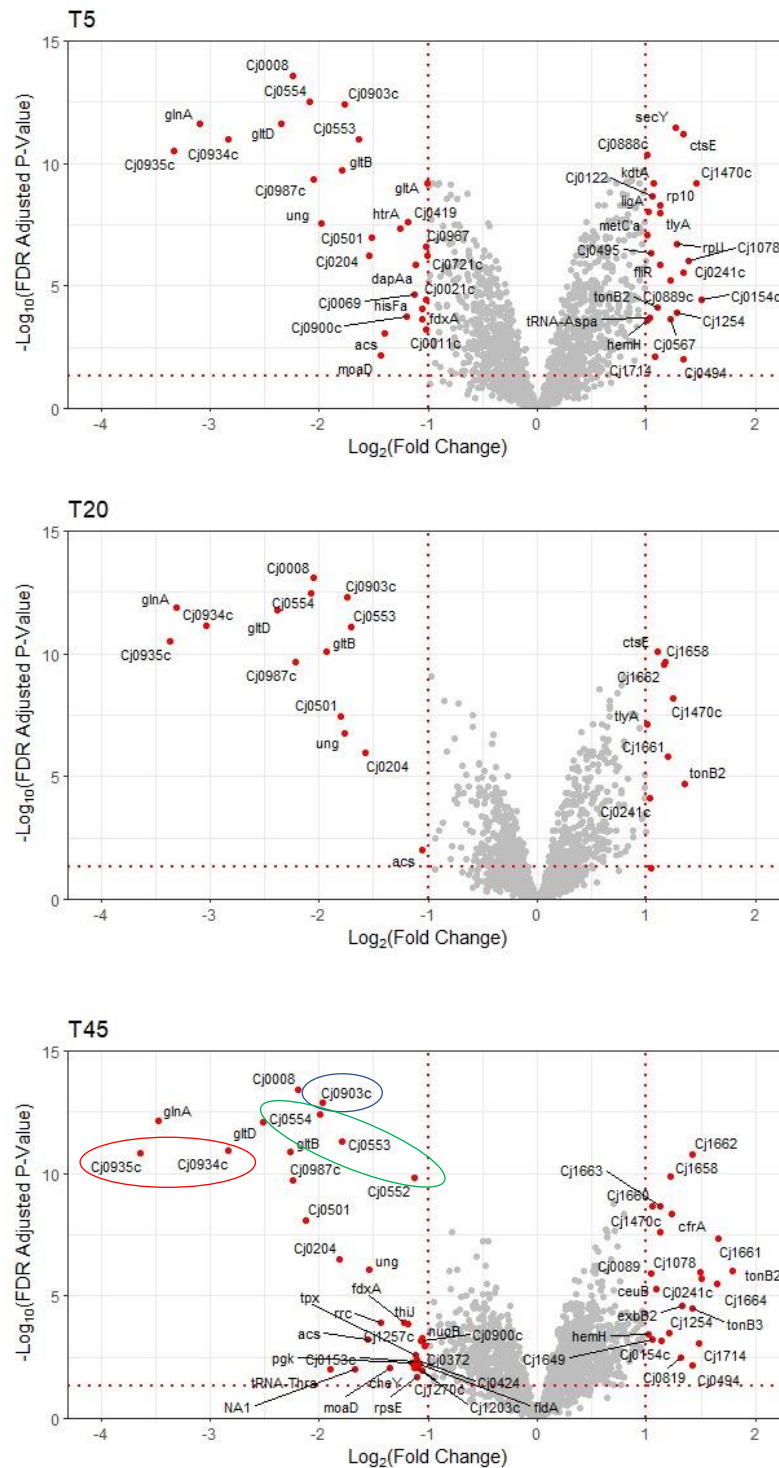


Figure 5.2 Volcano plot showing statistically significant RNA reads. Log_2 fold change in RNA reads were plotted against the difference Log_{10} FDR adjusted p-values in a glutamine limiting chemostat culture after the addition of excess glutamine at $T=5\text{min}$, $T=20\text{min}$ and $T=45\text{min}$. RNA reads circled in blue, green and red are putative transport proteins significantly regulated by glutamine.

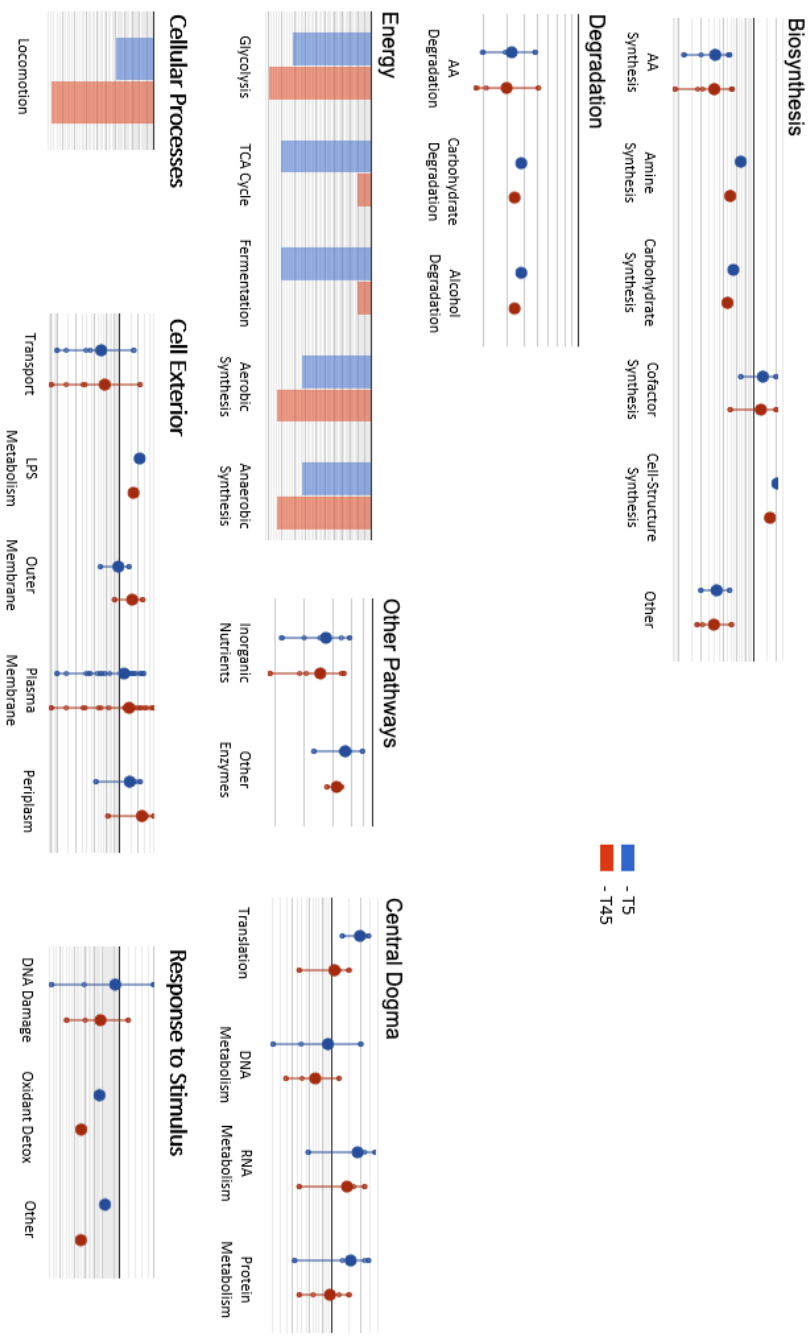


Figure 5.3 Cellular Processes associated with RNA-seq significant hits. Blue and red data points correspond to T=5 and T=45 significant hits. The graphs show foldchange in RNA reads on a 1-centered scale. Images taken from Biocyc Omics dashboard (Paley et al., 2017)

Table 5.1 Putative Glutamine Transporters of interest from RNA-seq

Gene	Description	Fold Change T=5	Fold Change T=20	Fold Change T=45	Adjusted p.value T=5	Adjusted p.value T=20	Adjusted p.value T=45
Cj0903c	amino acid transport protein	0.2933	0.2996	0.2566	3.77E-13	4.79E-13	1.36E-13
Cj0554	hypothetical protein	0.2358	0.2375	0.2513	3.15E-13	3.36E-13	3.78E-13
Cj0553	Integral membrane protein	0.3222	0.3069	0.2897	1.06E-11	7.74E-12	4.75E-12
Cj0552	membrane protein	0.5158	0.5083	0.4567	6.70E-10	8.61E-10	1.44E-10
Cj0934c	sodium:amino-acid symporter family protein	0.1407	0.1221	0.1398	1.06E-11	6.80E-12	1.20E-11
Cj0935c	sodium:amino-acid symporter family protein	0.0995	0.0973	0.0806	3.12E-11	3.18E-11	1.45E-11

Table 5.2 T=45 significant hits from RNA-seq

Gene	Description	FoldChange.T45	adj.p.value.T45
Cj0935c	sodium:amino-acid symporter family protein	0.0806	1.45E-11
glnA	glutamine synthetase	0.0898	6.88E-13
Cj0934c	sodium:amino-acid symporter family protein	0.1398	1.20E-11
gltD	glutamate synthase subunit beta	0.1751	8.40E-13
gltB	glutamate synthase large subunit	0.2084	1.26E-11
Cj0987c	NA	0.2115	1.80E-10
Cj0008	hypothetical protein	0.2195	3.65E-14
Cj0501	NA	0.2301	8.32E-09
Cj0554	hypothetical protein	0.2513	3.78E-13
Cj0903c	amino acid transport protein	0.2566	1.36E-13
tRNA-Thra	NA	0.2695	1.05E-02
Cj0204	oligopeptide transporter	0.2843	3.12E-07
Cj0553	integral membrane protein	0.2897	4.75E-12
NA1	NA	0.3147	1.05E-02
acs	acetyl-CoA synthetase	0.3395	5.76E-04
ung	uracil-DNA glycosylase	0.3438	8.61E-07
rrc	non-heme iron protein	0.3707	1.26E-04
moaD	molybdopterin converting factor subunit 1	0.3915	9.31E-03
fdxA	ferredoxin	0.4280	1.30E-04
thiJ	4-methyl-5(beta-hydroxyethyl)-thiazole monophosphate synthesis protein	0.4394	1.47E-04
pgk	phosphoglycerate kinase	0.4509	5.54E-03

Cj0552	membrane protein	0.4567	1.44E-10
cheY	chemotaxis protein CheY	0.4585	9.09E-03
tpx	2-Cys peroxiredoxin	0.4613	2.70E-03
Cj0153c	23S rRNA (guanosine(2251)-2'-O)-methyltransferase RlmB	0.4653	4.88E-03
rpsE	30S ribosomal protein S5	0.4661	1.98E-02
Cj0424	acidic periplasmic protein	0.4668	4.41E-03
Cj1203c	integral membrane protein	0.4671	8.81E-03
fldA	flavodoxin FldA	0.4744	6.33E-03
Cj1257c	efflux pump protein	0.4779	6.89E-04
Cj0900c	hypothetical protein	0.4805	6.68E-04
nuoB	NADH-quinone oxidoreductase subunit B	0.4810	5.60E-04
Cj1270c	2-nitropropane dioxygenase	0.4814	1.11E-02
Cj0372	glutathionylspermidine synthase	0.4900	1.11E-03
hemH	ferrochelatase	2.0229	3.70E-04
Cj0089	lipoprotein	2.0552	1.20E-06
Cj1660	integral membrane protein	2.0827	2.11E-09
Cj1649	lipoprotein	2.0828	5.75E-04
ceuB	enterochelin uptake permease	2.1259	5.16E-06
Cj1470c	NA	2.1877	2.40E-08
Cj1663	ABC transporter ATP-binding protein	2.1889	2.30E-09
Cj0154c	rRNA small subunit methyltransferase I	2.2071	6.70E-04
Cj1254	hypothetical protein	2.3106	3.36E-04
Cj1658	iron permease	2.3241	1.28E-10
cfrA	ferric enterobactin uptake receptor	2.3463	4.45E-09
Cj0819	hypothetical protein	2.4812	3.16E-03
exbB2	ExbB/TolQ family transport protein	2.5020	2.58E-05
tonB3	TonB transport protein	2.6826	3.43E-05
Cj0494	exporting protein	2.6837	7.06E-03
Cj1662	integral membrane protein	2.6874	1.71E-11
Cj1714	hypothetical protein	2.7798	9.14E-04
Cj1078	periplasmic protein	2.8044	1.15E-06
Cj0241c	bacteriohemerythrin	2.8425	1.99E-06
Cj1664	thiredoxin	3.1286	3.21E-06
Cj1661	ABC transporter permease	3.1651	4.67E-08
tonB2	TonB transport protein	3.4677	1.01E-06

5.2.2 Investigating the contribution of putative transport genes identified by RNA-seq to glutamine uptake

Deletion mutants were constructed in the genes in table 5.1. These genes encode putative transport proteins which are downregulated in response to excess glutamine. As seen in figure 5.4, when grown on pyruvate in minimal media with glutamine as N-source, a significant growth defect is observed in the *Cj0903c* mutant. Some residual growth can still be observed suggesting there is potentially an unidentified redundant mechanism for glutamine transport in *C. jejuni*. No significant phenotypes were observed in any of the other mutant strains tested with glutamine as the N-source. Complementation of the *cj0903c* mutant with the wild-type *Cj0903c* gene expressed from the *metK* promoter successfully restored growth on glutamine as seen in figure 5.4.

To explore the possibility of redundant glutamine transport mechanisms we constructed deletion mutants devoid of all putative glutamine transporters in this study (*Cj0903c*, *PaqPQ*, *GlnPQ*). The triple transporter mutant did not produce a phenotype which accounted for any of the residual growth on glutamine previously seen in the *11168Δ0903c* mutant (fig 5.5). A double mutant with deletions in both *cj0903c* and *glnH* did produce a significant phenotype when grown on glutamine (*11168Δ0903c* vs *11168Δ0903c+0817*, $p=0.010255$). However, this small change in OD_{600nm} of 0.03950 does not account for the residual growth of 0.2 OD_{600nm} seen in the *11168Δ0903c* strain when grown on glutamine (5 mM). Therefore, this small change in growth in combination with the thermoflour binding assay results discussed later suggests it is unlikely that this phenotype is glutamine specific. Finally, to explore the role of *Cj0903c* as a high affinity transporter we subjected the *11168Δ0903c* strain to growth on glutamine at limiting concentrations. As seen in figure 5.5 at limiting concentrations of glutamine (<0.2 mM) no significant increase in OD_{600nm} is observed in the *11168Δ0903c* strain. However, at excess glutamine levels (>2 mM) a small increase in OD_{600nm} is observed likely to be the result of non-specific/low-affinity uptake from other transport systems and not the result of an alternative glutamine transporter.

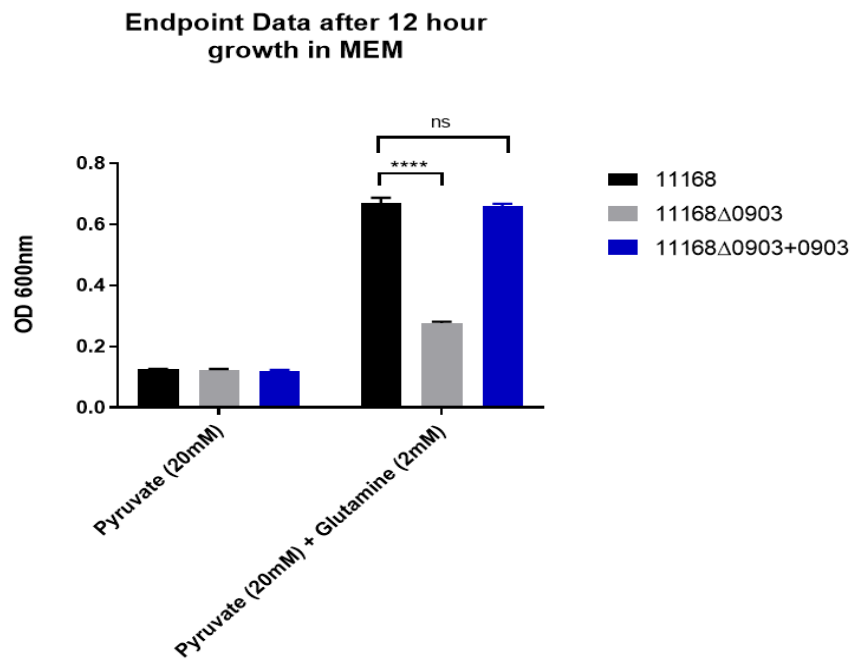
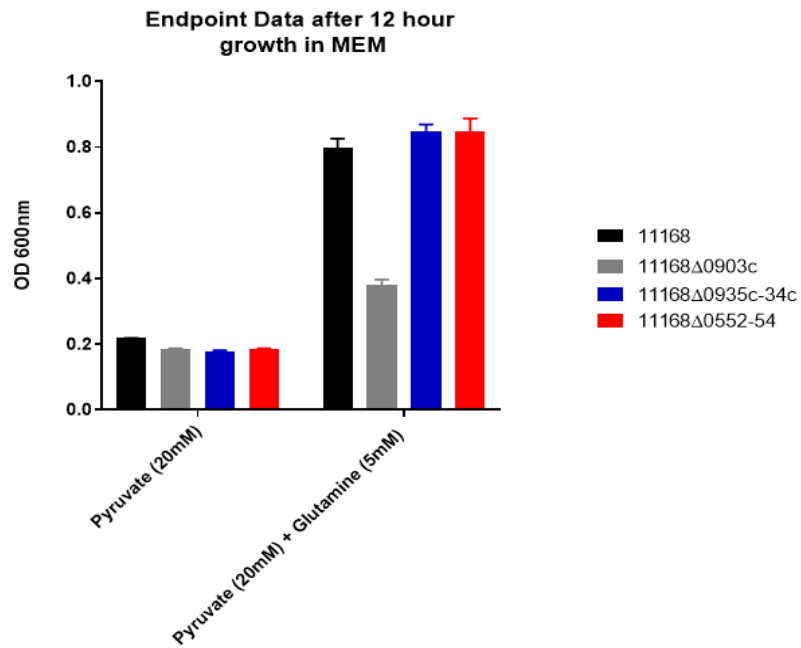


Figure 5.4 RNA-seq transport mutant growth on glutamine. *C. jejuni* cells were grown in BTS broth to mid-log phase and used to inoculate minimal media cultures to 0.1 OD_{600nm} in triplicate. Cultures were grown on Pyruvate 20 mM +/- Glutamine 5 mM. Data points are the means of 3 independent replicates with error bars showing standard deviation. **** $P \leq 0.0001$, ns indicates not statistically significant.

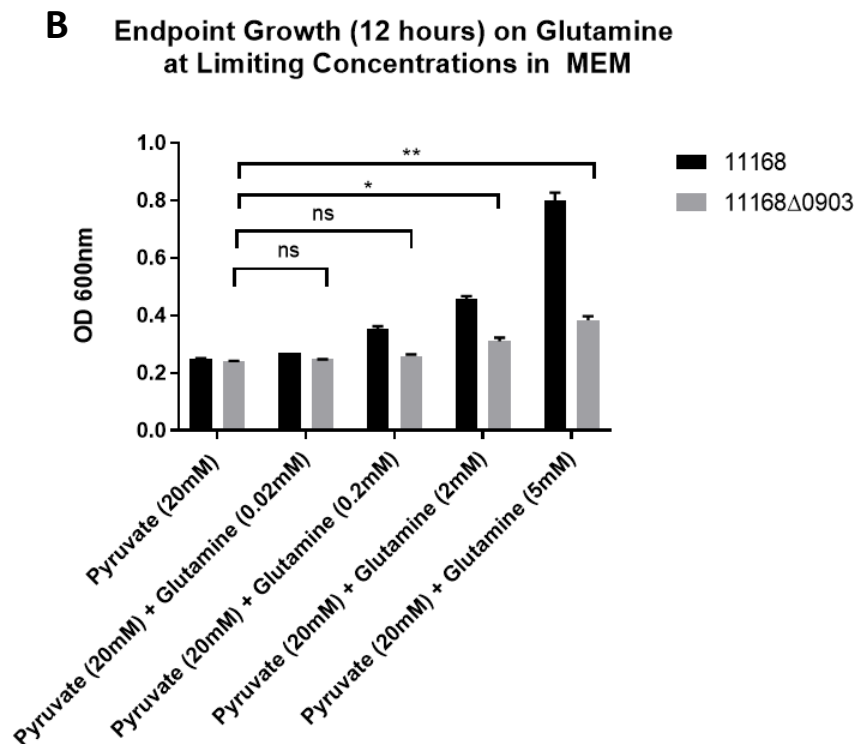
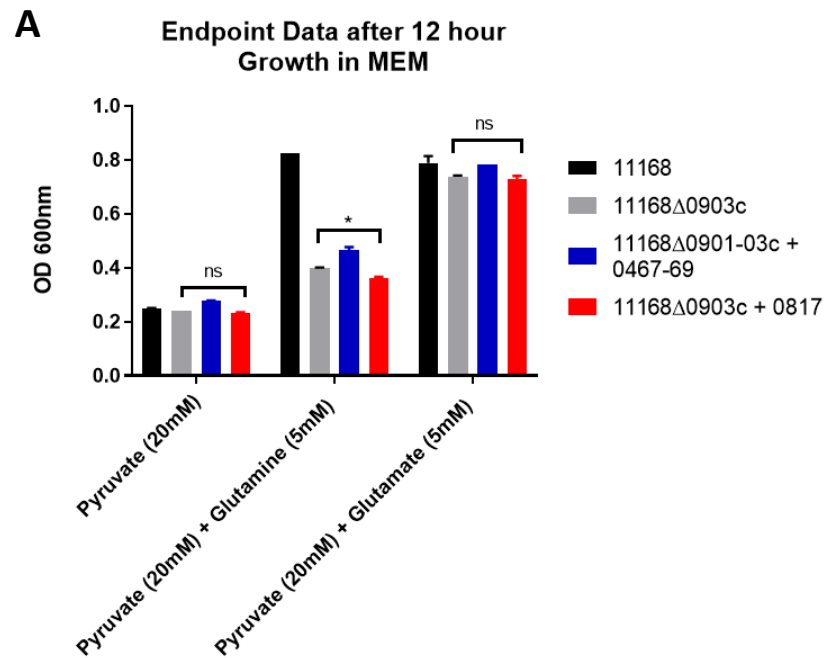


Figure 5.5 Endpoint Growth Data. A. Δ 0903c growth in multiple backgrounds including a Δ paqPQ+glnQ (Cj0467-69, Cj0901) and Δ glnH (Cj0817) strain. B. Exploring the role of Cj0903c as a high/low affinity transporter using growth at a range of glutamine limiting concentrations. C. *jejuni* cells were grown in BTS broth to mid-log phase and used to inoculate minimal media cultures to 0.1 OD_{600nm} in triplicate. Cultures were grown on Pyruvate 20 mM +/- Glutamine 5 mM. Data points are the means of 3 independent replicates with error bars showing standard deviation. * $P \leq 0.05$, * $P \leq 0.01$, ** $P \leq 0.001$, ns indicates not statistically significant.

5.2.3 Glutamine but not ammonia stimulates the growth of *C. jejuni* 11168 in minimal media containing serine as a carbon source

Ammonia can be assimilated in bacteria via ammonia specific transporters such as AmtB as well as glutamine transport. The striking glutamine requirement in *C. jejuni* for optimal growth as well as the presence of a pseudogene in a likely ammonia transporter (Cj0501) suggested that glutamine could potentially be the most important nitrogen source for *C. jejuni* growth. To explore this, we performed a growth experiment in MEM with the addition of glutamine and ammonia independently and together. As seen in figure 5.6 the addition of ammonium sulphate does not appear to replicate the growth advantage seen when grown on glutamine. An unpaired t-test suggests that growth in the presence of both glutamine and ammonium sulphate is not statistically different to growth in the presence of glutamine alone ($p=0.0744$). A significant albeit small increase in growth was observed when grown in the presence of ammonium sulphate compared to the no nitrogen source control ($p \leq 0.05$). This change of only 0.034 is within the usual variance seen between treatment groups in batch culture and therefore cannot conclusively be suggested to be the result of ammonia transport.

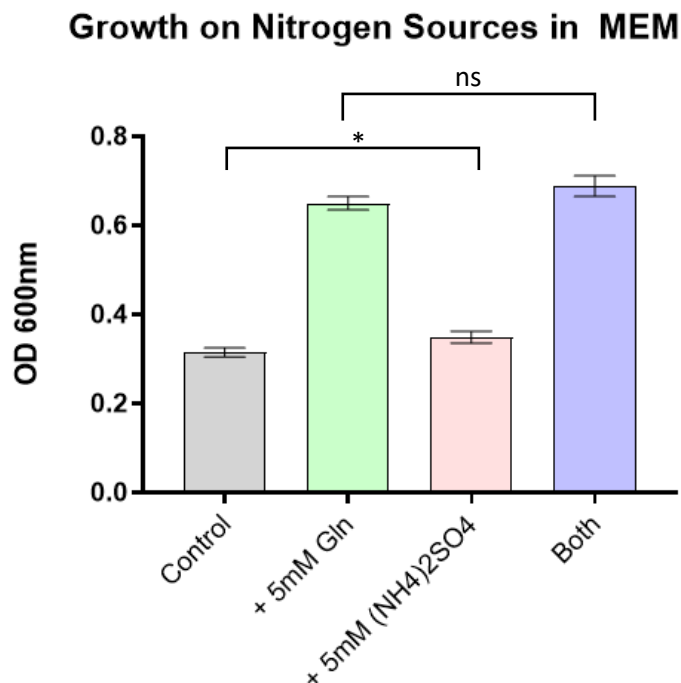


Figure 5.6 NCTC11168 Growth in MEM with multiple nitrogen sources. *C. jejuni* cells were grown in BTS broth to mid-log phase and used to inoculate minimal media cultures to 0.1 OD_{600nm} in triplicate. Cultures were grown on Serine 20 mM +/- Glutamine 5 mM, Ammonium sulphate or both together. Data points are the means of 3 independent replicates with error bars showing standard deviation. * $P \leq 0.05$, ns indicates not statistically significant.

5.2.4 Putative Amino Acid Binding Protein – GlnH

Cj0817 in the NCTC11168 genome is annotated as GlnH, a putative glutamine binding protein (Parkhill et al., 2000). To investigate this annotation, we constructed a deletion mutant strain 11168Δ0817 as well as purifying GlnH for use in amino-acid binding assays. Deletion of *Cj0817* had no effect on growth with 5 mM glutamine compared to WT (fig 5.7). Additionally, a preliminary tryptophan fluorescence assay revealed no significant changes in intensity when glutamine was added to the purified GlnH protein. Furthermore, using the HisTrap purified GlnH we performed a thermoflour binding assay, where ligand binding is expected to result in protein stabilisation and an increase in melting temperature. As seen in fig 5.6 we could not show binding to glutamine or any of the other 19 amino acids tested. The purified GlnH was urea treated in order to remove any potential substrates in complex with GlnH post purifications. The same results were observed when GlnH was purified without urea treatment.

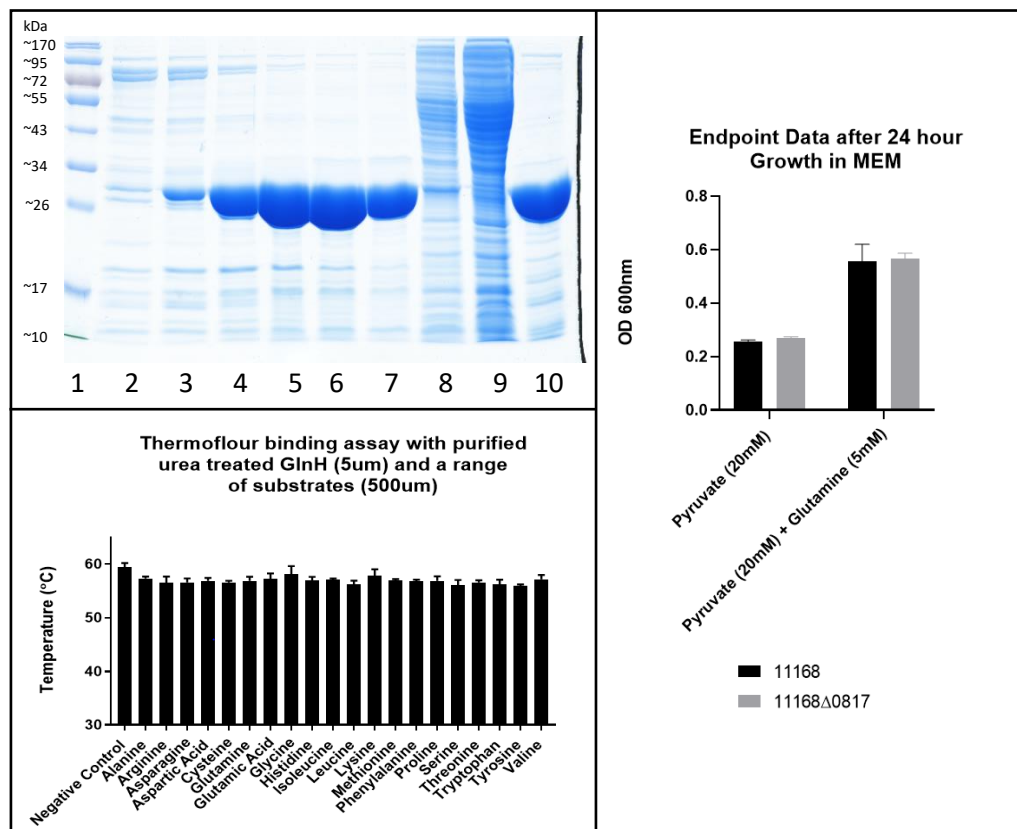


Figure 5.7 HisTrap Purified GlnH Binding Assay and Δ0817 growth on glutamine. (Top Left). 1% SDS-PAG of purified N-terminally His-tagged GlnH. pET21a_0817 was grown in LB to mid-log phase before induction with 0.4 mM IPTG and 24 hour growth at 25 °C. A cell free extract was produced and purified using a 5 ml HisTrap column. Lane 1, Hyperladder 1, Lanes 2-6, fractions 14-19, Lane 8 Flow through, Lane 9 CFE, Lane 10, purified GlnH by pooling and concentrating fractions 15-19. (Bottom Left) Thermoflour binding assay. The stability of GlnH (5 µm) was measured in the presence of 20 potential substrates (500 µm). (Right) *C. jejuni* strains were grown in BTS broth to mid-log phase and used to inoculate minimal media cultures to 0.1 OD_{600nm} in triplicate. Cultures were grown on Pyruvate 20 mM +/- Glutamine 5 mM. Data points are the means of 3 independent replicates with error bars showing standard deviation.

5.2.5 Inactivation of Cj0903c but not PaqPQ or GlnP reduces the susceptibility of C. jejuni to toxic glutamine analogue Gamma-L-Glutamyl hydrazide (GGH)

To further validate the findings from the glutamine growth experiments and verify that Cj0903c is the main glutamine transporter in *C. jejuni* we performed growth curves in the presence of 2 mM toxic glutamine analogue γ -L-glutamyl hydrazide. We included the 11168 Δ 0467-69 strain to provide further verification that the PaqPQ system is not acting as redundant glutamine transport system. Strains defective in glutamine uptake such as those with a deletion in a glutamine transporter are expected to show reduced susceptibility to GGH. Cells were grown on 20 mM serine with 1 mM glutamine to ensure expression of glutamine transport pathways and to stimulate sufficient growth to identify a clear phenotype in response to GGH treatment. As expected, addition of GGH reduced the growth of all strains however the 11168 Δ 0903c strain exhibited a significant reduction in sensitivity as seen in figure 5.8. Treatment with GGH resulted in WT cultures growing to 49% of growth seen in the untreated cultures compared to 79% in the 0903c deletional strain. This phenotype was successfully complemented. Interestingly the PaqPQ deletion appears to be more sensitive to GGH than WT which validates the observation in multiple growth experiments where deletion of the PaqPQ system increases the endpoint OD_{600nm} when grown on glutamine compared to WT.

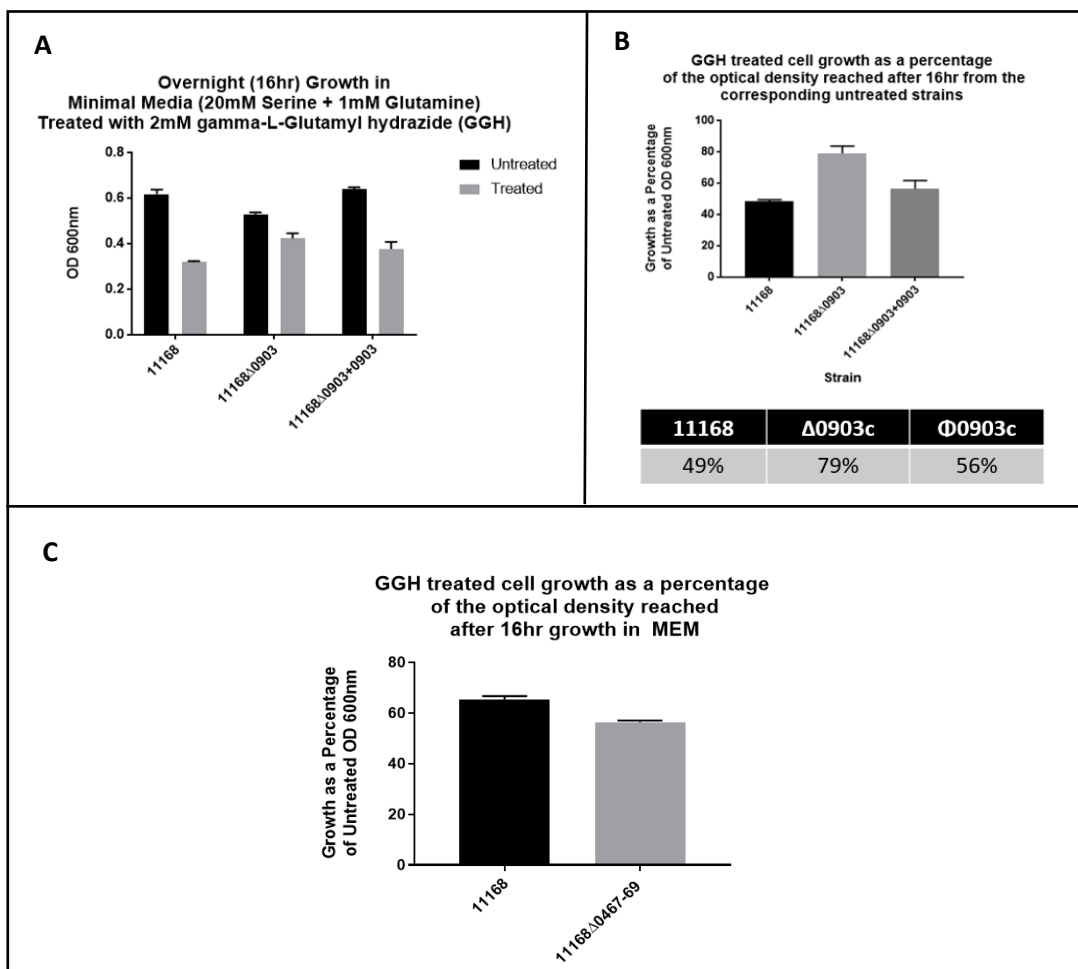


Figure 5.8 GGH Sensitivity in putative glutamine transport mutants compared to WT. *C. jejuni* cells were grown in BTS broth to mid-log phase and used to inoculate minimal media cultures to 0.1 OD_{600nm} in triplicate. Cultures were grown on Serine 20 mM and Glutamine 1mM +/- GGH 2 mM. Data points are the means of 3 independent replicates with error bars showing standard deviation. (A) 11168Δ0903c vs 11168 endpoint data. (B) GGH sensitivity shown as a percentage of untreated growth. The mean endpoint OD_{600nm} of the untreated group was used to calculate growth percentages individually in the treated group to allow for error bars showing standard deviation. (C) 11168Δ0467-69 vs 11168, *paqPQ* deletion strain.

5.2.6 *Cj0903c* is likely the sole glutamine transporter in NCTC11168 *Campylobacter jejuni*

To conclusively test if *Cj0903c* is the main glutamine transporter and verify all findings in this chapter we performed an uptake assay using radiolabelled glutamine. Uptake of glutamine was undetectable in the *Cj0903c* mutant and partially restored (~50.3%) in the complemented *Cj0903c* strain (fig 5.9). To confirm that *Cj0903c* is the sole glutamine transporter as indicated by the complete loss of uptake we performed uptake assays on *paqPQ*, *glnP*, *glnQ* and *glnH* mutant strains. All these transport genes have been previously implicated in glutamine transport either by homology or with experimental evidence in the case of *paqPQ*. As expected, based on our previous findings none of these other mutant strains showed a reduction in glutamine uptake compared to WT. Therefore, the data suggests that under the uptake assay conditions tested, *Cj0903c* functions as the sole glutamine transporter in *C. jejuni* NCTC11168. We cannot formally exclude that the *Cj0903c* is able to transport other amino acids. However, based on our findings **we propose to name the *Cj0903c* gene *guta* (glutamine uptake A).**

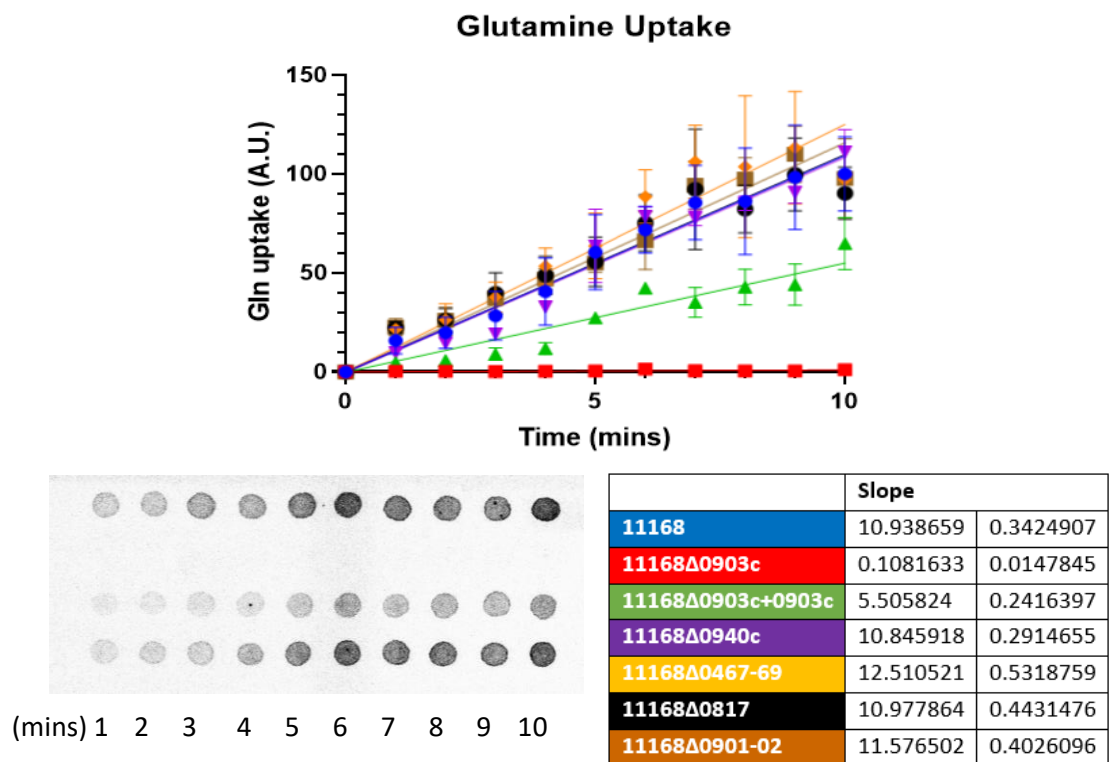


Figure 5.9 Radiolabelled Glutamine Uptake Assay. Cell suspensions in MEM and 0.5% sodium lactate were incubated at 42 °C. 1 uCi (1.78 μm) of C14 labelled glutamine and a final volume of 50 μm cold glutamine was added to the reaction and samples taken every minute for 10 minutes. Cells were washed with excess glutamine and spotted onto Whatman paper. Spots were exposed for 2 days and the IP imaged using phosphorimager. The immediate local background of each spot was normalised using an adapted DRaCALA equation (Roelofs et al. 2012). Data points are the means of 3 independent replicates with error bars showing standard deviation. Origins were forced to intercept X and Y at 0 and datasets normalised to WT 10 minute samples to allow direct comparison to WT. **(Bottom left)** Spotted Whatmann paper after exposure. **(Bottom right)** Straight line slopes of each strain.

5.3 Discussion

As discussed previously *C. jejuni* does not possess the classic Ntr nitrogen regulatory system seen in other “model” bacteria. Similarly, *C. jejuni* NCTC11168 does not possess a functional copy of an ammonium transporter. For this reason, we propose that the primary role of glutamine in *C. jejuni* is as a nitrogen source. This was verified by the lack of growth observed when *C. jejuni* was incubated in the presence of glutamine as the sole carbon source combined with the clear growth stimulation when glutamine was present in addition to known carbon sources. It has been previously suggested that two glutamine transport systems are present in the NCTC11168 genome, GlnPQ and PaqPQ. However, we have produced multiple pieces of experimental evidence to suggest that neither of these systems are responsible for glutamine transport. Firstly, as discussed in chapter 4 there is no glutamine related growth phenotype in strains with deletions in either of these systems. Secondly, as shown in this chapter, RNA transcripts for neither system appeared in the RNA-seq analysis of samples from a glutamine limited culture when exposed to excess glutamine. This suggests that neither *glnPQ* or *paqPQ* are subject to regulation by the presence of glutamine. Thirdly, a toxic glutamine analogue sensitivity assay has also shown that $\Delta glnP$ and $\Delta paqPQ$ strains are no more resistant to GGH than WT (data not shown). Finally, perhaps the most convincing evidence that these systems are not glutamine transporters comes from the result of the radio-labeled glutamine uptake assay. No significant reduction in glutamine uptake was seen in either mutant strain compared to WT. Interestingly, an unexplained phenotype that has been observed throughout this study was also observed in the glutamine uptake assay. It appears that a deletion in *paqPQ* may actually increase glutamine uptake, verified by a slight increase in growth on glutamine as well as a small but observable increase in radio labelled glutamine uptake. These results directly contradict the findings of Lin et al. (2009) that the deletion of either the ABC transporter permease (*paqP*) or the ATPase (*paqQ*) resulted in glutamine uptake levels <50% compared to WT. Lin et al. (2009) also suggest that GlnPQ could be responsible for residual glutamine uptake however provided no experimental evidence. However we must note that the published work by Lin et al. (2009) was performed in the *C. jejuni* strain 81-176. Our results do show that neither PaqPQ or GlnPQ are responsible for glutamine uptake in NCTC11168 but we cannot formally exclude that either of these systems is acting as a glutamine transporter in other strains such as 81-176.

The role of GlnH was also explored in chapter 5. GlnH is annotated as a putative glutamine binding periplasmic protein in NCTC11168 (Parkhill et al., 2000). However again our findings have shown *Campylobacter* gene annotations to be frequently misleading. We were unable to produce data to support this annotation. A thermoflour binding assay did not reveal any potential substrates from the 20 amino acids tested using both urea treated and untreated purified GlnH samples. At this time the substrate and cognate transport system of GlnH remain unclear. Another known periplasmic binding protein in *C. jejuni*, CjaA, has been found in complex with cysteine suggesting it to function as part of a cysteine transport system. An orthologue of *cjaA* in *H. pylori* is found in an operon containing orthologues for *paqP* and *paqQ*. It is possible that the PaqPQ transport system is indeed a cysteine transporter which is partially verified by Lin et al. (2009) who found strains with a deletion in either *paqP* or *paqQ* were defective in cysteine uptake albeit to a lesser extent than glutamine.

The RNA-seq results presented in section 5.2.1 revealed 81 different genes subject to regulation by the presence of excess glutamine. Multiple cellular processes were affected by the addition of glutamine including biosynthesis, degradation, ammonia assimilation, DNA metabolism and DNA repair. However the largest fold-changes were seen in genes encoding transport proteins, enzymes involved in the GS:GOGAT cycle as well as the pseudogene of the putative ammonia transporter *amt*. The three down-regulated transport systems identified are currently uncharacterised in *C. jejuni*, however *Cj0935c-34c* is annotated as a sodium:amino-acid symporter family protein with homology to the solute carrier 6 subfamily (SLC6). SLC6 family proteins in humans are functionally classified as sodium/glutamine co-transporters (Pochini et al., 2014). Bacterial SLC6 proteins include the LeuT amino acid transporter related to mammalian neurotransmitter transporters. LeuT is responsible for the transport of small hydrophobic amino acids such as alanine and leucine. The crystal structure of LeuT revealed a leucine molecule and 2 sodium ions in complex (Yamashita et al., 2005). However, L-alanine is also a substrate of LeuT and has been shown to competitive inhibit L-[3H]leucine transport as well as bind to LeuT with a K_d 15-fold greater than leucine (Singh et al., 2007). It is thus possible that *Cj0935c-0934c* is an alanine transporter, which should be further investigated. *Cj0552-54* form an operon encoding two putative membrane proteins and a hypothetical protein. Sequence homology revealed no further indication of the putative role however the genomic organisation was similar to that of a typical ABC transporter. Finally, *Cj0903c* encodes an annotated amino acid transport

protein that is homologous to AlST a bacterial sodium/alanine symporter. As seen in figure 5.3 only *cj0903c* mutant had a glutamine specific growth phenotype when grown in minimal media. The substrates of putative transporters *Cj0934c-35c* and *Cj0552-54* remain unclear. However, one hypothesis for the downregulation of *Cj0934c-35c* in response to glutamine could be linked to *Cj0903c*. Both *Cj0934c-35c* and *Cj0903c* are linked to the transport of small hydrophobic amino acids such as alanine by homology data. Potentially these transporters were both previously responsible for alanine transport in *C. jejuni* and therefore share regulatory pathways. It appears that *Cj0903c* has evolved to become responsible for glutamine transport subject to regulation by exogenous glutamine. Perhaps these two transport systems remain transcriptionally linked explaining the presence of *Cj0934c-35c* in the RNA-seq dataset. Another hypothesis arises from observations concerning eukaryotic glutamine transport. Glutamine transport in humans is well characterised due to glutamine's essentiality for body homeostasis, glutamine is also the most abundant amino acid in humans with intracellular concentrations between 2 to 20 mM, while extracellular concentrations range from 0.2 to 0.8 mM (Pochini et al., 2014). Glutamine has a similar role in humans as those seen in bacteria however glutamine is also responsible for regulating levels of glutamate and GABA in the brain as well as glucose regulation. Due to these multiple roles, glutamine transporters are often redundant and ubiquitous and often show specificity towards other amino acids. Perhaps both *Cj0903c* and *Cj0935c-45c* are glutamine transporters but the latter is not active under the conditions explored in this study. Alternatively, *Cj0934c-35c* is indeed a leucine/alanine transporter but can transport glutamine in a non-specific manner. This could explain some of the residual growth on glutamine seen in the 11168Δ*0903c* strain. Finally, alanine transport could be transcriptionally linked to glutamine transport. In mammals the Cahill Cycle (a.k.a. the alanine cycle) involves the breakdown of muscle protein to provide more glucose to generate additional ATP for muscle contraction (Sarabhai & Roden, 2019). After glycolysis in peripheral muscle tissues pyruvate can be transaminated to alanine which can then travel via the blood to the liver, in the liver alanine and 2-oxoglutarate are converted back to pyruvate and glutamate. Pyruvate then undergoes gluconeogenesis to produce glucose which can be transported back to peripheral muscles for energy generation by glycolysis (Felig et al., 1970). The transamination of alanine is catalyzed by alanine transaminase (ALT). This cycle is fueled by muscle protein breakdown yielding amino acid groups which are transferred by alanine transaminase to pyruvate to form alanine preventing ammonium accumulation in muscles. This type of muscle breakdown to provide further energy for

muscle contraction is induced in a fasting state where glucose availability is low (Sarabhai & Roden, 2019). It is possible that an ALT enzyme exists in the *C. jejuni* genome responsible for the transfer of the amino-group of alanine to 2-oxoglutarate to form glutamate which can then feed into the GS:GOGAT cycle. This would allow external alanine to be used as an N-source, providing a rationale for the existence of an alanine transporter. One possible candidate in *C. jejuni* which shows 22.43% identity with the human ALT is AspB. AspB has been shown to possess aspartate:glutamate aminotransferase activity responsible for conversion of glutamate to aspartate for growth on glutamate (Guccione et al., 2008). Type I aminotransferases have been shown to be active with a wide range of substrates (Mehta et al., 1993). Therefore, it is possible that AspB acts on both aspartate and alanine. This may in part explain why Guccione et al. (2008) observed a growth defect in a *aspB* mutant when grown on alternative carbon sources to glutamate. It is plausible that when glutamine is at excess concentrations that glutamate levels in the cytoplasm are also elevated due to the conversion of glutamine to glutamate via GOGAT. Therefore, the cell is not dependent on alanine transport for the production of glutamate triggering a reduction in the expression of alanine transporters. This hypothesis provides a metabolic link between glutamine and alanine, which could explain the glutamine-dependent down-regulation of a putative alanine transporter (Cj0935c-34c) in the RNA-seq dataset.

The presence of the pseudogene *Cj0501 (amt)* in the RNA-seq dataset suggested that glutamine is transcriptionally linked to ammonia assimilation. This provided further evidence for our hypothesis that glutamine acts more as a nitrogen source and less of a carbon source in *C. jejuni*. To explore the role of ammonia in NCTC11168 we performed a growth experiment in minimal media with both nitrogen sources, glutamine and ammonia independently and together. As expected, due to the multiple frameshifts and stop codons rendering *amt* a pseudogene it does not appear that ammonia is transported readily into the cytoplasm. However, glutamine stimulates a large increase in growth. When grown in the presence of both ammonia and glutamine there is also no statistical difference in growth compared to growth with glutamine alone. To explore the role of glutamine as a nitrogen source in *C. jejuni* we performed some phylogenetic analysis on the presence of *amt* and *Cj0903c* in *C. jejuni* (figure 5.10). A phylogenetically-representative subset of 100 strains from over 400 complete Campylobacter genomes in Genbank was collected and analysed for the presence of *amt* and *Cj0903c* as functional and non-functional gene copies. Ammonium transporter *amt* is present in the majority of *C. jejuni* strains however it exists

as a pseudogene in approximately half of the *C. jejuni* strains. *Cj0903c* on the other hand is functional and present across all *C. jejuni* strains. Interestingly, in other common lab strains such as 81-176 and 81116 *Cj0903c* is present and functional however *amt* is completely missing from the genome. This suggests that amongst *C. jejuni* it is likely that glutamine acts as the major nitrogen source and ammonia is not utilised. *Campylobacter coli* species appear to possess both *Cj0903c* and a functional copy of *amt*. Outside of the *C. jejuni* and *C. coli* species *amt* is largely missing from the genome of *Campylobacter* species and *Cj0903c* is fairly common, gut strain *C. lanienae* is an exception where *amt* is intact and functional and *Cj0903c* is missing. Some strains are devoid of both *amt* and *Cj0903c* and therefore must utilise an alternative nitrogen donor or ammonia/glutamine transport system. Overall, amongst *C. jejuni* and *C. coli* species it is likely that glutamine acts as the key nitrogen source and is essential for optimal growth.

Finally, this chapter concludes with the identification of a bona fide glutamine transporter, *Cj0903c*, which we propose to be named *gutA* (glutamine uptake **A**). RNA-seq analysis revealed *Cj0903c* to be downregulated in response to excess glutamine. A foldchange of 0.2566 (p. value <0.0001) was observed compared to WT. Bioinformatic analysis revealed *Cj0903c* to have homology to *AlST* a sodium alanine symporter in bacteria. However, we have discovered this gene to be involved in the uptake of glutamine. A 11168 Δ 0903c strain has a significant growth defect when grown on glutamine compared to WT which is complemented by the insertion of an *Cj0903c* gene copy under the *metK* promoter. Similarly, the 11168 Δ 0903c strain showed increased resistance to GGH a toxic glutamine analog. Finally, a radiolabelled glutamine uptake assay revealed a severe defect in glutamine uptake in the 11168 Δ 0903c strain which was partially complemented. Interestingly there appears to be some residual growth on glutamine in the 11168 Δ 0903c strain when growing on glutamine. This residual growth is only significant at excess glutamine concentrations >2 mM. However, in the glutamine uptake assay there was no detectable C14 labelled glutamine transport. We suggest that the residual growth observed is likely to be non-specific low affinity transport of glutamine by other systems, potentially *Cj0935c-34c*. Therefore, we conclude that *GutA* is likely the sole glutamine transporter in the NCTC11168 genome. In addition Hendrixson & DiRita, (2004) have also shown using signature-tagged transposon mutagenesis that a transposon insertion in *cj0903c* results in a dramatic colonization defect. This *in vivo* observation suggests that glutamine may be important in virulence as well as growth and survival. *AlST* in *Staphylococcus aureus* is

another example in the literature of a glutamine transporter being incorrectly annotated as an alanine/sodium symporter. No difference in the uptake of radiolabeled alanine was detected in an *alsT* mutant compared to WT (Zeden et al., 2018). They later discovered that glutamine uptake in an *alsT* mutant was severely reduced compared to WT. Interestingly *S. aureus* also contains a *glnPQ* operon as seen in *C. jejuni*. Zeden et al. (2020) have also shown that a *glnQ* mutant displays no difference in glutamine uptake or GGH sensitivity compared to WT. Glutamine was also shown to act as a nitrogen source in *S. aureus* and stimulates growth in defined medium containing a carbon source similar to what we have observed in *C. jejuni*. However, this stimulation was also observed with ammonia suggesting both glutamine and ammonia act as a nitrogen source in *S. aureus* (Zeden et al., 2020). The work by Zeden et al. (2020) further verifies our findings that glutamine is an essential nitrogen source transported into the cell solely by GutA and currently annotated transporters GlnPQ and PaqPQ are unlikely to be glutamine specific transporters. Further work will be required to identify the role of these transporters.

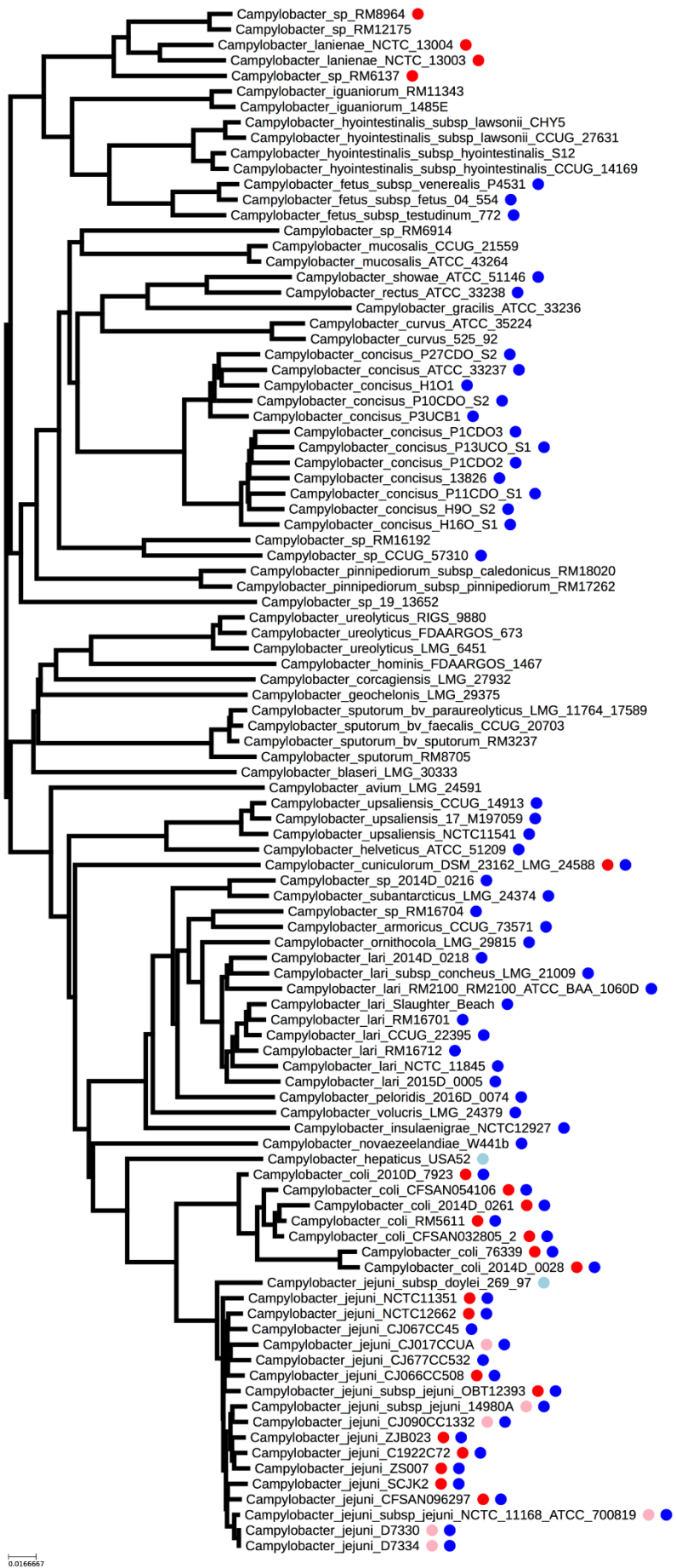


Figure 5.10 Distribution of *cj0903c* and *amt* in *C. jejuni*. A phylogenetically representative subset of 100 strains was generated from over 400+ complete *Campylobacter* genomes on Genbank using *mashtree* and *treemmer*. *Blast* (*tblastn* and *blastp*) searches were used to identify the presence of *cj0903c* and *amt* with a threshold of >50% identity and >50% query length. Red indicated the presence of a *amt* homologue and blue indicates the presence of a *cj0903c* homologue. These are shown as pink and light blue if the homologue is a likely pseudogene, respectively.

Chapter 6 Final conclusions and further work

This study has expanded on the current knowledge of the *Campylobacter jejuni* phosphoproteome revealing up to ten times the number of S/T/Y phosphorylated proteins previously known. We have shown that the annotated S/T phosphatase, Cj0184c, does indeed possess phosphatase activity. The mass spectrometry workflow we devised did provide us with putative targets of this phosphatase. However, in this case our chosen target, a glutamine ABC transport protein, did not perform its annotated function. We were therefore unable to provide a link between the dephosphorylating action of Cj0184c and GlnQ. However, this line of experiments did reveal the importance of glutamine as a nitrogen source in *C. jejuni*. In chapter 3 RNA-sequencing revealed a variety of possible glutamine transport candidates including an annotated putative amino-acid transport protein with homology to a sodium:alanine symporter that was highly down-regulated by excess glutamine. Growth analysis of the corresponding mutant on glutamine and treatment with toxic glutamine analogue, γ -l-glutamylhydrazide (GGH), indicate this gene to be responsible for the majority of glutamine-stimulated growth in culture. Further analysis using radio labelled glutamine in an uptake experiment confirmed this gene to encode the dominant glutamine transport protein. We now propose to name this gene to be named *gutA* (**g**lutamine **u**ptake **A**).

There are still multiple questions to be answered in this study. Firstly, if we could identify the substrate of the GlnPQ ABC transport system we could investigate the role of Cj0184c in the regulation of active transport driven by GlnQ. Radio labelled uptake assays with a range of substrates could identify the putative substrate of GlnPQ. Alternatively, growth experiments using defined medium could be valuable, proline is a key candidate based on the growth defect observed in the 11168 Δ 0184c strain. Additionally, the other significantly phosphorylated proteins in the 11168 Δ 0184c strain could be investigated. Although mostly uncharacterised a flagellar biosynthesis protein and CjaA are significantly phosphorylated in the absence of Cj0184c and therefore a role for phosphorylation in motility and cysteine transport could be explored. In regard to glutamine transport we need to establish if our findings are applicable to other strains. Currently all our observations are in NCTC11168, mutants must be constructed in strains such as 81-176 to verify that GutA is the dominant glutamine transporter and the PaqPQ system does not transport glutamine as previously suggested. Additionally, the regulation of nitrogen metabolism is unknown in *C. jejuni*. Using the RNA-seq data set we could potentially identify further targets subject to

regulation by glutamine. These targets may provide insights into the regulation of glutamine transport and thus nitrogen metabolism. Finally, the alanine hypothesis discussed in chapter 5 could be investigated. We suggest that alanine could be an alternative nitrogen source transported by Cj0935-34c. Using minimal media, a growth experiment could clearly identify an increase in OD_{600nm} in the presence of pyruvate and alanine compared to pyruvate alone. The role of ammonia in strains with a functional *amt* gene could be investigated in a similar manner.

This study has shown that gene annotations can be misleading and in the case of glutamine transport two currently annotated systems will now need to be characterised (PaqPQ and GlnPQ). Transcriptome analysis from chemostat culture has proven to be a valuable technique and could be used to explore the metabolism of substrates other than glutamine.

Chapter 7 References

- Afgan, E., Baker, D., Batut, B., van den Beek, M., Bouvier, D., Čech, M., Chilton, J., Clements, D., Coraor, N., Grüning, B. A., Guerler, A., Hillman-Jackson, J., Hiltmann, S., Jalili, V., Rasche, H., Soranzo, N., Goecks, J., Taylor, J., Nekrutenko, A., & Blankenberg, D. (2018). The Galaxy platform for accessible, reproducible and collaborative biomedical analyses: 2018 update. *Nucleic Acids Research*, *46*(W1), W537–W544. <https://doi.org/10.1093/NAR/GKY379>
- Ahmad, Z., Morona, R., & Standish, A. J. (2018). In vitro characterization and identification of potential substrates of a low molecular weight protein tyrosine phosphatase in streptococcus pneumoniae. *Microbiology (United Kingdom)*, *164*(4), 697–703. <https://doi.org/10.1099/mic.0.000631>
- Al-Haideri, H., White, M. A., & Kelly, D. J. (2016). Major contribution of the type II beta carbonic anhydrase CanB (Cj0237) to the capnophilic growth phenotype of *Campylobacter jejuni*. *Environmental Microbiology*, *18*(2), 721–735. <https://doi.org/10.1111/1462-2920.13092>
- Allos, B. M. (1997). Association between *Campylobacter* infection and Guillain-Barre syndrome. *Journal of Infectious Diseases*, *176*(6 SUPPL.). <https://doi.org/10.1086/513783>
- Altekruse, S. F., Stern, N. J., Fields, P. I., & Swerdlow, D. L. (1999). *Campylobacter jejuni* - An emerging foodborne pathogen. In *Emerging Infectious Diseases* (Vol. 5, Issue 1, pp. 28–35). Centers for Disease Control and Prevention (CDC). <https://doi.org/10.3201/eid0501.990104>
- Ashgar, S. S. A., Oldfield, N. J., Wooldridge, K. G., Jones, M. A., Irving, G. J., Turner, D. P. J., & Ala'Aldeen, D. A. A. (2007). CapA, an Autotransporter Protein of *Campylobacter jejuni*, Mediates Association with Human Epithelial Cells and Colonization of the Chicken Gut. *Journal of Bacteriology*, *189*(5), 1856. <https://doi.org/10.1128/JB.01427-06>
- Av-Gay, Y., & Everett, M. (2000). The eukaryotic-like Ser/Thr protein kinases of *Mycobacterium tuberculosis*. In *Trends in Microbiology* (Vol. 8, Issue 5, pp. 238–244). Trends Microbiol. [https://doi.org/10.1016/S0966-842X\(00\)01734-0](https://doi.org/10.1016/S0966-842X(00)01734-0)
- Avrain, L., Vernozy-Rozand, C., & Kempf, I. (2004). Evidence for natural horizontal transfer of tetO gene between *Campylobacter jejuni* strains in chickens. *Journal of Applied Microbiology*, *97*(1), 134–140. <https://doi.org/10.1111/j.1365-2672.2004.02306.x>
- Bach, H., Wong, D., & Av-Gay, Y. (2009). *Mycobacterium tuberculosis* PtkA is a novel protein tyrosine kinase whose substrate is PtpA. *Biochemical Journal*, *420*(2), 155–160. <https://doi.org/10.1042/BJ20090478>
- Barnes, I. H. A., Bagnall, M. C., Browning, D. D., Thompson, S. A., Manning, G., & Newell, D. G. (2007). γ -Glutamyl transpeptidase has a role in the persistent colonization of the avian gut by *Campylobacter jejuni*. *Microbial Pathogenesis*, *43*(5–6), 198. <https://doi.org/10.1016/J.MICPATH.2007.05.007>
- Bartell, S. M., & Batal, A. B. (2007). The Effect of Supplemental Glutamine on Growth Performance, Development of the Gastrointestinal Tract, and Humoral Immune Response of Broilers. *Poultry Science*, *86*(9), 1940–1947. <https://doi.org/10.1093/PS/86.9.1940>
- Blaser, M. J. (1997). Epidemiologic and Clinical Features of *Campylobacter jejuni* Infections.

- The Journal of Infectious Diseases*, 176(2), 103–105.
https://academic.oup.com/jid/article/176/Supplement_2/S103/841617
- Boll, J. M., & Hendrixson, D. R. (2013). A regulatory checkpoint during flagellar biogenesis in campylobacter jejuni initiates signal transduction to activate transcription of flagellar genes. *MBio*, 4(5). <https://doi.org/10.1128/MBIO.00432-13>
- Breitkopf, S. B., & Asara, J. M. (2012). Determining in vivo phosphorylation sites using mass spectrometry. *Current Protocols in Molecular Biology*, 1(SUPPL.98).
<https://doi.org/10.1002/0471142727.mb1819s98>
- Cain, J. A., Solis, N., & Cordwell, S. J. (2014). Beyond gene expression: The impact of protein post-translational modifications in bacteria. In *Journal of Proteomics* (Vol. 97, pp. 265–286). Elsevier. <https://doi.org/10.1016/j.jprot.2013.08.012>
- Caldwell, M. B., Guerry, P., Lee, E. C., Burans, J. P., & Walker, R. I. (1985). Reversible Expression of Flagella in Campylobacter jejuni. In *INFECTION AND IMMUNITY*.
- Cha, W., Mosci, R. E., Wengert, S. L., Vargas, C. V., Rust, S. R., Bartlett, P. C., Grooms, D. L., & Manning, S. D. (2017). Comparing the genetic diversity and antimicrobial resistance profiles of Campylobacter jejuni recovered from cattle and humans. *Frontiers in Microbiology*, 8(MAY). <https://doi.org/10.3389/fmicb.2017.00818>
- Champion, O. L., Karlyshev, A. V., Senior, N. J., Woodward, M., La Ragione, R., Howard, S. L., Wren, B. W., & Titball, R. W. (2010). Insect infection model for Campylobacter jejuni reveals that O-methyl phosphoramidate has insecticidal activity. *Journal of Infectious Diseases*, 201(5), 776–782. <https://doi.org/10.1086/650494>
- Chaudhuri, R. R., Yu, L., Kanji, A., Perkins, T. T., Gardner, P. P., Choudhary, J., Maskell, D. J., & Grant, A. J. (2011). Quantitative RNA-seq analysis of the Campylobacter jejuni transcriptome. *Microbiology*, 157(Pt 10), 2922.
<https://doi.org/10.1099/MIC.0.050278-0>
- Christensen, D. G., Baumgartner, J. T., Xie, X., Jew, K. M., Basisty, N., Schilling, B., Kuhn, M. L., & Wolfe, A. J. (2019). Mechanisms, Detection, and Relevance of Protein Acetylation in Prokaryotes. *MBio*, 10(2). <https://doi.org/10.1128/MBIO.02708-18>
- Cieśla, J., Frączyk, T., & Rode, W. (2011). *Phosphorylation of basic amino acid residues in proteins: important but easily missed*. www.actabp.pl
- Corcoran, A. T., Annuk, H., & Moran, A. P. (2006). The structure of the lipid anchor of Campylobacter jejuni polysaccharide. *FEMS Microbiology Letters*, 257(2), 228–235.
<https://doi.org/10.1111/j.1574-6968.2006.00177.x>
- Cozzone, A. J., Grangeasse, C., Doublet, P., & Duclos, B. (2004). Protein phosphorylation on tyrosine in bacteria. In *Archives of Microbiology* (Vol. 181, Issue 3, pp. 171–181). Arch Microbiol. <https://doi.org/10.1007/s00203-003-0640-6>
- Davies, C., Taylor, A. J., Elmi, A., Winter, J., Liaw, J., Grabowska, A. D., Gundogdu, O., Wren, B. W., Kelly, D. J., & Dorrell, N. (2019). Sodium Taurocholate Stimulates Campylobacter jejuni Outer Membrane Vesicle Production via Down-Regulation of the Maintenance of Lipid Asymmetry Pathway. *Frontiers in Cellular and Infection Microbiology*, 9(MAY), 177. <https://doi.org/10.3389/FCIMB.2019.00177>
- Debruyne, L., Gevers, D., & Vandamme, P. (2008). Taxonomy of the Family Campylobacteraceae. In *Campylobacter* (pp. 1–25). ASM Press.
<https://doi.org/10.1128/9781555815554.ch1>

- Deutscher, J., & Saier, M. H. (2006). Ser/Thr/Tyr protein phosphorylation in bacteria - For long time neglected, now well established. *Journal of Molecular Microbiology and Biotechnology*, *9*(3–4), 125–131. <https://doi.org/10.1159/000089641>
- Dixon, S. D., Huynh, M. M., Tamilselvam, B., Spiegelman, L. M., Son, S. B., Eshraghi, A., Blanke, S. R., & Bradley, K. A. (2015). Distinct Roles for CdtA and CdtC during Intoxication by Cytolethal Distending Toxins. *PLOS ONE*, *10*(11), e0143977. <https://doi.org/10.1371/JOURNAL.PONE.0143977>
- Duclos, B., Grangeasse, C., Vaganay, E., Riberty, M., & Cozzone, A. J. (1996). Autophosphorylation of a bacterial protein at tyrosine. In *Journal of Molecular Biology* (Vol. 259, Issue 5, pp. 891–895). Academic Press. <https://doi.org/10.1006/jmbi.1996.0366>
- Dworkin, J. (2015). Ser/Thr phosphorylation as a regulatory mechanism in bacteria. In *Current Opinion in Microbiology* (Vol. 24, pp. 47–52). Elsevier Ltd. <https://doi.org/10.1016/j.mib.2015.01.005>
- EFSA. (2010). Analysis of the baseline survey on the prevalence of *Campylobacter* in broiler batches and of *Campylobacter* and *Salmonella* on broiler carcasses in the EU, 2008 - Part A: *Campylobacter* and *Salmonella* prevalence estimates. *EFSA Journal*, *8*(3), 1–99. <https://doi.org/10.2903/j.efsa.2010.1503>
- Elmi, A., Watson, E., Sandu, P., Gundogdu, O., Mills, D. C., Inglis, N. F., Manson, E., Imrie, L., Bajaj-Elliott, M., Wren, B. W., Smith, D. G. E., & Dorrell, N. (2012). *Campylobacter jejuni* Outer Membrane Vesicles Play an Important Role in Bacterial Interactions with Human Intestinal Epithelial Cells. *Infection and Immunity*, *80*(12), 4089. <https://doi.org/10.1128/IAI.00161-12>
- Fauchère, J. L., Kervella, M., Rosenau, A., Mohanna, K., & Véron, M. (1989). Adhesion to HeLa cells of *Campylobacter jejuni* and *C. coli* outer membrane components. *Research in Microbiology*, *140*(5), 379–392. [https://doi.org/10.1016/0923-2508\(89\)90014-4](https://doi.org/10.1016/0923-2508(89)90014-4)
- Felig, P., Pozefsky, T., Marliss, E., & Cahill, G. (1970). Alanine: key role in gluconeogenesis. *Science (New York, N.Y.)*, *167*(3920), 1003–1004. <https://doi.org/10.1126/SCIENCE.167.3920.1003>
- Fiuza, M., Canova, M. J., Zanella-Cléon, I., Becchi, M., Cozzone, A. J., Mateos, L. M., Kremer, L., Gil, J. A., & Molle, V. (2008). From the characterization of the four serine/threonine protein kinases (PknA/B/G/L) of *Corynebacterium glutamicum* toward the role of PknA and PknB in cell division. *Journal of Biological Chemistry*, *283*(26), 18099–18112. <https://doi.org/10.1074/jbc.M802615200>
- Flanagan, R. C., Neal-McKinney, J. M., Dhillon, A. S., Miller, W. G., & Konkel, M. E. (2009). Examination of *Campylobacter jejuni* putative adhesins leads to the identification of a new protein, designated FlpA, required for chicken colonization. *Infection and Immunity*, *77*(6), 2399–2407. <https://doi.org/10.1128/IAI.01266-08>
- Forchhammer, K. (2007). Glutamine signalling in bacteria. *Frontiers in Bioscience : A Journal and Virtual Library*, *12*(1), 358–370. <https://doi.org/10.2741/2069>
- Forsythe. (2000). *The Microbiology of Safe Food, 3rd Edition | Wiley* (1st ed.). Blackwell Science Ltd. <https://www.wiley.com/en-gb/The+Microbiology+of+Safe+Food,+3rd+Edition-p-9781119405016>
- FSA. (2015). *A microbiological survey of campylobacter contamination in fresh whole UK-*

produced chilled chickens at retail sale (Y2/3/4) | Food Standards Agency.
<https://www.food.gov.uk/research/foodborne-diseases/a-microbiological-survey-of-campylobacter-contamination-in-fresh-whole-uk-produced-chilled-chickens-at-retail-sale-y234>

- Fuhrmann, J., Schmidt, A., Spiess, S., Lehner, A., Turgay, K., Mechtler, K., Charpentier, E., & Clausen, T. (2009). McsB Is a protein arginine kinase that phosphorylates and inhibits the heat-shock regulator ctsr. *Science*, *324*(5932), 1323–1327.
<https://doi.org/10.1126/science.1170088>
- Gao, B., Vorwerk, H., Huber, C., Lara-Tejero, M., Mohr, J., Goodman, A. L., Eisenreich, W., Galán, J. E., & Hofreuter, D. (2017). Metabolic and fitness determinants for in vitro growth and intestinal colonization of the bacterial pathogen *Campylobacter jejuni*. *PLOS Biology*, *15*(5), e2001390. <https://doi.org/10.1371/JOURNAL.PBIO.2001390>
- Garnak, M., & Reeves, H. C. (1979). Phosphorylation of isocitrate dehydrogenase of *Escherichia coli*. *Science*, *203*(4385), 1111–1112.
<https://doi.org/10.1126/science.34215>
- Gaynor, E., Wells, D., MacKichan, J., & Falkow, S. (2005). The *Campylobacter jejuni* stringent response controls specific stress survival and virulence-associated phenotypes. *Molecular Microbiology*, *56*(1), 8–27. <https://doi.org/10.1111/J.1365-2958.2005.04525.X>
- Ge, R., Sun, X., Xiao, C., Yin, X., Shan, W., Chen, Z., & He, Q. Y. (2011). Phosphoproteome analysis of the pathogenic bacterium *Helicobacter pylori* reveals over-representation of tyrosine phosphorylation and multiply phosphorylated proteins. *Proteomics*, *11*(8), 1449–1461. <https://doi.org/10.1002/pmic.201000649>
- Ge, Z., Feng, Y., Whary, M. T., Nambiar, P. R., Xu, S., Ng, V., Taylor, N. S., & Fox, J. G. (2005). Cytolethal Distending Toxin Is Essential for *Helicobacter hepaticus* Colonization in Outbred Swiss Webster Mice. *Infection and Immunity*, *73*(6), 3559.
<https://doi.org/10.1128/IAI.73.6.3559-3567.2005>
- Gilbert, M., Karwaski, M. F., Bernatchez, S., Young, N. M., Taboada, E., Michniewicz, J., Cunningham, A. M., & Wakarchuk, W. W. (2002). The genetic bases for the variation in the lipo-oligosaccharide of the mucosal pathogen, *Campylobacter jejuni*. Biosynthesis of sialylated ganglioside mimics in the core oligosaccharide. *Journal of Biological Chemistry*, *277*(1), 327–337. <https://doi.org/10.1074/jbc.M108452200>
- Grangeasse, C., Cozzone, A. J., Deutscher, J., & Mijakovic, I. (2007). Tyrosine phosphorylation: an emerging regulatory device of bacterial physiology. In *Trends in Biochemical Sciences* (Vol. 32, Issue 2, pp. 86–94). Trends Biochem Sci.
<https://doi.org/10.1016/j.tibs.2006.12.004>
- Grangeasse, C., Obadia, B., Mijakovic, I., Deutscher, J., Cozzone, A. J., & Doublet, P. (2003). Autophosphorylation of the *Escherichia coli* protein kinase Wzc regulates tyrosine phosphorylation of Ugd, a UDP-glucose dehydrogenase. *Journal of Biological Chemistry*, *278*(41), 39323–39329. <https://doi.org/10.1074/jbc.M305134200>
- Guccione, E. J., Kendall, J. J., Hitchcock, A., Garg, N., White, M. A., Mulholland, F., Poole, R. K., & Kelly, D. J. (2017). Transcriptome and proteome dynamics in chemostat culture reveal how *Campylobacter jejuni* modulates metabolism, stress responses and virulence factors upon changes in oxygen availability. *Environmental Microbiology*, *19*(10), 4326. <https://doi.org/10.1111/1462-2920.13930>

- Guccione, E., Leon-Kempis, M. D. R., Pearson, B. M., Hitchin, E., Mulholland, F., Diemen, P. M. Van, Stevens, M. P., & Kelly, D. J. (2008). Amino acid-dependent growth of *Campylobacter jejuni*: key roles for aspartase (AspA) under microaerobic and oxygen-limited conditions and identification of AspB (Cj0762), essential for growth on glutamate. *Molecular Microbiology*, *69*(1), 77–93. <https://doi.org/10.1111/J.1365-2958.2008.06263.X>
- Guerry, P., Alm, R. A., Power, M. E., Logan, S. M., & Trust2, T. J. (1991). Role of Two Flagellin Genes in *Campylobacter* Motility. *JOURNAL OF BACTERIOLOGY*, *173*(15), 4757–4764.
- Gupta, N., Tanner, S., Jaitly, N., Adkins, J. N., Lipton, M., Edwards, R., Romine, M., Osterman, A., Bafna, V., Smith, R. D., & Pevzner, P. A. (2007). Whole proteome analysis of post-translational modifications: Applications of mass-spectrometry for proteogenomic annotation. *Genome Research*, *17*(9), 1362–1377. <https://doi.org/10.1101/gr.6427907>
- Hanks, S. K., Quinn, A. M., & Hunter, T. (1988). The protein kinase family: Conserved features and deduced phylogeny of the catalytic domains. *Science*, *241*(4861), 42–52. <https://doi.org/10.1126/science.3291115>
- Harris, N. V., Weiss, N. S., & Nolan, C. M. (1986). The role of poultry and meats in the etiology of *Campylobacter jejuni/coli* enteritis. *American Journal of Public Health*, *76*(4), 407–411. <https://doi.org/10.2105/AJPH.76.4.407>
- Hazelbauer, G. L., & Lai, W.-C. (2010). BACTERIAL CHEMORECEPTORS: PROVIDING ENHANCED FEATURES TO TWO-COMPONENT SIGNALING. *Current Opinion in Microbiology*, *13*(2), 124. <https://doi.org/10.1016/J.MIB.2009.12.014>
- Heikema, A. P., Islam, Z., Horst-Kreft, D., Huizinga, R., Jacobs, B. C., Wagenaar, J. A., Poly, F., Guerry, P., van Belkum, A., Parker, C. T., & Endtz, H. P. (2015). *Campylobacter jejuni* capsular genotypes are related to Guillain-Barré syndrome. *Clinical Microbiology and Infection*, *21*(9), 852.e1-852.e9. <https://doi.org/10.1016/j.cmi.2015.05.031>
- Hendrixson, D. R., & DiRita, V. J. (2004). Identification of *Campylobacter jejuni* genes involved in commensal colonization of the chick gastrointestinal tract. *Molecular Microbiology*, *52*(2), 471–484. <https://doi.org/10.1111/J.1365-2958.2004.03988.X/FORMAT/PDF>
- Hofreuter, D. (2014). Defining the metabolic requirements for the growth and colonization capacity of *Campylobacter jejuni*. *Frontiers in Cellular and Infection Microbiology*, *4*(SEP). <https://doi.org/10.3389/FCIMB.2014.00137>
- Hofreuter, D., Novik, V., & Galán, J. E. (2008). Metabolic Diversity in *Campylobacter jejuni* Enhances Specific Tissue Colonization. *Cell Host & Microbe*, *4*(5), 425–433. <https://doi.org/10.1016/J.CHOM.2008.10.002>
- Hofreuter, D., Tsai, J., Watson, R. O., Novik, V., Altman, B., Benitez, M., Clark, C., Perbost, C., Jarvie, T., Du, L., & Galán, J. E. (2006). Unique Features of a Highly Pathogenic *Campylobacter jejuni* Strain. *Infection and Immunity*, *74*(8), 4694. <https://doi.org/10.1128/IAI.00210-06>
- Jackson, R. J., Elvers, K. T., Lee, L. J., Gidley, M. D., Wainwright, L. M., Lightfoot, J., Park, S. F., & Poole, R. K. (2007). Oxygen Reactivity of Both Respiratory Oxidases in *Campylobacter jejuni*: the *cydAB* Genes Encode a Cyanide-Resistant, Low-Affinity Oxidase That Is Not of the Cytochrome bd Type. *Journal of Bacteriology*, *189*(5), 1604. <https://doi.org/10.1128/JB.00897-06>

- Jers, C., Pedersen, M. M., Paspaliari, D. K., Schütz, W., Johnsson, C., Soufi, B., MacEk, B., Jensen, P. R., & Mijakovic, I. (2010). *Bacillus subtilis* BY-kinase PtkA controls enzyme activity and localization of its protein substrates. *Molecular Microbiology*, *77*(2), 287–299. <https://doi.org/10.1111/j.1365-2958.2010.07227.x>
- Jiang, P., & Ninfa, A. J. (1999). Regulation of Autophosphorylation of *Escherichia coli* Nitrogen Regulator II by the PII Signal Transduction Protein. *Journal of Bacteriology*, *181*(6), 1906. [/pmc/articles/PMC93592/](https://doi.org/10.1128/j.1365-2958.1999.02294.x)
- Jin, S., Joe, A., Lynett, J., Hani, E., Sherman, P., & Chan, V. (2001). JlpA, a novel surface-exposed lipoprotein specific to *Campylobacter jejuni*, mediates adherence to host epithelial cells. *Molecular Microbiology*, *39*(5), 1225–1236. <https://doi.org/10.1111/J.1365-2958.2001.02294.X>
- Jin, S., Song, Y., Emili, A., Sherman, P., & Chan, V. (2003). JlpA of *Campylobacter jejuni* interacts with surface-exposed heat shock protein 90alpha and triggers signalling pathways leading to the activation of NF-kappaB and p38 MAP kinase in epithelial cells. *Cellular Microbiology*, *5*(3), 165–174. <https://doi.org/10.1046/J.1462-5822.2003.00265.X>
- Karlyshev, A. V., Champion, O. L., Churcher, C., Brisson, J. R., Jarrell, H. C., Gilbert, M., Brochu, D., St Michael, F., Li, J., Wakarchuk, W. W., Goodhead, I., Sanders, M., Stevens, K., White, B., Parkhill, J., Wren, B. W., & Szymanski, C. M. (2005). Analysis of *Campylobacter jejuni* capsular loci reveals multiple mechanisms for the generation of structural diversity and the ability to form complex heptoses. *Molecular Microbiology*, *55*(1), 90–103. <https://doi.org/10.1111/j.1365-2958.2004.04374.x>
- Kendall, J. J., Barrero-Tobon, A. M., Hendrixson, D. R., & Kelly, D. J. (2014). Hemerythrins in the microaerophilic bacterium *Campylobacter jejuni* help protect key iron–sulphur cluster enzymes from oxidative damage. *Environmental Microbiology*, *16*(4), 1105. <https://doi.org/10.1111/1462-2920.12341>
- Kennelly, P. J., & Krebs, E. G. (1991). Consensus sequences as substrate specificity determinants for protein kinases and protein phosphatases. In *Journal of Biological Chemistry* (Vol. 266, Issue 24, pp. 15555–15558). Elsevier. [https://doi.org/10.1016/s0021-9258\(18\)98436-x](https://doi.org/10.1016/s0021-9258(18)98436-x)
- Ketley, J. M. (1997). Pathogenesis of enteric infection by *Campylobacter*. In *Microbiology* (Vol. 143, Issue 1, pp. 5–21). Microbiology Society. <https://doi.org/10.1099/00221287-143-1-5>
- Kobir, A., Shi, L., Boskovic, A., Grangeasse, C., Franjevic, D., & Mijakovic, I. (2011). Protein phosphorylation in bacterial signal transduction. In *Biochimica et Biophysica Acta - General Subjects* (Vol. 1810, Issue 10, pp. 989–994). Biochim Biophys Acta. <https://doi.org/10.1016/j.bbagen.2011.01.006>
- Komagamine, T., & Yuki, N. (2008). Ganglioside Mimicry as a Cause of Guillain-Barre Syndrome. *CNS & Neurological Disorders - Drug Targets*, *5*(4), 391–400. <https://doi.org/10.2174/187152706777950765>
- Konkel, M. E., Christensen, J. E., Keech, A. M., Monteville, M. R., Klena, J. D., & Garvis, S. G. (2005). Identification of a fibronectin-binding domain within the *Campylobacter jejuni* CadF protein. *Molecular Microbiology*, *57*(4), 1022–1035. <https://doi.org/10.1111/J.1365-2958.2005.04744.X>
- Konkel, M. E., Garvis, S. G., Tipton, S. L., Donald E. Anderson, J., & Witold Cieplak, J. (1997).

- Identification and molecular cloning of a gene encoding a fibronectin-binding protein (CadF) from *Campylobacter jejuni*. *Molecular Microbiology*, *24*(5), 953–963. <https://doi.org/10.1046/J.1365-2958.1997.4031771.X>
- Konkel, M. E., Talukdar, P. K., Negretti, N. M., & Klappenbach, C. M. (2020). Taking Control: *Campylobacter jejuni* Binding to Fibronectin Sets the Stage for Cellular Adherence and Invasion. *Frontiers in Microbiology*, *11*, 564. <https://doi.org/10.3389/FMICB.2020.00564>
- Kornberg, H. L. (1966). The role and control of the glyoxylate cycle in *Escherichia coli*. In *The Biochemical journal* (Vol. 99, Issue 1, pp. 1–11). Biochem J. <https://doi.org/10.1042/bj0990001>
- Korolik, V. (2019). The role of chemotaxis during *Campylobacter jejuni* colonisation and pathogenesis. *Current Opinion in Microbiology*, *47*, 32–37. <https://doi.org/10.1016/J.MIB.2018.11.001>
- Kuehn, M. J., & Kesty, N. C. (2005). Bacterial outer membrane vesicles and the host–pathogen interaction. *Genes & Development*, *19*(22), 2645–2655. <https://doi.org/10.1101/GAD.1299905>
- Lacey, J. M., & Wilrnore, D. W. (1990). Is Glutamine a Conditionally Essential Amino Acid? *Nutrition Reviews*, *48*(8), 297–309. <https://academic.oup.com/nutritionreviews/article/48/8/297/1830646>
- Lara-Tejero, M., & Galán, J. E. (2001). CdtA, CdtB, and CdtC Form a Tripartite Complex That Is Required for Cytolethal Distending Toxin Activity. *Infection and Immunity*, *69*(7), 4358. <https://doi.org/10.1128/IAI.69.7.4358-4365.2001>
- Laub, M. T., & Goulian, M. (2007). *Specificity in Two-Component Signal Transduction Pathways*. <https://doi.org/10.1146/annurev.genet.41.042007.170548>
- Leon-Kempis, M. D. R., Guccione, E., Mulholland, F., Williamson, M. P., & Kelly, D. J. (2006). The *Campylobacter jejuni* PEB1a adhesin is an aspartate/glutamate-binding protein of an ABC transporter essential for microaerobic growth on dicarboxylic amino acids. *Molecular Microbiology*, *60*(5), 1262–1275. <https://doi.org/10.1111/J.1365-2958.2006.05168.X>
- Lertsethtakarn, P., Ottemann, K. M., & Hendrixson, D. R. (2011). Motility and Chemotaxis in *Campylobacter* and *Helicobacter*. *Annual Review of Microbiology*, *65*, 389. <https://doi.org/10.1146/ANNUREV-MICRO-090110-102908>
- Li, X., Apel, D., Gaynor, E. C., & Tanner, M. E. (2011). 5'-Methylthioadenosine Nucleosidase Is Implicated in Playing a Key Role in a Modified Futasine Pathway for Menaquinone Biosynthesis in *Campylobacter jejuni*. *The Journal of Biological Chemistry*, *286*(22), 19392. <https://doi.org/10.1074/JBC.M111.229781>
- Lin, A., Krastel, K., Hobb, R. I., Thompson, S. A., Cvitkovitch, D. G., & Gaynor, E. C. (2009). Atypical Roles for *Campylobacter jejuni* Amino Acid ATP Binding Cassette Transporter Components PaqP and PaqQ in Bacterial Stress Tolerance and Pathogen-Host Cell Dynamics. *Infection and Immunity*, *77*(11), 4912. <https://doi.org/10.1128/IAI.00571-08>
- Lin, M. H., Sugiyama, N., & Ishihama, Y. (2015). Systematic profiling of the bacterial phosphoproteome reveals bacterium-specific features of phosphorylation. *Science Signaling*, *8*(394), rs10–rs10. <https://doi.org/10.1126/scisignal.aaa3117>

- Lin, W. J., Walther, D., Connelly, J. E., Burnside, K., Jewell, K. A., Kenney, L. J., & Rajagopal, L. (2009). Threonine phosphorylation prevents promoter DNA binding of the Group B Streptococcus response regulator CovR. *Molecular Microbiology*, *71*(6), 1477–1495. <https://doi.org/10.1111/j.1365-2958.2009.06616.x>
- Lindmark, B., Rompikuntal, P. K., Vaitkevicius, K., Song, T., Mizunoe, Y., Uhlin, B. E., Guerry, P., & Wai, S. N. (2009). Outer membrane vesicle-mediated release of cytolethal distending toxin (CDT) from *Campylobacter jejuni*. *BMC Microbiology*, *9*, 220. <https://doi.org/10.1186/1471-2180-9-220>
- Lu, P., Ma, D., Chen, Y., Guo, Y., Chen, G.-Q., Deng, H., & Shi, Y. (2013). L-glutamine provides acid resistance for *Escherichia coli* through enzymatic release of ammonia. *Cell Research* *23*(5), 635–644. <https://doi.org/10.1038/cr.2013.13>
- Lübke, A.-L., Minatelli, S., Riedel, T., Lugert, R., Schober, I., Spröer, C., Overmann, J., Groß, U., Zautner, A. E., & Bohne, W. (2018). The transducer-like protein Tlp12 of *Campylobacter jejuni* is involved in glutamate and pyruvate chemotaxis. *BMC Microbiology* *18*(1), 1–10. <https://doi.org/10.1186/S12866-018-1254-0>
- Macek, B., Gnad, F., Soufi, B., Kumar, C., Olsen, J. V., Mijakovic, I., & Mann, M. (2008). Phosphoproteome analysis of *E. coli* reveals evolutionary conservation of bacterial Ser/Thr/Tyr phosphorylation. *Molecular and Cellular Proteomics*, *7*(2), 299–307. <https://doi.org/10.1074/mcp.M700311-MCP200>
- Macek, B., Mijakovic, I., Olsen, J. V., Gnad, F., Kumar, C., Jensen, P. R., & Mann, M. (2007). The serine/threonine/tyrosine phosphoproteome of the model bacterium *Bacillus subtilis*. *Molecular and Cellular Proteomics*, *6*(4), 697–707. <https://doi.org/10.1074/mcp.M600464-MCP200>
- Malinverni, J. C., & Silhavy, T. J. (2009). An ABC transport system that maintains lipid asymmetry in the Gram-negative outer membrane. *Proceedings of the National Academy of Sciences*, *106*(19), 8009–8014. <https://doi.org/10.1073/PNAS.0903229106>
- Mangat, C. S., & Brown, E. D. (2008). Known Bioactive Small Molecules Probe the Function of a Widely Conserved but Enigmatic Bacterial ATPase, YjeE. *Chemistry and Biology*, *15*(12), 1287–1295. <https://doi.org/10.1016/j.chembiol.2008.10.007>
- Mashburn-Warren, L., Mclean, R. J. C., & Whiteley, M. (2008). Gram-negative outer membrane vesicles: beyond the cell surface. *Geobiology*, *6*(3), 214. <https://doi.org/10.1111/J.1472-4669.2008.00157.X>
- Maue, A. C., Mohawk, K. L., Giles, D. K., Poly, F., Ewing, C. P., Jiao, Y., Lee, G., Ma, Z., Monteiro, M. A., Hill, C. L., Ferderber, J. S., Porter, C. K., Trent, S. M., & Guerry, P. (2013). The polysaccharide capsule of *Campylobacter jejuni* modulates the host immune response. *Infection and Immunity*, *81*(3), 665–672. <https://doi.org/10.1128/IAI.01008-12>
- McNally, D. J., Jarrell, H. C., Li, J., Khieu, N. H., Vinogradov, E., Szymanski, C. M., & Brisson, J.-R. (2005). The HS:1 serostrain of *Campylobacter jejuni* has a complex teichoic acid-like capsular polysaccharide with nonstoichiometric fructofuranose branches and O-methyl phosphoramidate groups. *The FEBS Journal*, *272*(17), 4407–4422. <https://doi.org/10.1111/J.1742-4658.2005.04856.X>
- McNally, D. J., Lamoureux, M. P., Karlyshev, A. V., Fiori, L. M., Li, J., Thacker, G., Coleman, R. A., Khieu, N. H., Wren, B. W., Brisson, J. R., Jarrell, H. C., & Szymanski, C. M. (2007). Commonality and biosynthesis of the O-methyl phosphoramidate capsule

- modification in *Campylobacter jejuni*. *Journal of Biological Chemistry*, 282(39), 28566–28576. <https://doi.org/10.1074/jbc.M704413200>
- Mehta, P. K., Hale, T. I., & Christen, P. (1993). Aminotransferases: demonstration of homology and division into evolutionary subgroups. *European Journal of Biochemistry*, 214(2), 549–561. <https://doi.org/10.1111/J.1432-1033.1993.TB17953.X>
- Meins, M., Jenö, P., Müller, D., Richter, W. J., Rosenbusch, J. P., & Erni, B. (1993). Cysteine phosphorylation of the glucose transporter of *Escherichia coli*. *Journal of Biological Chemistry*, 268(16), 11604–11609. [https://doi.org/10.1016/s0021-9258\(19\)50244-7](https://doi.org/10.1016/s0021-9258(19)50244-7)
- Merrick, M. J., & Edwards, R. A. (1995). Nitrogen control in bacteria. *Microbiological Reviews*, 59(4), 604. [/pmc/articles/PMC239390/?report=abstract](https://pubmed.ncbi.nlm.nih.gov/10166121/)
- Monteiro, M. A., Baqar, S., Hall, E. R., Chen, Y. H., Porter, C. K., Bentzel, D. E., Applebee, L., & Guerry, P. (2009). Capsule polysaccharide conjugate vaccine against diarrheal disease caused by *Campylobacter jejuni*. *Infection and Immunity*, 77(3), 1128–1136. <https://doi.org/10.1128/IAI.01056-08>
- Monteville, M., Yoon, J., & Konkel, M. (2003). Maximal adherence and invasion of INT 407 cells by *Campylobacter jejuni* requires the CadF outer-membrane protein and microfilament reorganization. *Microbiology (Reading, England)*, 149(Pt 1), 153–165. <https://doi.org/10.1099/MIC.0.25820-0>
- Morona, J. K., Morona, R., Miller, D. C., & Paton, J. C. (2002). Streptococcus pneumoniae capsule biosynthesis protein CpsB is a novel manganese-dependent phosphotyrosine-protein phosphatase. *Journal of Bacteriology*, 184(2), 577–583. <https://doi.org/10.1128/JB.184.2.577-583.2002>
- Morooka, T., Umeda, A., & Amako, K. (1985). Motility as an intestinal colonization factor for *Campylobacter jejuni*. *Journal of General Microbiology*, 131(8), 1973–1980. <https://doi.org/10.1099/00221287-131-8-1973>
- Müller, A., Thomas, G. H., Horler, R., Brannigan, J. A., Blagova, E., Levdikov, V. M., Fogg, M. J., Wilson, K. S., & Wilkinson, A. J. (2005). An ATP-binding cassette-type cysteine transporter in *Campylobacter jejuni* inferred from the structure of an extracytoplasmic solute receptor protein. *Molecular Microbiology*, 57(1), 143–155. <https://doi.org/10.1111/J.1365-2958.2005.04691.X>
- Muraoka, W. T., & Zhang, Q. (2011). Phenotypic and Genotypic Evidence for L-Fucose Utilization by *Campylobacter jejuni*. *Journal of Bacteriology*, 193(5), 1065. <https://doi.org/10.1128/JB.01252-10>
- Musumeci, L., Bongiorni, C., Tautz, L., Edwards, R. A., Osterman, A., Perego, M., Mustelin, T., & Bottini, N. (2005). Low-molecular-weight protein tyrosine phosphatases of *Bacillus subtilis*. *Journal of Bacteriology*, 187(14), 4945–4956. <https://doi.org/10.1128/JB.187.14.4945-4956.2005>
- Newsholme, E. A., Crabtree, B., & Ardawi, M. S. M. (1985). GLUTAMINE METABOLISM IN LYMPHOCYTES: ITS BIOCHEMICAL, PHYSIOLOGICAL AND CLINICAL IMPORTANCE. *Quarterly Journal of Experimental Physiology*, 70(4), 473–489. <https://doi.org/10.1113/EXPPHYSIOL.1985.SP002935>
- Nguyen, H. A., El Khoury, T., Guiral, S., Laaberki, M. H., Candusso, M. P., Galisson, F., Foucher, A. E., Kesraoui, S., Ballut, L., Vallet, S., Orelle, C., Zucchini, L., Martin, J., Page, A., Attieh, J., Aghajari, N., Grangeasse, C., & Jault, J. M. (2017). Expanding the Kinome

- World: A New Protein Kinase Family Widely Conserved in Bacteria. *Journal of Molecular Biology*, 429(20), 3056–3074. <https://doi.org/10.1016/j.jmb.2017.08.016>
- Niemeyer, D., & Becker, A. (2001). The Molecular Weight Distribution of Succinoglycan Produced by *Sinorhizobium meliloti* Is Influenced by Specific Tyrosine Phosphorylation and ATPase Activity of the Cytoplasmic Domain of the ExoP Protein. *Journal of Bacteriology*, 183(17), 5163. <https://doi.org/10.1128/JB.183.17.5163-5170.2001>
- Oelschlaeger, T. A., Guerry, P., & Kopecko, D. J. (1993). Unusual microtubule-dependent endocytosis mechanisms triggered by *Campylobacter jejuni* and *Citrobacter freundii*. *Proceedings of the National Academy of Sciences of the United States of America*, 90(14), 6884. <https://doi.org/10.1073/PNAS.90.14.6884>
- Paley, S., Parker, K., Spaulding, A., Tomb, J.-F., O'Maille, P., & Karp, P. D. (2017). The Omics Dashboard for interactive exploration of gene-expression data. *Nucleic Acids Research*, 45(21), 12113–12124. <https://doi.org/10.1093/NAR/GKX910>
- Parkhill, J., Wren, B. W., Mungall, K., Ketley, J. M., Churcher, C., Basham, D., Chillingworth, T., Davies, R. M., Feltwell, T., Holroyd, S., Jagels, K., Karlyshev, A. V., Moule, S., Pallen, M. J., Penn, C. W., Quail, M. A., Rajandream, M. A., Rutherford, K. M., Van Vliet, A. H. M., ... Barrell, B. G. (2000). The genome sequence of the food-borne pathogen *Campylobacter jejuni* reveals hypervariable sequences. *Nature*, 403(6770), 665–668. <https://doi.org/10.1038/35001088>
- Parsons, C. M. (1984). Influence of caectomy and source of dietary fibre or starch on excretion of endogenous amino acids by laying hens. *British Journal of Nutrition*, 51(3), 541–548. <https://doi.org/10.1079/BJN19840059>
- Pei, Z., & Blaser, M. J. (1993). PEB1, the Major Cell-binding Factor of *Campylobacter jejuni*, Is a Homolog of the Binding Component in Gram-negative Nutrient Transport Systems*. *THE JOURNAL OF BIOLOGICAL CHEMISTRY*, 268(26), 18717–18735. [https://doi.org/10.1016/S0021-9258\(17\)46689-0](https://doi.org/10.1016/S0021-9258(17)46689-0)
- Pochini, L., Scalise, M., Galluccio, M., & Indiveri, C. (2014). Membrane transporters for the special amino acid glutamine: structure/function relationships and relevance to human health. *Frontiers in Chemistry*, 0, 61. <https://doi.org/10.3389/FCHEM.2014.00061>
- Post, A., Martiny, D., van Waterschoot, N., Hallin, M., Maniewski, U., Bottieau, E., Van Esbroeck, M., Vlieghe, E., Ombelet, S., Vandenberg, O., & Jacobs, J. (2017). Antibiotic susceptibility profiles among *Campylobacter* isolates obtained from international travelers between 2007 and 2014. *European Journal of Clinical Microbiology and Infectious Diseases*, 36(11), 2101–2107. <https://doi.org/10.1007/s10096-017-3032-6>
- Pratt, J. S., Sachen, K. L., Wood, H. D., Eaton, K. A., & Young, V. B. (2006). Modulation of Host Immune Responses by the Cytolethal Distending Toxin of *Helicobacter hepaticus*. *Infection and Immunity*, 74(8), 4496. <https://doi.org/10.1128/IAI.00503-06>
- Prisic, S., Dankwa, S., Schwartz, D., Chou, M. F., Locasale, J. W., Kang, C. M., Bemis, G., Church, G. M., Steene, H., & Husson, R. N. (2010). Extensive phosphorylation with overlapping specificity by *Mycobacterium tuberculosis* serine/threonine protein kinases. *Proceedings of the National Academy of Sciences of the United States of America*, 107(16), 7521–7526. <https://doi.org/10.1073/pnas.0913482107>
- Radomska, K. A., Wösten, M. M. S. M., Ordoñez, S. R., Wagenaar, J. A., & Putten, J. P. M. van. (2017). Importance of *Campylobacter jejuni* FliS and FliW in Flagella Biogenesis

- and Flagellin Secretion. *Frontiers in Microbiology*, 8(JUN), 1060.
<https://doi.org/10.3389/FMICB.2017.01060>
- Rees, J., Soudain, S., Gregson, N., & Highes, R. (1995). Campylobacter jejuni Infection and Guillain–Barré Syndrome. *New England Journal of Medicine*, 333(21), 1374–1379.
<https://doi.org/10.1056/NEJM199603213341216>
- Reuse, H. De, & Skouloubris, S. (2001). Nitrogen Metabolism. *Cyanidioschyzon Merolae: A New Model Eukaryote for Cell and Organelle Biology*, 283–296.
<https://www.ncbi.nlm.nih.gov/books/NBK2412/>
- Rivera-Amill, V., Kim, B. J., Seshu, J., & Konkel, M. E. (2001). Secretion of the Virulence-Associated Campylobacter Invasion Antigens from Campylobacter jejuni Requires a Stimulatory Signal. *The Journal of Infectious Diseases*, 183(11), 1607–1616.
<https://doi.org/10.1086/320704>
- Roier, S., Zingl, F. G., Cakar, F., Durakovic, S., Kohl, P., Eichmann, T. O., Klug, L., Gadermaier, B., Weinzerl, K., Prassl, R., Lass, A., Daum, G., Reidl, J., Feldman, M. F., & Schild, S. (2016). A novel mechanism for the biogenesis of outer membrane vesicles in Gram-negative bacteria. *Nature Communications* 2016 7:1, 7(1), 1–13.
<https://doi.org/10.1038/ncomms10515>
- Rollins, D. M., & Colwell, R. R. (1986). Viable but nonculturable stage of Campylobacter jejuni and its role in survival in the natural aquatic environment. *Applied and Environmental Microbiology*, 52(3), 531–538. <https://doi.org/10.1128/aem.52.3.531-538.1986>
- Sarabhai, T., & Roden, M. (2019). Hungry for your alanine: when liver depends on muscle proteolysis. *The Journal of Clinical Investigation*, 129(11), 4563.
<https://doi.org/10.1172/JCI131931>
- Schirm, M., Soo, E. C., Aubry, A. J., Austin, J., Thibault, P., & Logan, S. M. (2003). Structural, genetic and functional characterization of the flagellin glycosylation process in Helicobacter pylori. *Molecular Microbiology*, 48(6), 1579–1592.
<https://doi.org/10.1046/J.1365-2958.2003.03527.X>
- Sellars, M., Hall, S., & Kelly, D. (2002). Growth of Campylobacter jejuni supported by respiration of fumarate, nitrate, nitrite, trimethylamine-N-oxide, or dimethyl sulfoxide requires oxygen. *Journal of Bacteriology*, 184(15), 4187–4196.
<https://doi.org/10.1128/JB.184.15.4187-4196.2002>
- Shibayama, K., Wachino, J., Arakawa, Y., Saidijam, M., Rutherford, N., & Henderson, P. (2007). Metabolism of glutamine and glutathione via gamma-glutamyltranspeptidase and glutamate transport in Helicobacter pylori: possible significance in the pathophysiology of the organism. *Molecular Microbiology*, 64(2), 396–406.
<https://doi.org/10.1111/J.1365-2958.2007.05661.X>
- Singh, S. K., Yamashita, A., & Gouaux, E. (2007). Antidepressant binding site in a bacterial homologue of neurotransmitter transporters. *Nature* 2007 448:7156, 448(7156), 952–956. <https://doi.org/10.1038/nature06038>
- Sørensen, M. C. H., van Alphen, L. B., Harboe, A., Li, J., Christensen, B. B., Szymanski, C. M., & Brøndsted, L. (2011). Bacteriophage F336 recognizes the capsular phosphoramidate modification of Campylobacter jejuni NCTC11168. *Journal of Bacteriology*, 193(23), 6742–6749. <https://doi.org/10.1128/JB.05276-11>

- South, S. L., Nichols, R., & Montie, T. C. (1994). Tyrosine kinase activity in *Pseudomonas aeruginosa*. *Molecular Microbiology*, *12*(6), 903–910. <https://doi.org/10.1111/j.1365-2958.1994.tb01078.x>
- Stahl, M., Friis, L. M., Nothaft, H., Liu, X., Li, J., Szymanski, C. M., & Stintzi, A. (2011). l-Fucose utilization provides *Campylobacter jejuni* with a competitive advantage. *Proceedings of the National Academy of Sciences of the United States of America*, *108*(17), 7194. <https://doi.org/10.1073/PNAS.1014125108>
- Stanley, K., & Jones, K. (2003). Cattle and sheep farms as reservoirs of *Campylobacter*. *Journal of Applied Microbiology Symposium Supplement*, *94*(32). <https://doi.org/10.1046/j.1365-2672.94.s1.12.x>
- Stel, A.-X. van der, Mourik, A. van, Łaniewski, P., Putten, J. P. M. van, Jagusztyn-Krynicka, E. K., & Wösten, M. M. S. M. (2015). The *Campylobacter jejuni* RacRS two-component system activates the glutamate synthesis by directly upregulating γ -glutamyltranspeptidase (GGT). *Frontiers in Microbiology*, *6*(JUN). <https://doi.org/10.3389/FMICB.2015.00567>
- Sterner, D. E., & Berger, S. L. (2000). Acetylation of Histones and Transcription-Related Factors. *Microbiology and Molecular Biology Reviews*, *64*(2), 435. <https://doi.org/10.1128/MMBR.64.2.435-459.2000>
- Stevenson, G., Andrianopoulos, K., Hobbs, M., & Reeves, P. R. (1996). Organization of the *Escherichia coli* K-12 gene cluster responsible for production of the extracellular polysaccharide colanic acid. *Journal of Bacteriology*, *178*(16), 4885. <https://doi.org/10.1128/JB.178.16.4885-4893.1996>
- Sultan, A., Jers, C., Ganief, T. A., Shi, L., Senissar, M., Køhler, J. B., Macek, B., & Mijakovic, I. (2021). Phosphoproteome Study of *Escherichia coli* Devoid of Ser/Thr Kinase YeaG During the Metabolic Shift From Glucose to Malate. *Frontiers in Microbiology*, *0*, 771. <https://doi.org/10.3389/FMICB.2021.657562>
- Szymanski, C. M., Logan, S. M., Linton, D., & Wren, B. W. (2003). *Campylobacter* – a tale of two protein glycosylation systems. *Trends in Microbiology*, *11*(5), 233–238. [https://doi.org/10.1016/S0966-842X\(03\)00079-9](https://doi.org/10.1016/S0966-842X(03)00079-9)
- Szymanski, C. M., Yao, R., Ewing, C. P., Trust, T. J., & Guerry, P. (1999). Evidence for a system of general protein glycosylation in *Campylobacter jejuni*. *Molecular Microbiology*, *32*(5), 1022–1030. <https://doi.org/10.1046/J.1365-2958.1999.01415.X>
- Taheri, N., Mahmud, A. K. M. F., Sandblad, L., Fällman, M., Wai, S. N., & Fahlgren, A. (2018). *Campylobacter jejuni* bile exposure influences outer membrane vesicles protein content and bacterial interaction with epithelial cells. *Scientific Reports 2018 8:1*, *8*(1), 1–14. <https://doi.org/10.1038/s41598-018-35409-0>
- Thibault, P., Logan, S., Kelly, J., Brisson, J., Ewing, C., Trust, T., & Guerry, P. (2001). Identification of the carbohydrate moieties and glycosylation motifs in *Campylobacter jejuni* flagellin. *The Journal of Biological Chemistry*, *276*(37), 34862–34870. <https://doi.org/10.1074/JBC.M104529200>
- Thomas, D. K., Lone, A. G., Selinger, L. B., Taboada, E. N., Uwiera, R. R. E., Abbott, D. W., & Inglis, G. D. (2014). Comparative Variation within the Genome of *Campylobacter jejuni* NCTC 11168 in Human and Murine Hosts. *PLoS ONE*, *9*(2), 88229. <https://doi.org/10.1371/JOURNAL.PONE.0088229>

- Tolkatchev, D., Shaykhutdinov, R., Xu, P., Plamondon, J., Watson, D. C., Young, N. M., & Ni, F. (2006). Three-dimensional structure and ligand interactions of the low molecular weight protein tyrosine phosphatase from *Campylobacter jejuni*. *Protein Science*, *15*(10), 2381–2394. <https://doi.org/10.1110/ps.062279806>
- Van Alphen, L. B., Wenzel, C. Q., Richards, M. R., Fodor, C., Ashmus, R. A., Stahl, M., Karlyshev, A. V., Wren, B. W., Stintzi, A., Miller, W. G., Lowary, T. L., & Szymanski, C. M. (2014). Biological roles of the O-methyl phosphoramidate capsule modification in *Campylobacter jejuni*. *PLoS ONE*, *9*(1), 87051. <https://doi.org/10.1371/journal.pone.0087051>
- VanDrisse, C. M., & Escalante-Semerena, J. C. (2019). Protein Acetylation in Bacteria. *Annual Review of Microbiology*, *73*, 111. <https://doi.org/10.1146/ANNUREV-MICRO-020518-115526>
- Velayudhan, J., Jones, M. A., Barrow, P. A., & Kelly, D. J. (2004). l-Serine Catabolism via an Oxygen-Labile l-Serine Dehydratase Is Essential for Colonization of the Avian Gut by *Campylobacter jejuni*. *Infection and Immunity*, *72*(1), 260. <https://doi.org/10.1128/IAI.72.1.260-268.2004>
- Velayudhan, J., & Kelly, D. J. (2002). Analysis of gluconeogenic and anaplerotic enzymes in *Campylobacter jejuni*: an essential role for phosphoenolpyruvate carboxykinase. *Microbiology*, *148*(3), 685–694. <https://doi.org/10.1099/00221287-148-3-685>
- Véron, M., Lenois-Furet, A., & Beaune, P. (1981). Anaerobic respiration of fumarate as a differential test between *Campylobacter fetus* and *Campylobacter jejuni*. *Current Microbiology* *1981* *6:6*, *6*(6), 349–354. <https://doi.org/10.1007/BF01567010>
- Vincent, C., Duclos, B., Grangeasse, C., Vaganay, E., Riberty, M., Cozzone, E., & Doublet, P. (2000). Relationship between exopolysaccharide production and protein-tyrosine phosphorylation in gram-negative bacteria. *Journal of Molecular Biology*, *304*(3), 311–321. <https://doi.org/10.1006/JMBI.2000.4217>
- Vincent, Carole, Doublet, P., Grangeasse, C., Vaganay, E., Cozzone, A. J., & Duclos, B. (1999). Cells of *Escherichia coli* contain a protein-tyrosine kinase, Wzc, and a phosphotyrosine-protein phosphatase, Wzb. *Journal of Bacteriology*, *181*(11), 3472–3477. <https://doi.org/10.1128/jb.181.11.3472-3477.1999>
- Voisin, S., Watson, D. C., Tessier, L., Ding, W., Foote, S., Bhatia, S., Kelly, J. F., & Young, N. M. (2007). The cytoplasmic phosphoproteome of the Gram-negative bacterium *Campylobacter jejuni*: Evidence for modification by unidentified protein kinases. *Proteomics*, *7*(23), 4338–4348. <https://doi.org/10.1002/pmic.200700483>
- Waldroup, P., Waldroup, P. W., Mussini, F. J., Goodgame, S. D., Lu, C., Bradley, C. D., & Fiscus, S. M. (2012). A Nutritional Approach to the Use of Anticoccidial Vaccines in Broilers: Glutamine Utilization in Critical Stages of Immunity Acquisition. *Article in International Journal of Poultry Science*, *11*(4), 243–246. <https://doi.org/10.3923/ijps.2012.243.246>
- Wang, X., Ni, M., Niu, C., Zhu, X., Zhao, T., Zhu, Z., Xuan, Y., & Cong, W. (2014). Simple detection of phosphoproteins in SDS-PAGE by quercetin. *EuPA Open Proteomics*, *4*, 156–164. <https://doi.org/10.1016/J.EUPROT.2014.07.002>
- Wassenaar, T. M., Bleumink-Pluym, N. M. C., & Van Der Zeijst, B. A. M. (1991). Inactivation of *Campylobacter jejuni* flagellin genes by homologous recombination demonstrates that flaA but not flaB is required for invasion. In *The EMBO Journal* (Vol. 10, Issue 8).

- Watson, R. O., & Galán, J. E. (2008). *Campylobacter jejuni* Survives within Epithelial Cells by Avoiding Delivery to Lysosomes. *PLoS Pathogens*, *4*(1), 0069–0083. <https://doi.org/10.1371/JOURNAL.PPAT.0040014>
- Weingarten, R. A., Grimes, J. L., & Olson, J. W. (2008). Role of *Campylobacter jejuni* Respiratory Oxidases and Reductases in Host Colonization. *Applied and Environmental Microbiology*, *74*(5), 1367. <https://doi.org/10.1128/AEM.02261-07>
- Whitmore, S. E., & Lamont, R. J. (2012). Tyrosine phosphorylation and bacterial virulence. In *International Journal of Oral Science* (Vol. 4, Issue 1, pp. 1–6). *Int J Oral Sci*. <https://doi.org/10.1038/ijos.2012.6>
- Wilson, DJ, Gabriel, E., Leatherbarrow, A., Cheesbrough, J., Gee, S., Bolton, E., Fox, A., Fearnhead, P., Hart, C. A., & Diggle, P. J. (2008). Tracing the source of campylobacteriosis. *PLoS Genetics*, *4*(9). <https://doi.org/10.1371/journal.pgen.1000203>
- Wilson, David, Bell, J. A., Young, V. B., Wilder, S. R., Mansfield, L. S., & Linz, J. E. (2003). Variation of the natural transformation frequency of *Campylobacter jejuni* in liquid shake culture. *Microbiology*, *149*(12), 3603–3615. <https://doi.org/10.1099/mic.0.26531-0>
- Wright, J. A., Grant, A. J., Hurd, D., Harrison, M., Guccione, E. J., Kelly, D. J., & Maskell, D. J. (2009). Metabolite and transcriptome analysis of *Campylobacter jejuni* in vitro growth reveals a stationary-phase physiological switch. *Microbiology*, *155*(1), 80–94. <https://doi.org/10.1099/MIC.0.021790-0>
- Xue, G. D., Barekatin, R., Wu, S. B., Choct, M., & Swick, R. A. (2018). Dietary L-glutamine supplementation improves growth performance, gut morphology, and serum biochemical indices of broiler chickens during necrotic enteritis challenge. *Poultry Science*, *97*(4), 1334–1341. <https://doi.org/10.3382/PS/PEX444>
- Yamashita, A., Singh, S. K., Kawate, T., Jin, Y., & Gouaux, E. (2005). Crystal structure of a bacterial homologue of Na⁺/Cl⁻-dependent neurotransmitter transporters. *Nature* *2005* *437*:7056, *437*(7056), 215–223. <https://doi.org/10.1038/nature03978>
- Young, K. T., Davis, L. M., & DiRita, V. J. (2007). *Campylobacter jejuni* : molecular biology and pathogenesis. *Nature Reviews Microbiology* *2007* *5*:9, *5*(9), 665–679. <https://doi.org/10.1038/nrmicro1718>
- Young, N. M., Brisson, J.-R., Kelly, J., Watson, D. C., Tessier, L., Lanthier, P. H., Jarrell, H. C., Cadotte, N., Michael, F. St., Aberg, E., & Szymanski, C. M. (2002). Structure of the N-Linked Glycan Present on Multiple Glycoproteins in the Gram-negative Bacterium, *Campylobacter jejuni* *. *Journal of Biological Chemistry*, *277*(45), 42530–42539. <https://doi.org/10.1074/JBC.M206114200>
- Yu, B., Kim, J., Moon, J., Ryu, S., & Pan, J. (2008). The diversity of lysine-acetylated proteins in *Escherichia coli*. *Journal of Microbiology and Biotechnology*, *18*(9), 1529–1536. <https://europepmc.org/article/med/18852508>
- Zautner, A. E., Tareen, A. M., Groß, U., & Lugert, R. (2012). Chemotaxis in *Campylobacter jejuni*. *European Journal of Microbiology & Immunology*, *2*(1), 24. <https://doi.org/10.1556/EUJMI.2.2012.1.5>
- Zeden, M. S., Kviatkovski, I., Schuster, C. F., Thomas, V. C., Fey, P. D., & Gründling, A. (2020). Identification of the main glutamine and glutamate transporters in *Staphylococcus*

aureus and their impact on c-di-AMP production. *Molecular Microbiology*, 113(6), 1085. <https://doi.org/10.1111/MMI.14479>

Zeden, M. S., Schuster, C. F., Bowman, L., Zhong, Q., Williams, H. D., & Gründling, A. (2018). Cyclic di-adenosine monophosphate (c-di-AMP) is required for osmotic regulation in *Staphylococcus aureus* but dispensable for viability in anaerobic conditions. *The Journal of Biological Chemistry*, 293(9), 3180. <https://doi.org/10.1074/JBC.M117.818716>

Zheng, J., & Jia, Z. (2010). Structure of the bifunctional isocitrate dehydrogenase kinase/phosphatase. *Nature*, 465(7300), 961–965. <https://doi.org/10.1038/nature09088>